High Frequency electrical breakdown of gases at low pressures

Mallalieu, P.

HIGH FREQUENCY ELECTRICAL BREAKDOWN OF GASES AT LOW PRESSURES

by

P. Pallaton, B.Sc.

Being an account of the work carried out at Sunderland Technical College during the two years ending September 1960.

Thesis submitted to the University of Durham in candidature for the degree of M.Sc.

ACKNOWLEDGEMENTS

The author is most indebted to Dr. J.L. Clark who, as Research Supervisor, has given unfailing guidance and warm friendship.

He also wishes to thank the Governors and Principal of the Technical College and Mr. K.E. Pattinson for the facilities made available at the Physics Department, Sunderland.

Finally, he wishes to record his gratitude to Dr. W.A. Prowse, of the Physics Department, Durham Colleges, Durham, for his advice and direction.

SYMBOLS

α	-	Townsend primary coefficient; ion pairs per cm. drift in field direction.
γ	-	Townsend's secondary coefficient.
δ	-	secondary emission coefficient.
λ	-	wavelength of applied field, cm.
ν	-	quantum radiation frequency, $sec.^{-1}$.
ν_c	-	collision frequency between electrons and gas molecules, $sec.^{-1}$.
ν_i	-	ionization energy of a gas, e.v.
Λ	-	characteristic diffusion length, cm.
Φ	-	work function of surface, e.v.
$\bar{c}$	-	mean random electron velocity, $cm.sec.^{-1}$.
d	-	electrode separation, cm.
e	-	electron charge, coulomb.
f	-	field frequency, $sec.^{-1}$.
h	-	Plancks radiation constant, joules.sec.
n	-	electron density, cm^{-3}.
p	-	gas pressure, mm. Hg.
$\bar{u}$	-	mean electron energy, e.v.
v	-	drift velocity of electrons, $cm.sec.^{-1}$.
z	-	ionizing efficiency.

D_e - electron diffusion coefficient.

E - instantaneous field strength, volt.cm.$^{-1}$.

E_e - effective field strength, volt. cm.$^{-1}$.

E_p - peak field strength, volt.cm.$^{-1}$.

E_R - R.M.S. field strength, volt.cm.$^{-1}$.

I - electron current, amp.

J - electron current density, amp.cm.$^{-2}$.

P_c - probability of collision.

S_e - electron ionizing efficiency.

LIST OF CONTENTS

CHAPTER 2

Introduction to the Breakdown Studies at 10 Mc/s and 20 Mc/s

CHAPTER 3

Apparatus

CHAPTER 4

Experimental Results in Hydrogen at 10 Mc/s and 20 Mc/s : Basic Equations

CHAPTER 5

Breakdown in Hydrogen at 20 Mc/s

1. PRE-BREAKDOWN PHENOMENA IN GASES AT HIGH FREQUENCIES

1.1 The Breakdown Criterion

When a neutral gas is subjected to a weak electric field it generally possesses good, though imperfect, insulation properties. No practical gas-filled electrode system can completely prevent "casual" sources of irradiation (e.g. energetic cosmic radiations, natural radioactivity) from causing local ionization within the gas. Conduction currents of the order of 10^{-19} to 10^{-16} A. amps. are normally observed. By deliberately irradiating the system with high-energy quantum radiation, for example γ -rays, X-rays, or ultra-violet light, the current density can be increased by several orders. In none of these cases is the physical nature of the gas sensibly altered and an 'insulating state' may be said to exist.

As the applied electric stress is increased, however, a point is reached at which the gas, quite suddenly, exhibits a considerable increase in electrical conductivity. The increase in current is usually accompanied by a characteristic visible glow from the gas, and by a drop in the potential difference across the electrode system. Under these conditions

an electrical discharge or 'break-down' is said to have occurred.

A satisfactory definition of the breakdown criterion is not, however, as clear-cut as may be supposed. Discharges are not necessarily accompanied by strong light emission or by perceptible changes in a voltmeter reading. Even a definition based upon "change in conductivity" is not altogether acceptable, as the pre-breakdown current is not a true characteristic of the gas; being dependent on the strength of the external ionizing agent. One definition makes use of an important physical distinction between currents flowing in the 'insulating' and 'conducting' states: whereas pre-breakdown currents cease when the external ionizing source is removed, the current in a true discharge is self-sustained i.e. will continue to flow when the irradiation is removed.

The onset of breakdown can be said to have occurred when the current ceases to depend upon the existence of an external ionizing source.

The rapid changes in electrical conductivity accompanying breakdown are brought about by the generation of charged particles within the gas and/or at the walls of the discharge chamber. Electrons are the most important of the conducting

particles, though positive ions and in certain gases negative ions, sometimes play a significant part in initiating the discharge.

The motion of the particles in the body of a gas, controlled by such factors as the gas pressure, field strength, frequency and electrode geometry, consists of 'random' thermal motion with a superimposed mobility 'drift' in the direction of the electric field gradient. Essentially, the difference between the action of weak electric fields on the gas and of fields the order of the threshold breakdown value, is that the latter must be of sufficient magnitude to promote effects, either in the gas itself or on the walls of the container, which result in the generation of further particles, and in particular, electrons. Moreover, for a discharge to occur, the rate of (electron) production must exceed the rate of loss; breakdown may thus be conveniently defined from a quantitative standpoint as a failure of equilibrium in the above process, in the direction favouring growth of electron population.

In developing a breakdown theory the physical problem is to account for net growth in electron density (from a small number of initiatory electrons) in terms of fundamental electronic, ionic, and atomic collision processes in the gas

and at the electrode surfaces. Experiments have shown that the efficiencies of the processes, controlling electron generation and loss are functions of the quantities describing the discharge system. As a consequence, the mechanism by which a discharge occurs, may become modified, even radically changed, as each particular parameter is varied.

The main purpose of this chapter is to give an account of the pre-breakdown and initiation processes relevant to the experimental work carried out. Processes having only an indirect bearing upon the subject matter are dealt with briefly.

1.2 Generation of Charged Particles in the body of a Gas

1.2.1 Motion of charged particles in a field-free gas

Classical kinetic theory gives a number of results which are quite adequate in expressing the thermal motion of gas molecules in an enclosure.

In cases where Maxwellian distributions of molecular velocities may be assured, calculations may be made of many of the fundamental quantities describing thermal motion e.g. R.M.S. velocities and energies, and diffusion rates, as functions of temperature and pressure. Determination can also be made of energy interchanges between colliding atoms and extended to impacts between charged particles, provided

no change of internal energy is involved, i.e. the collisions must be perfectly elastic.

When charged particles, particularly electrons, are present in a gas the useful application of kinetic theory is limited, and resort must sometimes be made to the wave mechanics.

At normal room temperatures (the usual working conditions for experimental glow-discharge studies) the maximum thermal velocities of gas molecules are much too low to stimulate inelastic collisions. Casual electrons and ions present in a field-free gas are likewise not sufficiently energetic and, if time permits, they eventually acquire thermal equilibrium with their surroundings. Usually, however, before the equilibrium energy is attained, recombination occurrs, either in the volume of the gas or by a three-body process involving the walls of the containing vessel. Under the influence of a sufficiently powerful field mobility drift is superimposed upon the random motion of the charged particles present. This gives rise to two effects normally characterizing a gas discharge, namely optical excitation and collision ionization. Excitation, though an inherent accompaniment to a discharge, frequently contributes only indirectly to the mechanisms of charge multiplication and for this reason will not

be given the same prominence as the important ionization processes.

1.2.2 Ionization processes

Ionization of a gas atom may be effected by a variety of processes, provided always that the total energy available for transfer to atom (or molecule) exceeds the characteristic ionizing energy, V_i e.v.

The necessary exchanges can be brought about in the following ways:

(a) by collisions between electrons and neutral atoms.

(b) by collisions between positive ions and neutral atoms.

(c) by collisions between neutral atoms.

(d) by absorption of radiation quanta by neutral atoms and ions.

(e) by cumulative ionization, in which the necessary energy is received by the atom in two (or more) distinct parcels.

(f) by 'thermal' ionization, a term used to describe the ionizing action of molecular, ionic and electronic collisions and radiation absorption occurring in gases at high temperatures.

In the initiation of a gas discharge the processes may occur either singly or in combinations, with efficiencies

determined by the physical conditions imposed.

1.2.3 Ionization by electron impact

Contrary to Townsend's original supposition that any electron possessing ionizing energy or greater will always ionize a gas atom by collision, the effectiveness of electrons in promoting ionization by impact depends upon their energy. Experimental evidence[2,3,4] shows that the ionizing probability (number of ion pairs produced per electron travelling 1 cm. through at gas at unit pressure) rises from zero for electron energies the order of the ionizing potential V_i, passes through a relatively broad maximum for energies a few times V_i and falls away gradually for impacts involving even more energetic electrons. The residual electron kinetic energy arising from an ionizing event may, partly, be retained by the electron, transferred to the released electron or used in further ionization or excitation. Instantaneous directions of both primary and daughter electrons are orientated almost at random. In the absence of some external stimulant e.g. an electric field, it is not possible for a sustained build-up of charge to take place. Fast electrons shot into a gas may well produce a number of ion-pairs ('ion-pair' used in this context refers to an electron and a positive ion), but

once their velocities fall below a minimum value they cease to function as ionizing agents and, given time, acquire thermal equilibrium with the gas. The same conditions apply to ejected electrons.

Field-intensified ionization by electrons

When a gas enclosed by a suitable container is subjected to a strong electric field, one electron starting at a convenient point in the gap can in its lifetime create a large number of ion-pairs, by virtue of acquiring from the field sufficient energy to ionize a gas atom, subsequent to a previous ionizing encounter.

Townsend's primary coefficient α (number of ion-pairs created by an electron per cm. drift in the negative field direction), is the parameter most widely used in describing multiplication of change under the action of a unidirectional or low-frequency electric field. By definition it follows that n_o electrons starting at a point x = o, will have created $n_o \exp. \int_o^x \alpha \, dx$ fresh electrons in travelling a distance x cm. in the field direction. For a uniform field, stressing a gas enclosed by electrodes of separation d cm., the number of electrons entering the anode, n, is related to the number n_o generation at the cathode by

$$n = n_o \exp. \int_o^d \alpha \, dx = n_o \exp (\alpha d)$$

or in terms of current

$$I = I_o \exp. (\alpha d) \quad \ldots \quad \ldots \quad \ldots \quad (1)$$

When n_o is used to indicate a rate of generation of initiatory electrons, the term 'electron avalanche' is used to indicate exp.(α d) electrons per second reaching the plane of d per electron leaving the plane x = 0.

α is a complex function of the reduced field E/p and of the nature of the gas. No theory has yet been proposed which successfully correlates the observed variation of α with E/p [5], due probably to lack of evidence regarding the exact form of the electron energy distribution - assumed Maxwellian. Since $1/\alpha$ represents the average distance travelled between ionizing events, the number of electrons in an avalanche, exp.(α d), is essentially an average number: the statistical fluctuations have been represented by a probability equation[6].

No mention has yet been made of the positive ions created during ionization. Due to their large mass relative to the electron, they migrate only slowly in the positive field

direction, towards the cathode. Under normal laboratory conditions they do not acquire sufficient energy to ionize by collision, as was originally assumed by Townsend. Their presence, however, cannot be ignored, both by virtue of the space-charge they create in the body of the gas and their ability to liberate fresh electrons by impact on the cathode.

1.2.4 Ionization by quantum absorption (photo-ionization)

Radiation quanta, passing through a gas, may promote ionization provided the characteristic quantum energy $h\nu$ is greater than $e V_i$; in practice this condition almost entirely excludes direct ionization by visible radiations. Several distinct mechanisms are possible, depending upon the order of energy of the quanta and the complexity of the extra-nuclear structure of the target atoms or molecules. When $h\nu$ is the same order of magnitude as eV_i it is found[7] that the probability of an ionizing event in a given gas depends upon ν and the gas pressure p, and that absorption and ionization are a maximum when the quantum has just enough energy to ionize.

The ionizing capabilities of highly-energetic quanta (e.g. X-rays, γ-rays) depend very largely upon the gas undergoing irradiation. An atom of low atomic number is preferentially ionized by one of its innermost extranuclear

electrons absorbing a large fraction of the energy of the incident quantum. The ejected K-electron thus leaves the atom with high velocity (corresponding to nearly the full quantum energy) and is capable of intense local ionization.

As the atom returns to a state of minimum energy quanta will be released. They may be preferentially absorbed and an atom may be stripped of several electrons. (Auger effect).

Photons released by optical excitation of gas atoms, by virtue of their possessing energy $< v_i$ e.v. are incapable of stimulating direct photo-ionization by any of the mechanisms described above. However, such atoms may be ionized if they receive the necessary energy in steps.

1.2.5 Other Processes

It has been established, that energies not less than several hundred electron volts must be imparted to ions before their ionizing efficiencies become in any way comparable with electrons.

The effect may be neglected under conditions other than high gas temperatures and/or powerful applied fields.

The velocity distribution of neutral particles at room temperatures precludes direct ionization by thermal impact; ionization by atom-atom collisions becomes important only at very high temperatures.

The proportion of gas atoms having relatively high velocities increases with increasing temperature, leading to ionization at temperatures exceeding a few thousand ^{o}C. Photoionization will in general occur (radiation from the high temperature enclosing walls and the so-called "imprisoned" radiation), electrons and positive ions will also contribute towards the efficiency of the process.

1.2.6 Generation at solid surfaces

Possible emission processes from solid surfaces include thermionic emission, field emission, secondary emission, by ion impact, photoelectric emission and secondary emission as the result of electron impact. Of these only the last mentioned seems likely to play a significant role in the present work.

A primary electron which falls on the surface of a solid either returns to the gas (or vacuum) or penetrates into the solid and is captured or releases secondary electrons. For a secondary electron to be released the energy of the primary particle has to exceed the work function, Φ , of the solid. One possible mode of secondary emission occurs when incident primary electrons transfer energy to the valence electrons of the solid atoms. Alternatively, interaction

between the primary electrons and the free electrons of the solids atomic lattice may cause multiple collisions and enable secondaries to pass through the boundary into the gas or vacuum.

Stimulated emission, attributed to the formation of internal electric fields, has been reported[41] by a number of workers using specially prepared surface layers. Thin film field emission of this type is referred to as the Malter effect.

The yield or coefficient of secondary emission, δ , is defined as the number of secondaries per normally incident primary particle.

All emission curves show a characteristic rapid rise of δ with increasing primary electron energy up to a value $\delta_{max.}$: further increase of primary energy causes a gradual descrease in δ (assocated with increased primary penetration into the lattice). For pure metals, $\delta_{max.}$ usually lies between 0.9 and 1.5; the associated values of primary electron energy vary over a wide range. Higher values of δ have been observed from metal compounds, particularly from oxides and halides. Workers have concentrated attention upon determinations of δ_{max} rather than the primary energy values for $\delta \approx 1$.

Some work has been reported on emission from metal alloys and evidence from the available data is significant. Certain alloys have been shown to give exceptionally high yields and values of δ_{max} up to 16 have been obtained [8,9,10].

Monatomic layers of absorbed oxygen cause a reduction in secondary yield. With thicker layers, δ shows either little change or exhibits a marked increase, particularly for metals having a strong oxygen affinity.

1.3 Removal processes

The growth of electron density by ionization and other processes is opposed by a number of possible depopulating mechanisms.

1.3.1 Mobility Capture

This process takes place when an electron is carried to a bounding surface by virtue of the drift imparted by an applied electric field. Impacts taking place with sufficiently high energy may cause the release of secondary electrons (1.2.6) giving rise to the possibility of an overall increase in electron population.

1.3.2 Recombination and Attachment

If a suitable encounter takes place between particles of opposite charge, recombination may occur, with consequent

neutralisation of charge.

In a system containing equal numbers of oppositely charged particles the rate of recombination is proportional to the square of the charge density and hence to the square of the pressure.

The efficiency of recombination processes is thus small at low pressures. Theoretical and experimental evidence suggests that direct electron-ion recombination, in the body of a gas, may be neglected.

A three body process is more effective, eg. the formation of a negative ion and its subsequent encounter with a positive ion. Such collisions are unlikely at low pressures, however, furthermore hydrogen and inert gases are virtually non-attaching.

A special type of dissociative recombination has been described in a paper by Fucks[11]. Firstly, dissociation of a hydrogen molecule occurs whereby

$$H_2 \rightarrow H + H^{*} + \nu_1$$

(H^{*} represents an excited atom, ν_1 a radiation quantum). Then three body volume-recombination takes place in the presence of a third body M,

$$H + H^{*} + M \rightarrow H_2 + M + \nu_2.$$

This process lead to an emission spectrum below 1,100 Å and gives rise to 'gas-ionizing radiation' since the first ionizing potential of hydrogen is equivalent to a quantum energy of $\lambda = 805$ Å. More recently, Corrigan and von Engel [12] have shown that a large proportion of the energy of an electron swarm is used in the dissociation of hydrogen molecules. However, the sequence of events is most improbable below a few mm.Hg. - Corrigan & Von Engel dismiss volume recombination in the pressure range 0.7 - 12 mm.Hg.

Surface recombination between electrons and ions is an efficient process being a special case of three body recombination. This mechanism is frequently dominant in the ultimate neutralisation of charged particles in a discharge chamber where the walls are remote from the electrode system, irrespective of the removal processes taking place in the intense field region.

1.3.3 Diffusion

When a non-uniform particle density exists in a gaseous medium, thermal motion gives rise to a net transfer of momentum in the direction of the negative concentration gradient.

The particles thus flow as though they possess a directed velocity, v_D, and for electrons the flow across unit area per second is given by

$$J = n v_D = - D_e \nabla n$$

where D_e = diffusion coefficient in cm^2 per sec.

Kinetic theory shows that $D_e \propto \lambda_e$, where λ_e is the mean distance travelled by electrons between collision, and therefore suggests that $D_e \propto \frac{1}{p}$, though the dependence of λ_e upon electron energy must be taken into account.

The mean time, t_D, spent by an electron in diffusing from its point of origin to a given bounding surface is determined by the geometry of the surface and the concentration gradient (expressed mathematically in terms of D_e).

These quantities are related by the general expressions:

$$t_D D_e = \Lambda^2 \quad \ldots \quad \ldots \quad \ldots \quad (11)$$

where Λ is a quantity, called the Diffusion Length[13], having units of length and describing the shape of the bounding surface.

1.4 Breakdown Mechanisms in Gases

1.4.1 Requirements of Breakdown Theory

A gaseous electrical discharge in a given system, occurs when the application of an external field of suitable magnitude stimulates the production of large numbers of charged particles within the body of the gas or at the walls of the containing vessel, multiplication starting from a small number of initiatory

electrons and leading ultimately to change from the 'insulating' to 'conducting' state (Section 1.1). The transition may be considered complete when the discharge ceases to depend upon the existence of the external irradiating source.

The descriptions of ionizing processes, Sections 1.2.2 - 1.2.5 show that electrons are by far the most powerful agents in the production of fresh charged particles. In general, any breakdown theory must satisfactorily account for a net growth of electron density with time. Further, relationships describing the mechanisms of electron multiplication and loss must be formulated in terms of measurable quantities (e.g. onset field strength, gas pressure etc., and atomic data such as charge, mass and mean free path) for the purpose of verifying theoretical predictions.

1.4.2 Parameters: Order of Presentation

Disregarding any special physical conditions imposed, the threshold breakdown field is in general a function of the pressure and nature of the gas, electrode geometry, field frequency and the nature of the electrode surfaces. The variables are frequently used in reduced form e.g. E/p, α/p, f/p, since, together with the quantity p.d., the applicability of the Similarity Rules [14,15] can be readily

checked.

In certain cases of high-frequency breakdown controlled by diffusion, a different though analogous set of variables are employed[13], namely E/p, $p\Lambda$, $p\lambda$.

Under the action of a unidirectional field, an electron is accelerated by the field between collisions, whereupon its instantaneous direction of motion is redirected almost at random. The influence of the field then re-orientates the electron in the field direction (a parabolic path is approximately followed). The electron then continues to move with the field until the termination of its free path, whence the above process is repeated. For elastic collisions, the electron will on the average gain a net amount of energy per collision time, notwithstanding the small amount transferred to the neutral atom during impact. Energy transfer between field and electron, a function of E/p, is completely efficient insofar as the particle is continuously subjected to an accelerating force constant in magnitude and direction. If, on the other hand, the d.c. source is replaced by an a.c. field of R.M.S. value equal to that in the d.c. case, the energy transferred to the electron can only equal that under the corresponding d.c. conditions in the special cases of high gas

pressure and/or low field frequency. If either the frequency is raised or the gas pressure lowered, transfer becomes gradually less efficient. The cause of this may be attributed directly to electron inertia. Increase in the amplitude of electron oscillation (due to decrease in frequency) or mean free path (due to reduction in pressure) results in electron-atom collisions occurring too infrequently for the electron motion to keep in phase with the field. It is to be expected that the more out-of-phase the electron motion becomes, the less energy will be transferred, on the average, from the field, to the electron. An extreme limit of the argument leads to the well-known result that an electron in a vacuum will oscillate in quadrature with the applied field and will take no power from it.

An equation expressing the above has been derived in Section 4.5.2 .

$$V = \frac{e\,E_p\;10^7}{m(\omega^2 + \nu_c^2)^{\frac{1}{2}}}\;\sin(\omega t - \alpha) \quad \ldots \quad \ldots \quad (27)$$

where V is the average drift velocity of electrons in an ocean of gas acted upon by a field

$$E = E_p \sin \omega t.$$

ν_c is the collision frequency of electrons with gas atoms and

$$\alpha = \tan^{-1} \frac{\omega}{\nu_c} \quad \ldots \quad \ldots \quad \ldots \quad \ldots \quad (26)$$

Over a range of electron energies, in several gases, experimental evidence[16] suggests that $\nu_c \propto p$.

Hence when $\omega >> \nu_c$ (i.e. at high frequencies or low pressures)

$$\alpha \rightarrow \tan^{-1} \infty = \frac{\pi}{2} \text{ rdns.}$$

i.e. $V \propto \cos \omega t$.

i.e. velocity is in quadrature with field.

Again when $\omega << \nu_c$, corresponding to high pressures or low frequencies (which may, with reservations, be taken to include d.c.)

$$V \propto \sin \omega t.$$

i.e. velocity in phase with field.

In terms of energy transfer, an expression by Margeneau[17]

$$E_e^2 = E_R^2 \left[\frac{\nu_c^2}{\nu_c^2 + \omega^2} \right] \quad \ldots \quad \ldots \quad (2)$$

relates "effective" field E_e to the R.M.S. value of the applied field. It is seen that when $\omega >> \nu_c$: $E_e \rightarrow 0$ and when $\omega << \nu_c$: $E_e = E_R$

1.4.3 Breakdown under conditions where $\omega << \nu_c$

(a) d.c. breakdown

The physical problem has been to propose a theory to satisfactorily explain the development of a discharge current not dependent upon the existence of an external source of electrons. Referring to equation 1 it is evident that an α - mechanism alone is not sufficient, since the current I, being directly proportional to the rate at which 'casual' electrons are being produced, would cease subsequent to the removal of the irradiating source, irrespective of the magnitude of the applied field.

Townsend originally proposed that the necessary 'secondary' mechanism resulted from the ionizing action of positive ions (produced by collision ionization) migrating towards the cathode. However, calculations showed that under normal experimental conditions the ions could not receive ionizing energy from the field (ref. section 1.2.5). Subsequently Townsend modified his ideas and introduced his celebrated γ - mechanism, in which

secondary emission from the cathode due to positive ions, excited ions, photons etc., was considered to play the vital role in producing the 'internal' source of secondary electrons.

Mathematically, this led to the well-known Townsend equation

$$I = \left[\frac{I_o \exp(\alpha d)}{1 - \gamma\{\exp(\alpha d)-1\}} \right] \quad \ldots \quad \ldots \quad \ldots \quad (3)$$

where γ, for simplicity, may be defined as the number of electrons released from the cathode per positive ion impinging upon it, (the general form of the equation is not altered by including other effects in the definition of γ). It was found that for low values of p.d. equation (3) agreed quite adequately with experimental plots of pre-breakdown current.

On the other hand, investigation by Masch[18] and Paavola[19] indicated the absence of a γ - mechanism, at least for high p.d. values. This evidence was based upon ln I/I_o d plots in the vicinity of breakdown yielding straightlines, instead of the upcurving of the required hyperexponential increase of pre-breakdown current.

The situation was further obscured by the studies of time-lags associated with discharge. According to Townsend's theory, the time taken for a discharge to develop subsequent

to the appearance of a suitable 'triggering' electron (the formative time, t_f) should be of the order of the transit time of positive ions across the gap. Oscillographic studies of pulsed gaps, however, indicated values of t_f two or three orders less.

As an alternative, photoionization was considered as the additional electron multiplication process. It was suggested[20] that photons produced in the gap by exciting collisions would move ahead of the main avalanche and cause ionization by virtue of their absorption by the molecules of the gas mixture having low ionization potential. The subsequent creation of fresh electron avalanches, assisted by field intensification due to positive ion space charges, would cause the gap to be bridged in a time interval corresponding to the observed formative period. Support for this view was provided by Raether's[20] cloud chamber photographs of spark development, which enable calculations to be made of the diameter of the spark channels and the rate of growth of the discharge. Such 'streamer' theories were neverl fully developed and post World War II investigations immediately demanded a re-appraisal of ideas. In particular, accurate oscillographic studies of formative times showed that with threshold fields applied to a test gap

(as distinct from severe overvolting in pre-war studies) t_f is large enough to include the possibility of positive ions crossing the gap, at least for small separations. Doubt was expressed about the interpretations of Raether's cloud chamber tracks, which were based upon the assumption that the first stages of spark development had been photographed. Finally a critical analysis of previous work by Llewellyn Jones and Parker[22] revealed that incorrect conclusions had been reached concerning lack of evidence of the role of positive ions in assisting the initiation of a discharge.

Modern views on the inception of the d.c. discharge owe much to a series of precision experiments by Llewellyn Jones[22] et al. at Swansea. Using gases of high purity and well-regulated power supplies, Jones showed that the development of a discharge could, in fact, be satisfactorily explained by mechanisms of the Townsend type i.e. an α -process sustained by a γ - process. Good agreement between theory and experiment is in evidence over an extended range of p.d.

Jones[23] concludes that the secondary mechanism must be considered complex in character, with all processes, which may lead to the supply of fresh electrons from the cathode, possibly contributing - no single process can be said, in general, to

to dominate, relative efficiencies being governed by such factors as cathode surface and geometry.

By putting the denominator of equation (3) equal to zero, a mathematical statement of the breakdown criterion may be made, viz:-

$$1 - \gamma \left[\exp. (\alpha d) - 1 \right] = 0 \quad \ldots \quad \ldots \quad (4)$$

The above equation may be regarded as representing a condition whereby electron production processes replace the initiatory electrons, giving rise to a self-sustained current. Thus, when in practice the breakdown criterion is realised, I_o may be reduced to zero, and I should remain finite with the breakdown potential independent of current. The above has been adequately verified under strict experimental conditions.

This summary of d.c. breakdown acts as an essential preliminary to the study of breakdown under alternating electric fields.

(b) Low Frequency and High Frequency Breakdown at High Gas Pressures

Energy transfer between field and gas is still efficient under a.c. conditions provided the electron- gas molecule collision frequency is substantially greater than the angular field frequency. The collision frequency has been found by

1. Breakdown in Air at fixed pd. Compiled by Prowse (19--)
Variation of Breakdown Voltage with Field Frequency

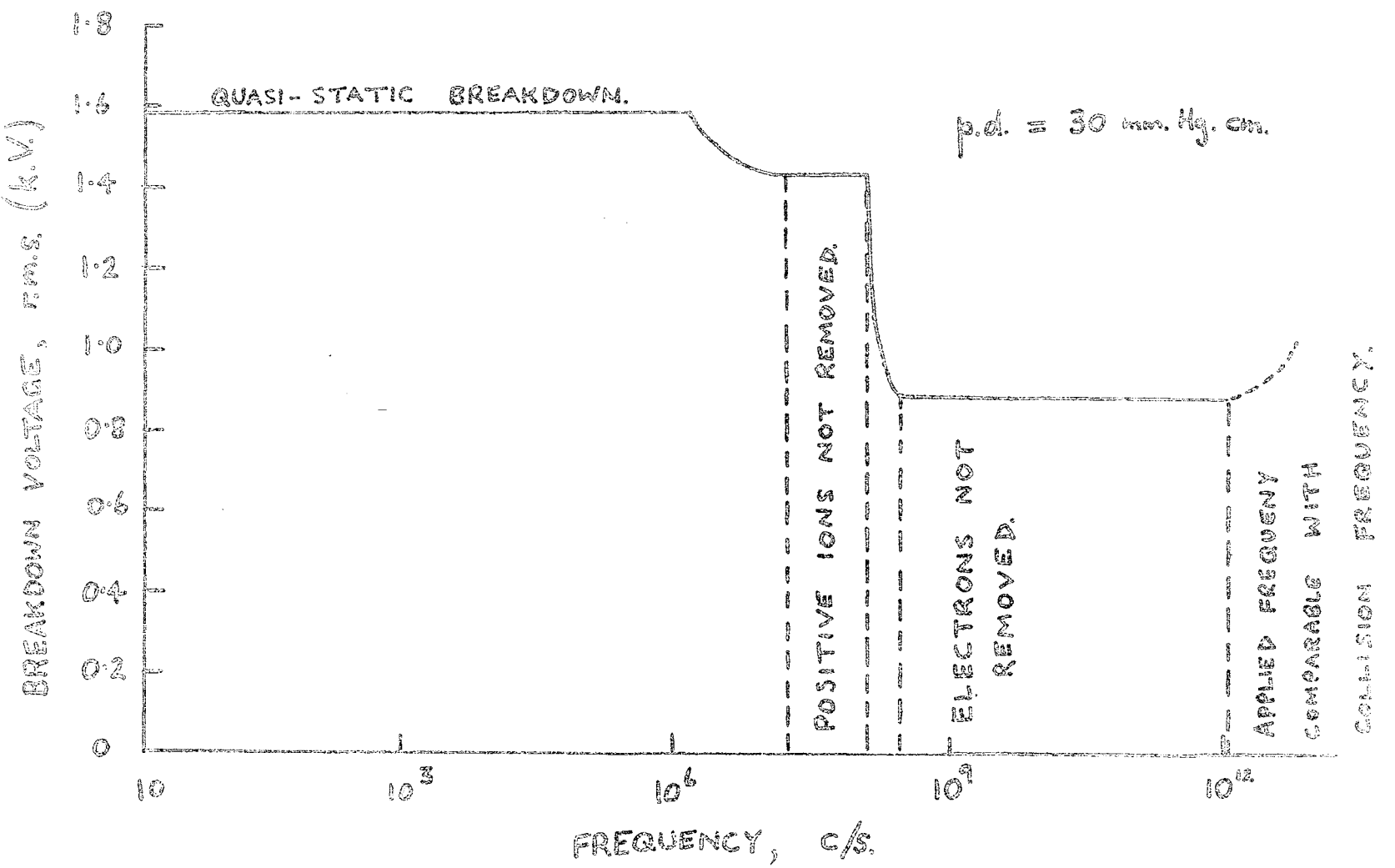

experiment to depend upon electron energy as well as gas pressure. We may write

$$\nu_c \quad \alpha \quad p$$

$$= \quad 5.10^9 \text{ sec.}^{-1} \text{ mm.Hg.}^{-1} \text{ (approximately, for a number of gases)}$$

$$\therefore \quad \frac{\nu_c}{\omega} = \frac{5.10^9 p}{2\pi f} \simeq \frac{10^9 p}{f}$$

In practice a ratio $\frac{\nu_c}{\omega} > 100$ is necessary to ensure the condition $\nu_c >> \omega$. Hence $\frac{10^9 p}{f} > 10^2$

$$\text{i.e.} \quad p > f.\, 10^{-7}$$

Hence for frequencies the order of a few megacycles, gas pressures not less than a few mm. Hg. must be used to ensure efficient energy transfer. At these relatively 'high' pressures the breakdown mechanisms over a wide range of frequency are now quite well established.

For convenience in the description of starting mechanisms, a hypothetical test gap will be considered, enclosing a pure gas at a suitable pressure and subjected to a voltage source of variable frequency. It may be seen from Figure 1 that for low frequencies the R.M.S. starting field E_R rises slowly but

steadily from the corresponding d.c. value , until a critical frequency is reached, at which E_R shows a small drop; quite distinct and fairly sudden. At frequencies beyond this value a further decrease, more pronounced than the first, occurs at a second critical point. Still higher up the frequency scale a further transition occurs characterised by a sudden and continuous rise in onset field strength.

Discussion of this phenomenon (the collision-frequency transition) is referred to the following section, as the condition $\nu_c >> \omega$ no longer applies.

Not only are the starting field strengths similar at low frequencies and d.c., the discharge mechanism is also essentially the same. Here the transit times of the electrons, and even positive ions across the gap, are short compared with the half period of the applied field.

Figure 1 shows that as the first critical frequency fc_1 is approached the amplitude of oscillation of the positive ions is progressively decreased until they are just unable to reach an electrode face during a half-cycle of the field. The consequent existence of positive ions within the gap has been shown[24] to lead to 'enhanced' values of the primary coefficient α . Clearly a relatively smaller field is sufficient to initiate the discharge.

Comparison between the results of different workers, in this range, is not easy, but all adopt explanations in terms of the effect of positive space charge.

Until fairly recently, the experimental data available indicated constancy of sparking potential at frequencies intermediate between low frequencies and fc_1. A publication by Fuchs,[11] however, suggests the gradual rise mentioned earlier. An explanation is given in terms of the behaviour of positive ions. The frequency fc_1 is not unique, but depends upon the nature of the gas and the electrode separation; in many experiments it is observed in the region of a few hundred Kc/s.

The second critical frequency fc_2 is associated with the non-removal of electrons from the test-gap. Under these circumstances the previously dominant agency of electron loss-mobility capture by the electrodes - is no longer operative. Hence breakdown, which may be regarded as due to the failure of equilibrium between rates of electron generation and loss, can therefore be expected to start with a relatively less energetic field.

Several workers,[25,26,27] have confirmed by experiment this lowering of the threshold field value.

The origin of breakdown theory at frequencies exceeding the second transition is rooted in the work of S.C. Brown et al. at the M.I.T. Experimental results on gases confined within a resonant cavity and subjected to microwave oscillations, led to the proposition[28] that breakdown in a non-attaching gas could (subject to certain limiting conditions) be explained simply in terms of electron production by collision ionization, and their loss from the system by diffusive processes.

The total flow of particles from a region of high concentration may be written as

$$J = - D_e \nabla n,$$

Assuming that an external irradiating source is providing a small rate of ionization S in the gap, the continuity equation may be written as

$$\frac{dn}{dt} = \nu_i n + S - \nabla \cdot J$$

$$= \nu_i n + S + D_e \nabla^2 n \quad \ldots \quad \ldots \quad \ldots \quad (5)$$

Equation 5 may be modified to include depopulation by electron attachment to neutral atoms, (leading to recombination in the volume of the gas) by rewriting the equation in the form

$$\frac{dn}{dt} = (\nu_i - \nu_a)\, n + S + D_e \nabla^2 n$$

$$= \nu_n + S + D_e \nabla^2 n \quad \ldots \quad \ldots \quad \ldots \quad (6)$$

ν_a is the rate of attachment and hence

ν_n is the net rate of electron generation.

Assuming that the approach of breakdown is so slow that $\frac{dn}{dt}$ may be neglected, the equation for a non-attaching gas becomes:

$$D_e \nabla^2 n + \nu_i n = - S \quad \ldots \quad \ldots \quad \ldots \quad (7)$$

The solution of equation 7 expresses the electron density n at some arbitary distance x from the median plane between parallel plates of separation d, viz:

$$n = \frac{\frac{4\,S}{\pi} \cos \frac{\pi x}{d}}{D_e (\frac{\pi}{d})^2 - \nu_i} \quad \ldots \quad \ldots \quad \ldots \quad (8)$$

Breakdown may be defined as the condition that the electron density goes to infinity, i.e. it occurs when

$$\nu_i = D_e (\frac{\pi}{d})^2 \quad \ldots \quad \ldots \quad \ldots \quad (9)$$

An alternative way of stating the equilibrium condition is that an electron created in the gap must make one ionizing collision in its mean lifetime, t_D, as limited by diffusion

$$\text{i.e.} \quad \nu_i = \frac{1}{t_D} = \alpha v \quad \ldots \quad \ldots \quad (10)$$

t_D is related to diffusion length and diffusion coefficient by equation (11), viz:

$$t_D = \frac{\Lambda^2}{D_e} \quad \ldots \quad \ldots \quad \ldots \quad \ldots \quad (11)$$

Λ is a convenient quantity, the 'diffusion' length (introduced by McDonald & Brown)[13] which describes the geometry of the discharge chamber.

The solution of Λ^6 for a cylinder of length d and radius R, is

$$\frac{1}{\Lambda^2} = \left(\frac{\pi}{d}\right)^2 + \left(\frac{2.405}{R}\right)^2 \quad \ldots \quad \ldots \quad (12)$$

The first term on the R.H.S. of the equation describes diffusion to the electrodes of a parallel plate system, the second term relates radial diffusion away from the electric field.

From equations 10, 11, and 12:

$$\nu_i = \frac{D_e}{\Lambda^2} = D_e \left[\left(\frac{\pi}{d}\right)^2 + \left(\frac{2.405}{R}\right)^2 \right] \quad \ldots \quad \ldots \quad (13)$$

Comparing equations 9 and 13 it is seen that the threshold expressions for ν_i are identical for large values of R i.e. the simple equation is a special case of the more general expression in which sideways diffusion is taken into account.

Agreement between theory and experiment

Herlin & Brown[28] tested the diffusion theory at microwave frequencies in the pressure range 1 - 1,000 mm. Hg. Good agreement was found between experimental and theoretical values of t within the limiting condition of theory.

Prowse & Clark[29] extended the applicability of the theory into the radio-frequency region. They have shown quantitatively that, if diffusion is the dominant removal mechanism, the curve relating $E\Lambda$ to $p\Lambda$ will be unique for any one gas.

1.4.4 Breakdown under conditions where ν_c is the same order of magnitude as ω.

Changes in discharge behaviour are to be expected when the collision - and field-frequencies are the same order of magnitude. In this region the change takes place between many collisions per oscillation ($\nu_c >> \omega$) and many oscillations per collision ($\omega >> \nu_c$). Using the data introduced in Section

1.3.3, it is seen that since

$$\frac{\nu_a}{\omega} = \frac{10^9 p}{2\pi f}$$

then for $\nu_c = \omega$

$$\frac{p}{f} = \frac{2\pi}{10^9}$$

Hence for a test-gap maintained at a pressure of a few mm.Hg, frequencies of the order of 10^9 c/s. are required to study the transition region.

The rapid advances in microwave techniques during 1939-1945, and particularly the development of high-power cavity magnetrons, extended the available frequency coverage into the desired band; in 1948 S.C. Brown and his colleagues published their first paper[28] on C.W. breakdown at 10,000 Mc/s. As indicated in Section 1.4.3, plots of breakdown field against gas pressure established diffusion as the controlling method of electron loss. But whereas, at the higher pressures used, E decreased regularly with decreasing p (conforming to simple diffusion theory), the fall was not maintained and below a certain pressure E was observed to rise again quite rapidly.

Calculations showed that such minima coincide with the condition $\nu_c = \omega$, confirming predictions that the efficiency of energy transfer from the field falls off when the electrons cease to make many collisions during an oscillation of the field.

1.4.5 Breakdown under conditions where $\nu_c << \omega$.

So far, discharge behaviour has only been reported under circumstances where the gas pressure has exceeded a few mm. Hg. In fact, experimental data, covering an extended range in the low pressure region, are scarce.

Gill and Von Engel[30], however, have made important studies in evacuated glass enclosures, using external parallel-plate electrodes and a variable frequency supply. Breakdown under these conditions is attributed to a type of electron resonance, brought about by secondary emission from the glass walls of the tube.

At the low pressures involved ($\sim 10^{-3}$ mm.Hg.) electron motion under the influence of the external field is not impeded to any significant extent by collisions with gas molecules. The build-up of population requires that electrons leave one wall with favourable velocity in a suitable phase with the field, traverse the gap in a half-cycle and strike the opposite wall with sufficient energy to cause the near-instantaneous release

of further electrons by secondary emission. (These secondary particles may in turn be returned to the original face thereby causing the release of further electrons). Hence, provided that the effective secondary emission coefficient δ exceeds unity, a regular build-up will take place culminating in breakdown. For the glass vessel involved, impact velocities of 40 e.v. are necessary to give unit emission coefficient δ .

The experimentally observed values of break-down field were plotted as a function of wavelength. For a tube of give size the breakdown field was observed initially to decrease with increasing λ . Further increase in λ was found to cause an abrupt out-off, following a region of fairly constant field.

Gill and Von Engel have based their quantitative study upon equations derived from the motion of electrons in vacuo, namely:

$$v_i = v_o + \frac{2e E_p \cos \phi}{m \omega} \quad \ldots \quad \ldots \quad \ldots \quad (14)$$

and $$d = \left(v_o + \frac{e E_p}{m \omega} \cos \phi\right) \frac{\pi}{\omega} + \frac{2e E_p}{m\omega^2} \sin \phi \ \ldots \quad (15)$$

where v_i is the impact velocity, and v_o the initial velocity

of an electron moving with favourable phase ϕ in the field. A constant relationship between ν_i and ν_o was assumed, and by assigning a suitable value to their ratio (obtained by trial and error), a theoretical curve was obtained and found to conform closely to the experimental plot.

2. INTRODUCTION TO THE BREAKDOWN STUDIES AT 10 Mc/s. and 20 Mc/s.

2.1 Radio-frequency breakdown at pressures exceeding a few mm. Hg.

In discussing a.c. breakdown in gases (Chapter 1), theories concerning the starting of a discharge were categorised in terms of the efficiency of energy transfer between the source of electrical power and the charged particles present in the gas.

On the other hand, breakdown under prescribed experimental conditions may sometimes be conveniently studied by investigating the applicability of the diffusion theory to the results obtained, experience showing that in this way any departures from the theory are more readily made explainable. Thus, Prowse and Clark[29] investigated the onset of electrical discharges in a variety of gases, both monatomic and diatomic, attaching and non-attaching, with a view to establishing the mechanism of breakdown. Only relatively high pressures were employed, (beyond a few mm. Hg.).

Previous to these studies, considerable doubt existed as to the nature of such discharges under such conditions that electrons both oscillated between the electrode faces

during a half-cycle of the field, and made many collisions per oscillation ($\nu_c >> \omega$). Data from the work of Pim[31], and Prowse and Lane[25], for example, indicate that the starting field for a gas at a given pressure is independent of the electrode separation; the view was taken, therefore, that breakdown stress is a constant quantity, characteristic of the pressure and nature of the gas in question. These results were, however, not in accord with other measurements, notably by Githens[26] and Thompson[27]. In these cases the results were consistent with a diffusion-controlled build-up of electron population.

By quantitative analysis, Prowse and Clark were able to demonstrate that in a gas at constant pressure, breakdown over a wide range of electrode geometries can be brought about by the application of a high frequency field whose magnitude is sufficient to promote a rate of collision ionization just in excess of the losses from the system by diffusion.

The conclusions reached regarding the inconsistencies referred to, were that they could be attributed to the use of undesirable electrode shapes, and, possibly, impure gases.

2. Breakdown Curves for Various Gases, Prowse & Clark (1958)
Breakdown Field as a function of Gap Width

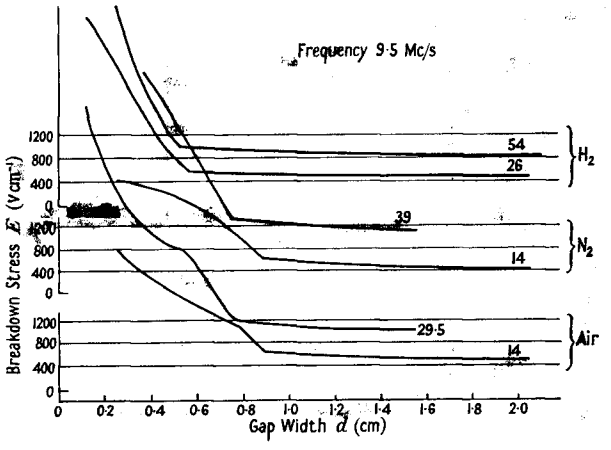

2.2 Results of Prowse and Clark at 9.5 Mc/s.

Typical experimental runs at fixed pressures in hydrogen, nitrogen and air are illustrated in Figure 2, with peak breakdown stress plotted against electrode separation. It is seen that each curve is characterised by two distinct regions. For short gaps E_p decreases rapidly with increasing d. However, beyond a certain value of d (determined by the gas pressure) further increase in electrode separation is associated with a small but steady lowering of field strength.

Diffusion theory was found to apply in the less steep parts of the curves. In these regions electrons oscillate to and fro within the test gap, their lifetime limited by the time taken to diffuse either to the electrodes or radially out of the intense field region. Further, the electrons oscillate in phase with the field since $\nu_c >> \omega$ even at the lowest pressures used.

The initiation process on the steep parts of the curve is not dominated by diffusion losses. Bearing in mind that electron oscillation amplitude is determined by gas pressure, field-frequency and field strength - and not by gap width - a steady reduction in d from a high value (with E_p changing only slowly) must result in a critical separation d_c below

which the electrons are able to span the electrodes, during a half-period of the field, by mobility motion i.e. the transition values of d correspond to the second transition region referred to in Section 1.4.3. The increases in field strength required to start the discharge for values of $d < d_c$ are evidence of the necessity for increased field-intensified ionization to counterbalance the increased rate of loss due to capture by the electrodes.

It is thus seen that the magnitude of the breakdown field under diffusion controlled conditions in 'high-pressure' gases at short-wave frequencies is characterised by:

(a) a sharp rise, whenever limiting conditions are such that electrons reach the electrodes by oscillatory drift.

(b) a slow but steady decrease, for increased electrode separation at fixed gas pressures.

(c) a decrease, whenever pressure is reduced at constant electrode separation.

2.3. Measurements at somewhat lower pressures

Having established the ability of a diffusive mechanism to operate at radio-frequencies as well as in the micro-wave region, further measurements were made by Clark[32] at

3. Breakdown in Hydrogen at 9.5 kc/s. Clark (1957)
Breakdown Stress as a function of Gas Pressure

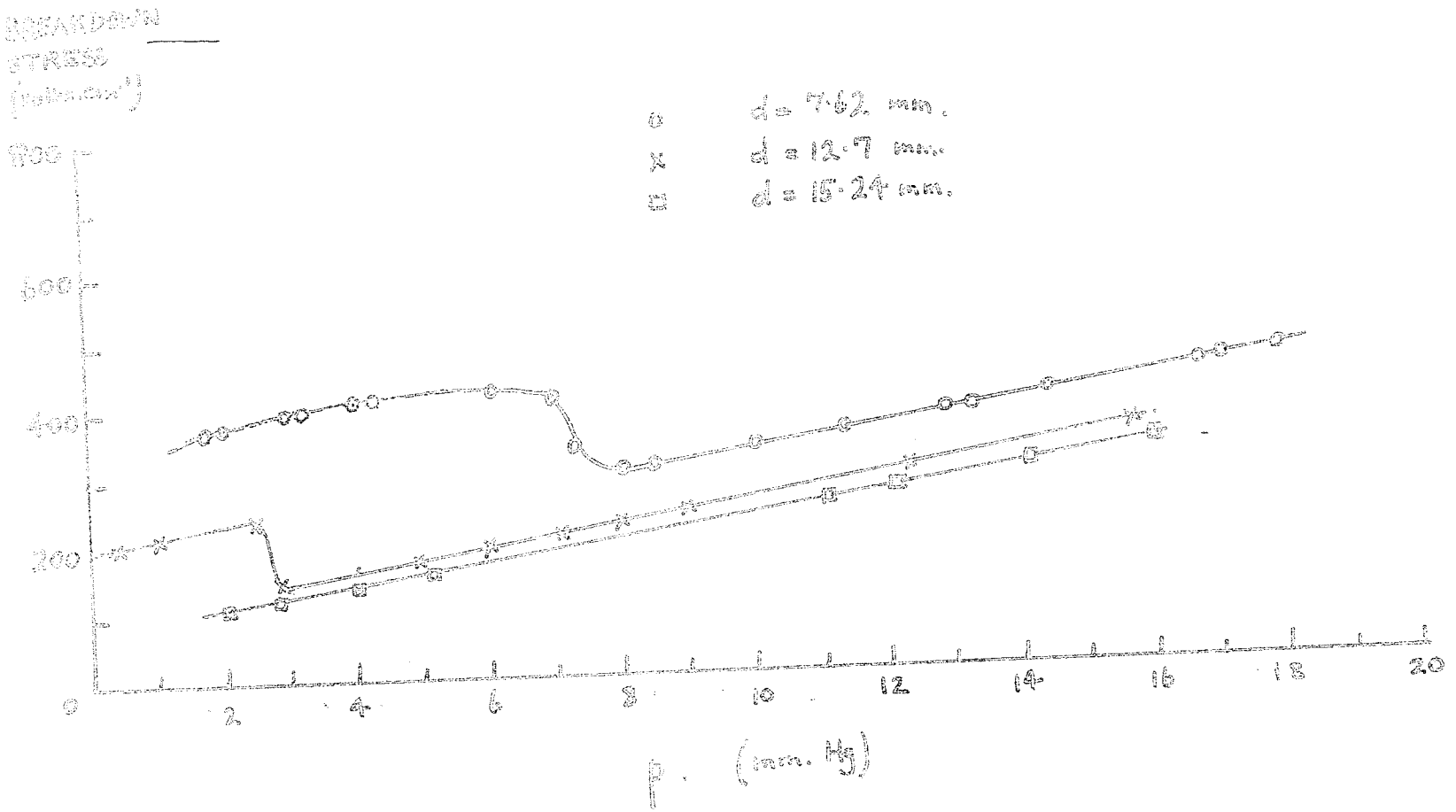

somewhat lower pressures, to enable calculations to be made of ionizing efficiencies over an extended range of E/p. Typical plots are shown in Figure 3, for hydrogen.

Calculations show that for the two smallest separations, 5.08 and 7.62 mm. electrons were able to reach the electrodes by mobility drift for all pressures used. For gap widths 10.16 → 15.24 mm, the transition to diffusion controlled breakdown is clearly indicated, at pressures ranging from 2 → 6 mm. H.g. (the 'critical pressures' p_c correspond to the critical gaps d_c in Figure 2). But, at the largest separations, 20 → 32 mm., the onset field shows a continuous decrease down to the lowest pressures used. This run in particular was considered to be of great interest. Values of breakdown field recorded were lower than any hitherto published under uniform field conditions and were significantly smaller than those obtained at micro-wave frequencies. However, no firm interpretations could be made regarding the significance of the measurements, for two reasons. Firstly, the pressure-measuring device used for the lowest pressures was a simple differential gauge, linear scale, which did not permit recordings below about 0.3 mm. Hg. Further, the accuracy of the instrument below 5 mm.Hg. was questionable. Secondly, the voltage-

measuring system, based upon square-law detection, though quite suitable for measuring voltages in excess of 200 volts, was inherently insensitive for values below this figure.

Thus, only tentative suggestions may be made regarding an explanation of why the starting field can be driven lower down at radio-frequencies compared with micro-wave values.

Analysis by McDonald and Brown[13] shows (Section 1.4.4) that the collision-frequency transition using micro-wave sources occurs at pressure values about two orders higher than at short-wave radio-frequencies. Breakdown at pressurss below the transition value is characterised by a rise in onset field values. Hence, given a system at radio-frequencies, in which the electrode separation is large enough to enable electrons to oscillate within the gap, diffusion control of electron loss, with inherent ease of starting a discharge, should be expected to operate at lower pressures than is possible under microwave conditions.

Such an explanation could not be tested from Clark's measurements for the reasons described. Also, it was far from certain that the rates of electron multiplication and loss continued to be dominated by collision ionization and diffusion, respectively, under the conditions of fairly low pressure and

wide electrode spacing; the possibility of other mechanism becoming active could not be ignored.

2.4 The experimental problem - breakdown at radio-frequencies under low pressure conditions.

In view of the uncertainties with regard to the physical processes involved it was decided to make a systematic investigation of the breakdown of relatively large gaps in the radio-frequency region, using pure gases at pressures less than 1 mm.H.g., with sensitive and accurate equipment to measure the parameters involved. Also, it was considered that measurements involving extremely low values of breakdown stress under uniform field conditions would be of some teahnical interest. One example of this was the failure of radio signals from high-altitude rockets which led PasKa[33] to study low pressure breakdown in air at 77 Mc/s. Interesting results were obtained, including lownumerical values of starting field. However, to simulate the transmitting antenna of a rocket, concentric cylinder geometry was used, giving radial non-uniformity of electric field and undesirable edge effects. Also, from the physicist's point of view, air is not the simplest gas from which to make deductions regarding fundamental processes.

The apparatus described in Chapter 3 was designed and constructed to meet the requirements previously discussed.

4. Schematic Diagram of Apparatus

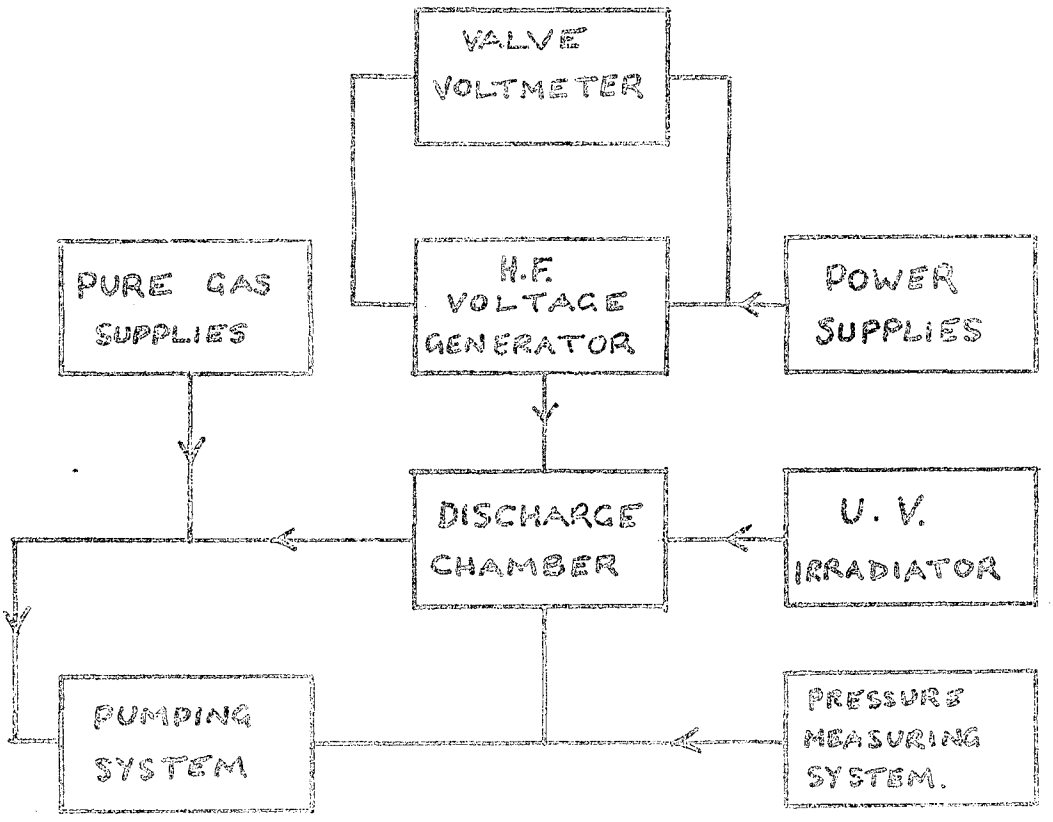

3. APPARATUS

3.1 Basic Requirements

The essential requirements of the apparatus were as follows:

(i) A glass discharge chamber surrounding (but sufficiently remote from) a pair of uniform field electrodes, and containing the gas under test.

(ii) A high frequency voltage source of given frequency and variable, but known amplitude, having sufficient strength to break down the gas.

(iii)A vacuum system capable of pumping down the test line to low pressures, maintaining a given pressure under static conditions and provided with pressure measuring equipment.

(iv) A supply of spectrally pure gases, with facility for pipetting test samples into the main vacuum line and thence into the discharge chamber.

(v) A steady supply of initiatory electrons, to reduce statistical time-lags.

The variable quantities involved included:

Gas Pressure,

5. Discharge Chamber and Accessories

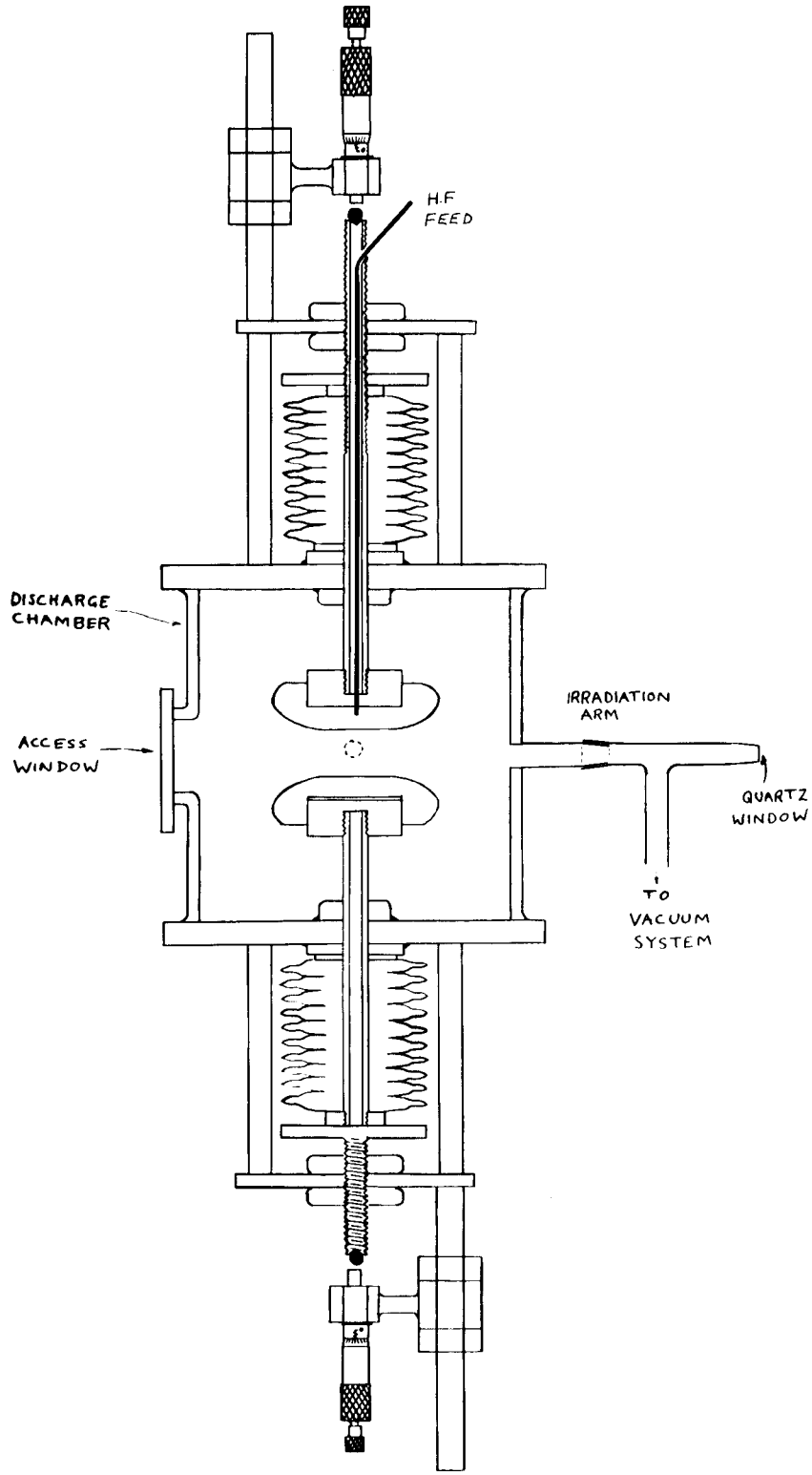

Electrode Separation,

Field frequency,

Field Strength.

Care was taken in design to allow the adequate variation of these quantities and to measure them with accuracy.

A schematic diagram of the apparatus is shown in Figure 4.

3.2 The Discharge Chamber

3.2.1 Constructional Details

Design details of the chamber and its accessories are given in Figure 5. The vessel was made to specification at the Wear Glass Works, from 17.8 cm. (I.D.) Pyrex pipeline 17.8 cm. in length with wall thickness 4.7 mm. The open ends of the chamber were made parallel and accurately ground.

Two short arms with B.19 cones were set at right-angles in the centre of the chamber. By making connection from both these points to the pumping and gas-injection systems, continuous circulation of gas was ensured in dynamic working. One of these arms also acted as the path for the ultra-violet irradiating beam. In addition, two 10 cm. diameter windows provided easy access to the interior of the chamber for the purposes of assembling and aligning the electrodes. During

the pumping process these windows were sealed with 4.7 mm. thick ground glass cover plates, lightly smeared with Apeizon 'N' high vacuum grease.

The ends of the chamber were closed by mild steel plates, accurately turned and ground. Metal-to-glass seals were made with Araldite 103 Epoxy Resin, to give vacuum-tight unions. These remained leak-free for the whole period during which measurements were taken.

To permit variation of electrode separation without disturbing vacuum conditions, 1.27 cm. diameter brass tubes were set into the backs of the electrodes and passed out of the chamber through brass bushes sealed to the end-plates, into specially constructed vacuum bellows.

The bellows, constructed to specification by Negretti and Zambra Ltd., each consisted of a stack of 10 capsules made from reinforced heat-hardened beryllium-copper. Collars fitted to the ends of the stacks enabled the electrode rods to be securely connected to the bellows. Each pair of bellows, of diameter 7.4 cm., had a maximum working deflection of 3.5 cm. giving rise to a maximum electrode separation of 7 cm.

3.2.2 Variation and Measurement of Electrode Separation

The distance between electrodes was varied by screwing

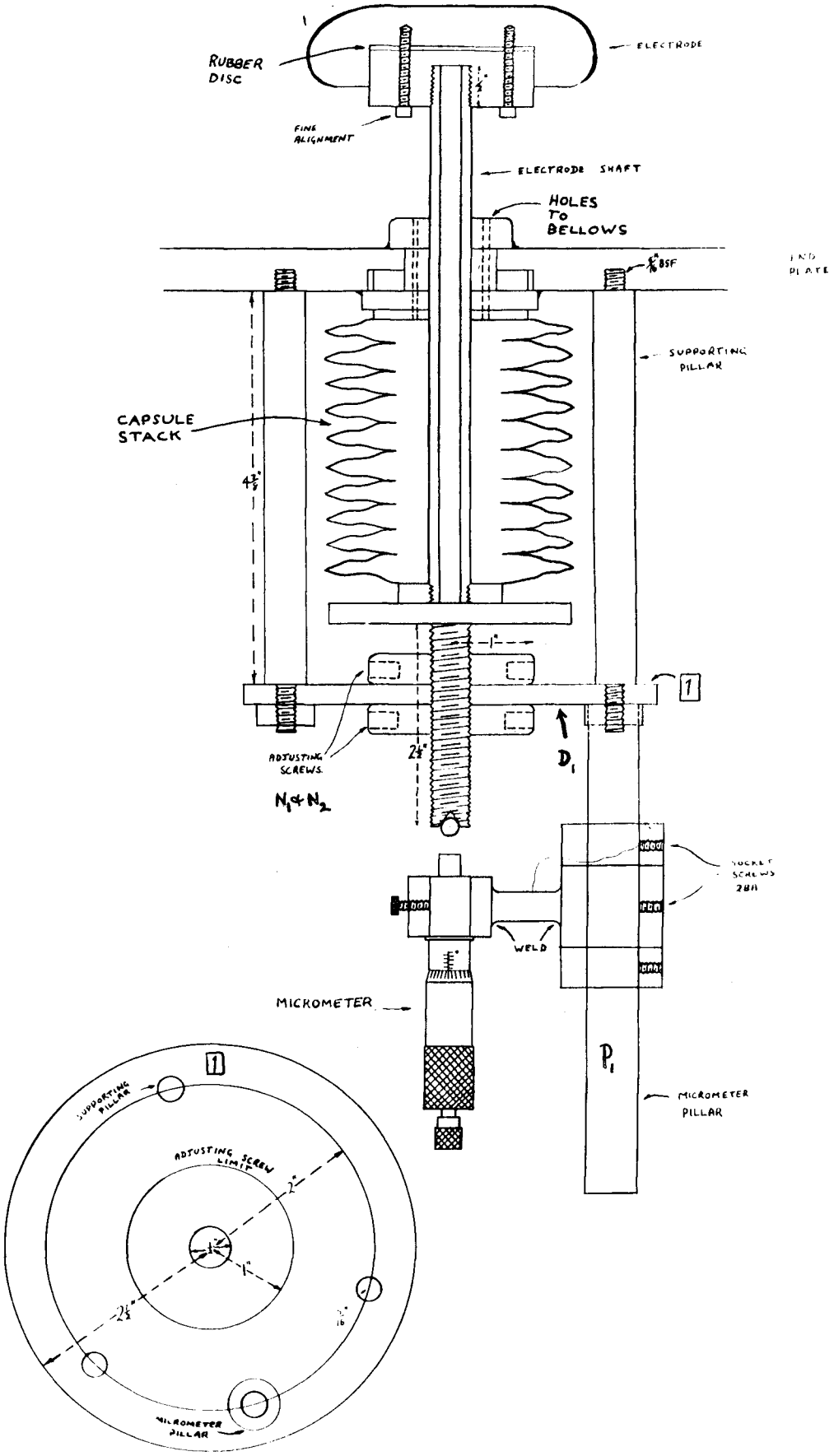
RUBBER DISC
ELECTRODE
FINE ALIGNMENT
ELECTRODE SHAFT
HOLES TO BELLOWS
END PLATE
SUPPORTING PILLAR
CAPSULE STACK
ADJUSTING SCREWS
N_1 & N_2
D_1
SOCKET SCREWS
WELD
MICROMETER
P_1
MICROMETER PILLAR
SUPPORTING PILLAR
ADJUSTING SCREW LIMIT
MICROMETER PILLAR

6. Electrode System & Bellows

(a) Upper Electrode

(b) Lower Electrode

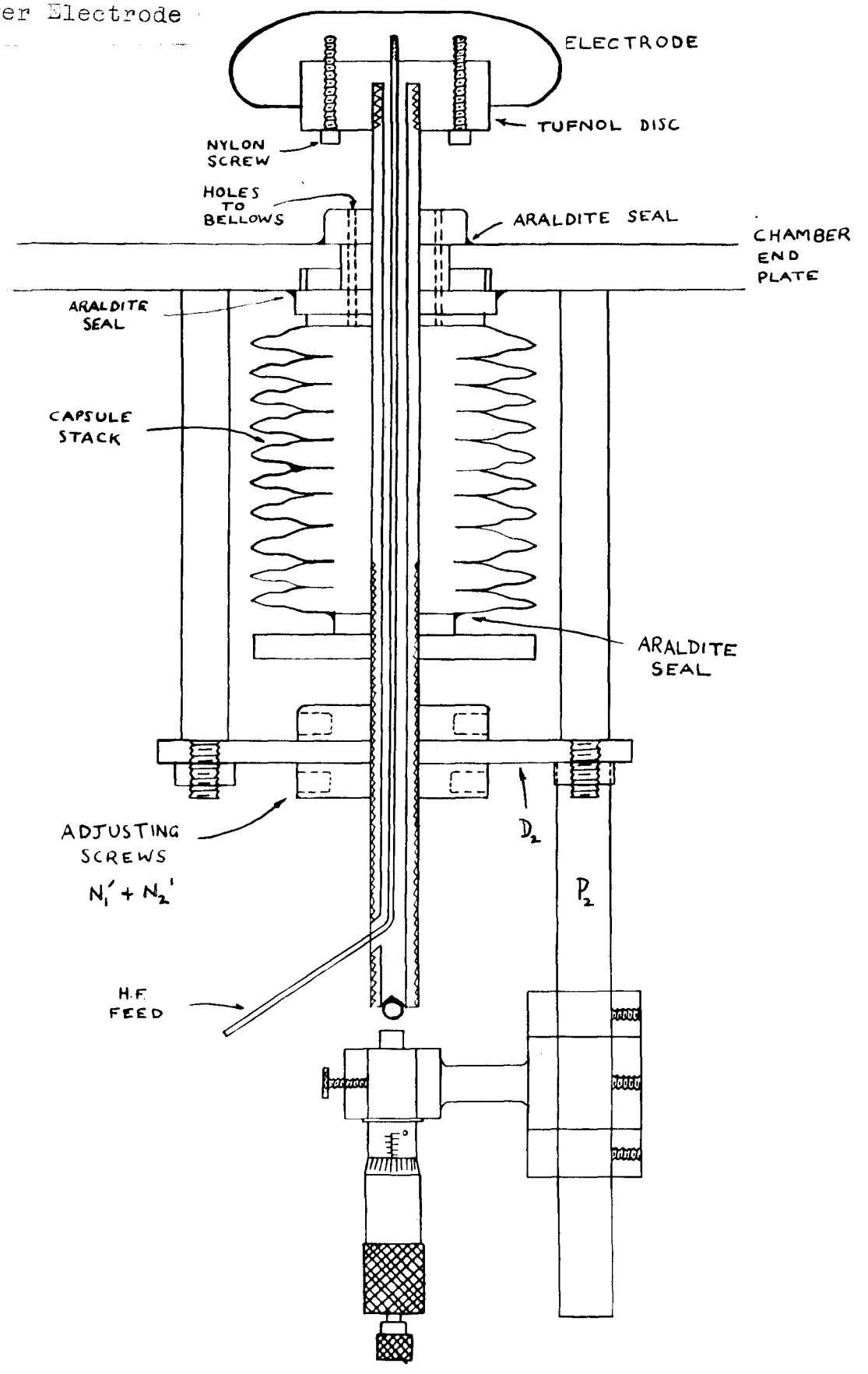

the two pairs of large bevelled nuts (N_1 N_2 and N_1' N_2') on the electrode shafts against fixed mild steel discs (D_1 and D_2) causing the bellows to be expanded or contracted and hence the electrode spacing to be varied.

Figures 6a and 6b show the micrometer screw gauges used to monitor electrode separation. These gauges were fixed by horizontal arms to rigid vertical pillars (P_1 and P_2) and could be swung away by releasing the screwed collars on P_1 and P_2. The micrometers were referred to steel balls sealed into 90° countersinkings at the ends of the electrode shafts. Zero separation was determined electrically using a d.c. voltage source, current limiting resistor and a milliammeter.

It was appreciated that any attempt to isolate the interiors of the bellows from the main chamber would fail due to leakage down the outer walls of the electrode shafts. To avoid this difficulty, a series 0.8 mm. holes was drilled through the brass bushes into the interiors of the bellows, giving pressure equalization.

3.2.3 Electrode Profiling: Stephenson Profile

(a) Importance of correct profiling

The usefulness of much breakdown data has been lessened by the choice of undesirable electrode shapes, particularly

plane-parallel discs. Whilst the existence of inherent field intensification at the electrode edges has been realized, several workers have concluded that since such discharges are commonly observed within the uniform central region, they were initiated there. More recently, evidence strongly suggests[34] that the locality in which a discharge is initiated cannot be readily deduced from the position of a sustained discharge.

The ideal uniform field electrode system would consist of a pair of infinite parallel plates. In 1926 Rogowski[35] demonstrated mathematically that electrodes of finite size may be suitably shaped to fulfil the condition that electric field strength is nowhere greater than in the central uniform field region. Such electrodes have frequently been used : electrolytic tank tests confirm a gradual decrease in field intensity away from the centre.

From a purely empirical approach Stephenson[36] has derived electrode profiles which fulfil the same conditions as Rogowski profiles but which have the advantage that they are simpler to construct geometrically. In addition, the Stephenson profile offers, per unit area of the electrode, a greater constant field region than the Rogowski envelope. In essence, the Stephenson profile has a plane central region, leading to a section which

7. Stephenson Profile

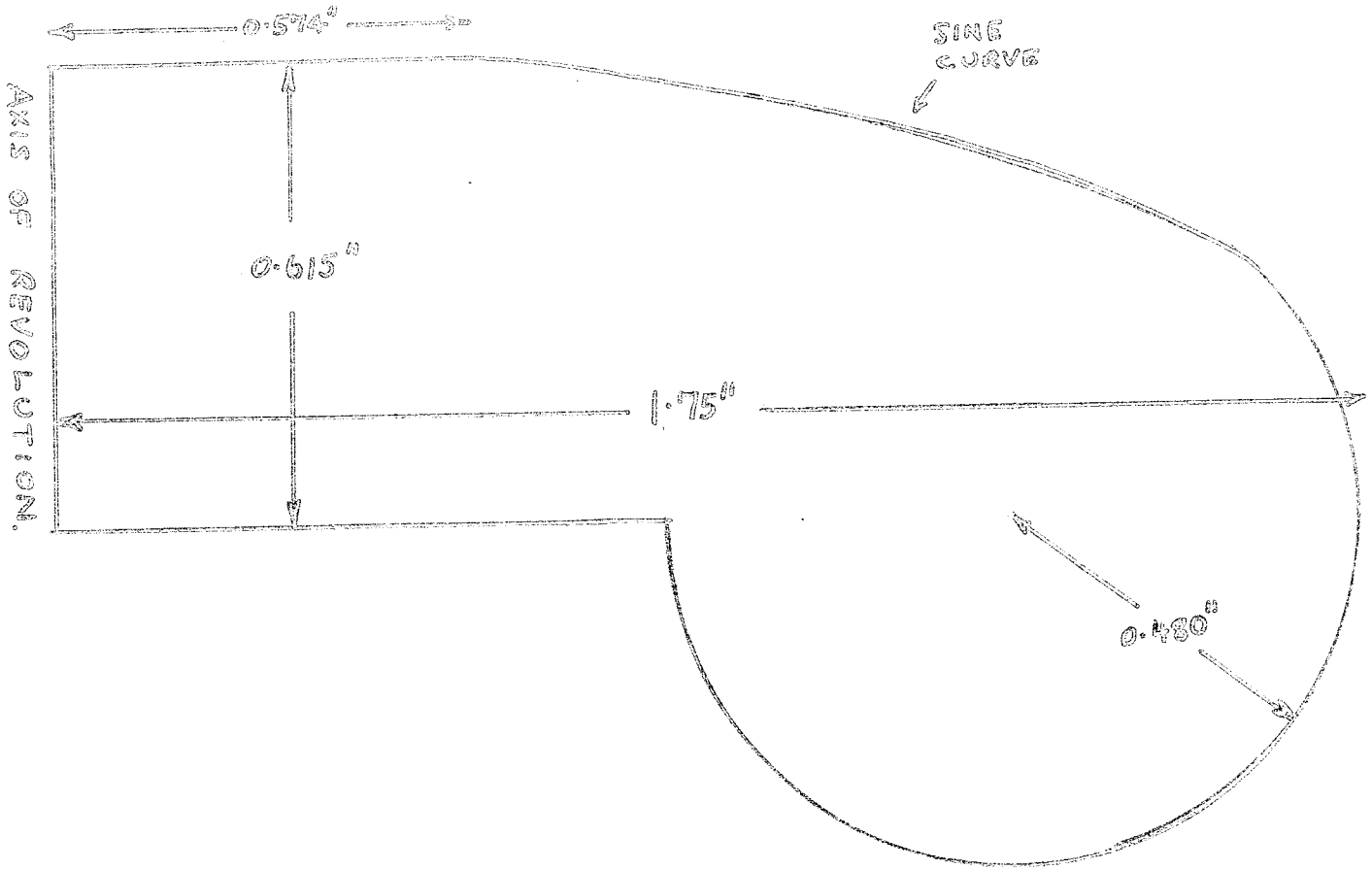

follows a sine curve and culminates in an arc of a circle.

The shape and dimensions of the adopted Stephenson profile are shown in Figure 7.

(b) Choice of Electrode Material : Profiling

At the time of construction of the apparatus it was not believed that the physical properties of the electrode surfaces would have any important effect upon the initiation of discharges - in most cases of high-frequency breakdown the electrodes serve only to stress the gas and limit the extent of the discharge.

Brass was, therefore, selected, largely because of the ease with which it could be turned and ground.

This choice was later a source of trouble because secondary emission from the electrode faces became an important part of the breakdown mechanism at 20 Mc/s and no data are available for secondary emission from brasses.

A tinplate former of half an electrode profile was constructed. Cylinders of brass were turned in the lathe until their profiles roughly corresponded to the former.

An accurate curve representing the desired profile envelope (magnified ten times) was drawn on a screen. Optical means were used whereby a parallel beam of light from a small

intense source (passed through a good quality condenser lens) projected an image of the rough profile on to the screen (via another lens), Very careful alignment was made of the source, lenses, electrodes and screen.

The electrode in the lathe was carefully filed until the projected image corresponded more closely to the accurately drawn profile on the screen. Final accuracy (limited by the diffraction edge of the light beam) was obtained by a series of grinding materials. Firstly, emery paper of varying grades, followed in turn by optical grinding paste and finally metal polish until the projected profile corresponded to the master profile. The electrodes were cleaned using carbon tetrachloride, acetone, and finally distilled water, before being carefully dried.

3.2.4 Attachment of Electrodes

A 'tufnol' disc was sunk into a recess at the back of the upper electrode (Figure 6a) and fixed with nylon screws. The disc was internally tapped to accommodate the electrode shaft. Figure also shows that the disc and the back of the electrode were drilled and tapped for the 16 S.W.G. copper wire used to feed the high frequency supply to the electrode.

Care was taken to ensure that the feed wire was coaxial

with the electrode shaft, though as an added precaution against a possible short circuit, a hollow P.V.C. tube was inserted between the wire and the inner wall of the shaft. The remaining space contained air at atmospheric pressure. A vacuum seal of epoxy resin was used (around the tufnol disc) to prevent leakage of air into the discharge chamber. The possibility of electrical breakdown between wire and shaft was most unlikely. For geometries similar to these employed, a voltage of between 20-30KV is required to initiate a discharge at atmospheric pressure, many times in excess of the maximum value used. Breakdown between coaxial cylinders under A.C. conditions has been studied by Uhlmann[46a].

The attachment of the lower electrode is shown in Figure 6b. A brass disc was fixed, by Allen screws, into the drilled hole in the back of this electrode. A 1/40 cm. rubber disc was fitted between the brass disc and the electrode (with suitable holes for the passage of the fixing screws) so that the electrodes could be accurately aligned horizontally, when the final assembly was made. This was done by using the fixing screws as adjusting screws, the rubber disc permitting a small amount of angular rotation. Electrical connection between this electrode and the earthed side of the supply was made by external

8. Vacuum System

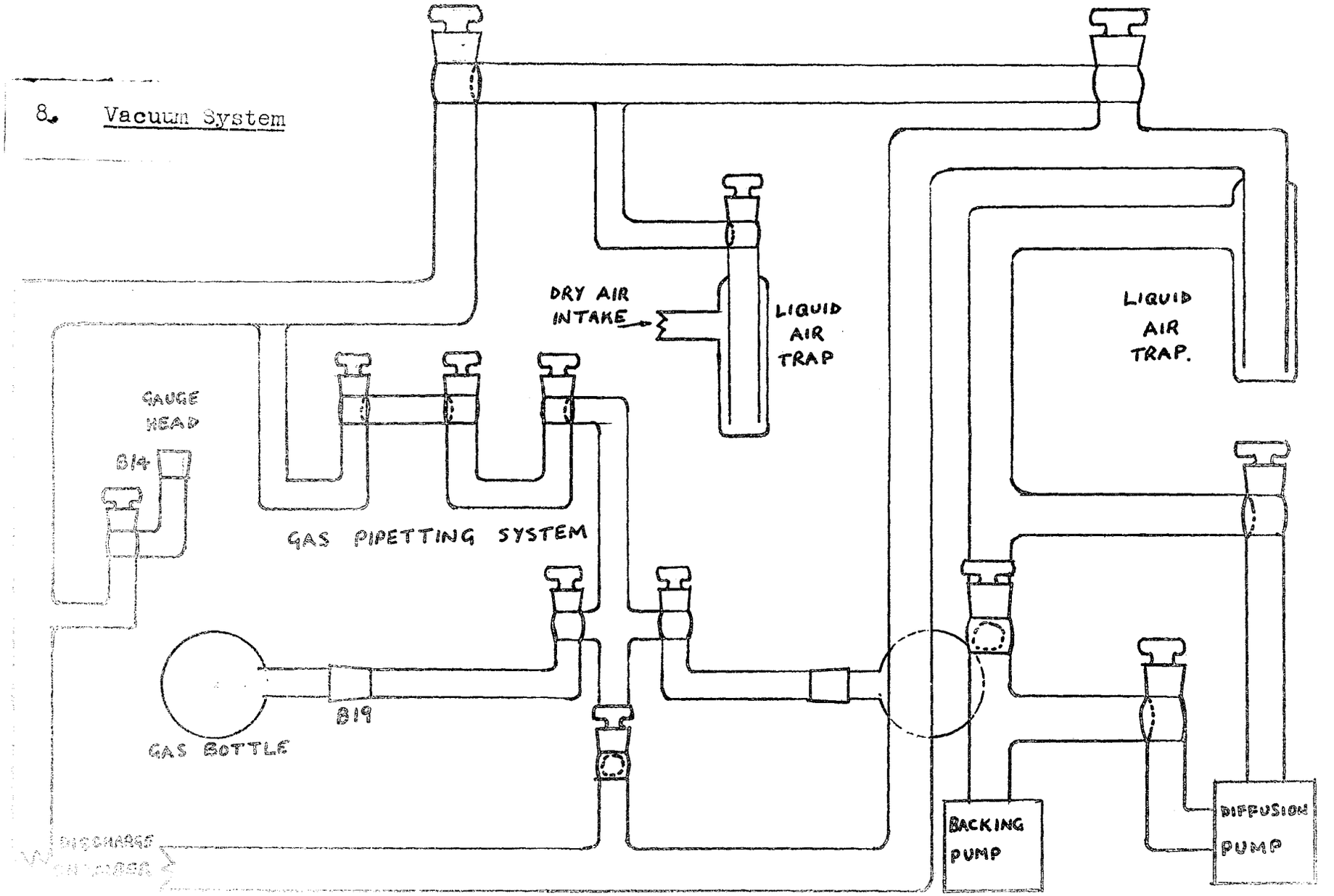

connection to the electrode shaft.

3.2.5 Alignment

The two end plates were drilled together to ensure that the electrode shafts and hence the electrodes themselves would be aligned vertically after final assembly.

Since the two central 10 cm. windows in the chamber were at right-angles to one another, a straightforward optical method of checking the electrode alignment was possible, using a cathetometer mounted in turn in front of each window. Only a fractional adjustment to the alignment was found necessary.

3.3 The Vacuum System : Pressure Measurement

3.3.1 General Features

Figure 8 shows the final design of the system.

The main vacuum lines were constructed from 20 mm. Pyrex tubing, ensuring rapid throughput when outgassing the system. Continuous circulation of the gas was ensured by the inclusion of an inlet and an outlet arm in the centre of the discharge chamber.

Permanent ground joints and metal-to-glass unions from the pumps to the glass vacuum line were sealed with Apiezon wax. 20 mm. bore high-vacuum stopcocks were used on the main vacuum line; otherwise 10 mm. bore stopcocks were incorporated.

Both types were fitted with sealed hollow plugs. Any section of the system could be isolated; all taps were readily accessible.

Initial pressure reduction was obtained using an Edward's "Speedivac" rotary oil pump, and the high vacuum from an air-cooled two-stage "Speedivac" silicone oil diffusion pump, fitted with an isolation baffle.

Various methods were used to remove occluded gases from the walls of the system:

(a) by wrapping "Electrothermal" heating tapes round the walls of the system.

Using energy regulators a temperature of 325°C was obtainable, which is the optimum temperature for the removal of occluded gas from Pyrex glass.

Temperatures were measured using thermocouples and a calibrated galvanometer.

(b) by running a 'Tesla' coil along the glass walls of the system.

(c) the electrodes were cleaned by applying a glow discharge between them at regular intervals.

(d) a liquid air trap was inserted between the pumps and the main vacuum line.

(e) a phosphorous pentoxide trap was placed in the vacuum line,

situated on top of the backing pump.

It was found that an ultimate pressure of less than 10^{-4} mm.Hg. was obtainable. No observable change in pressure occured during breakdown measurement, with the discharge chamber isolated from the pumping system.

3.3.2 Gas supplies

Samples of spectroscopically pure gases were obtained from B.O.C. Ltd. in 1 litre flasks. The flasks were fitted to the system using B 19 cones. The seals were broken magnetically when required.

Small quantities of gas were introduced into the system via the pipetting line shown in Figure 8.

The whole system was regularly flushed with samples of gas to assist purification, particularly when a change of gas was in process.

Doubt as to the purity of the neon samples is discussed in Chapter 6.

3.3.3 Pressure measurement

During all experimental runs an Edwards Pirani Gauge was used (GS/2) fitted with two gauge-heads. Gas pressure in the discharge vessel was monitored by one head sited near the chamber (Figure 8). The second head, fixed above the diffusion

pump, was used simply as an indicator and safety check.

Accurate measurements were possible in the range 0.0001 mm. Hg. to 0.1 mm.Hg. Measurements were also possible between 0.1 mm. Hg. and 1 mm. Hg. but no great accuracy could be claimed in this region due to scale cramping.

Calibration of the gauge was carried out by the manufacturers for dry air; corresponding pressures for other gases were obtained by reference to calibration curves provided. The calibration was checked in the laboratory using a McLeod gauge.

3.4 The High-Frequency Voltage Generator

3.4.1 General Description

Basically the requirement of the generator was to provide a stable source of alternating voltage with low harmonic content across the test gap, with facility for varying and measuring the amplitude and frequency of the supply.

Several designs were considered. It was finally decided to base the generator upon a crystal-controlled master oscillator. It was felt that the disadvantage of being restricted in frequency coverage (to the fundamental and one or two harmonics) was overshadowed by the advantages of such a system i.e. purity of waveform, frequency stability over

9. R.F. Voltage Generator. Crystal Oscillator and Driver Circuit

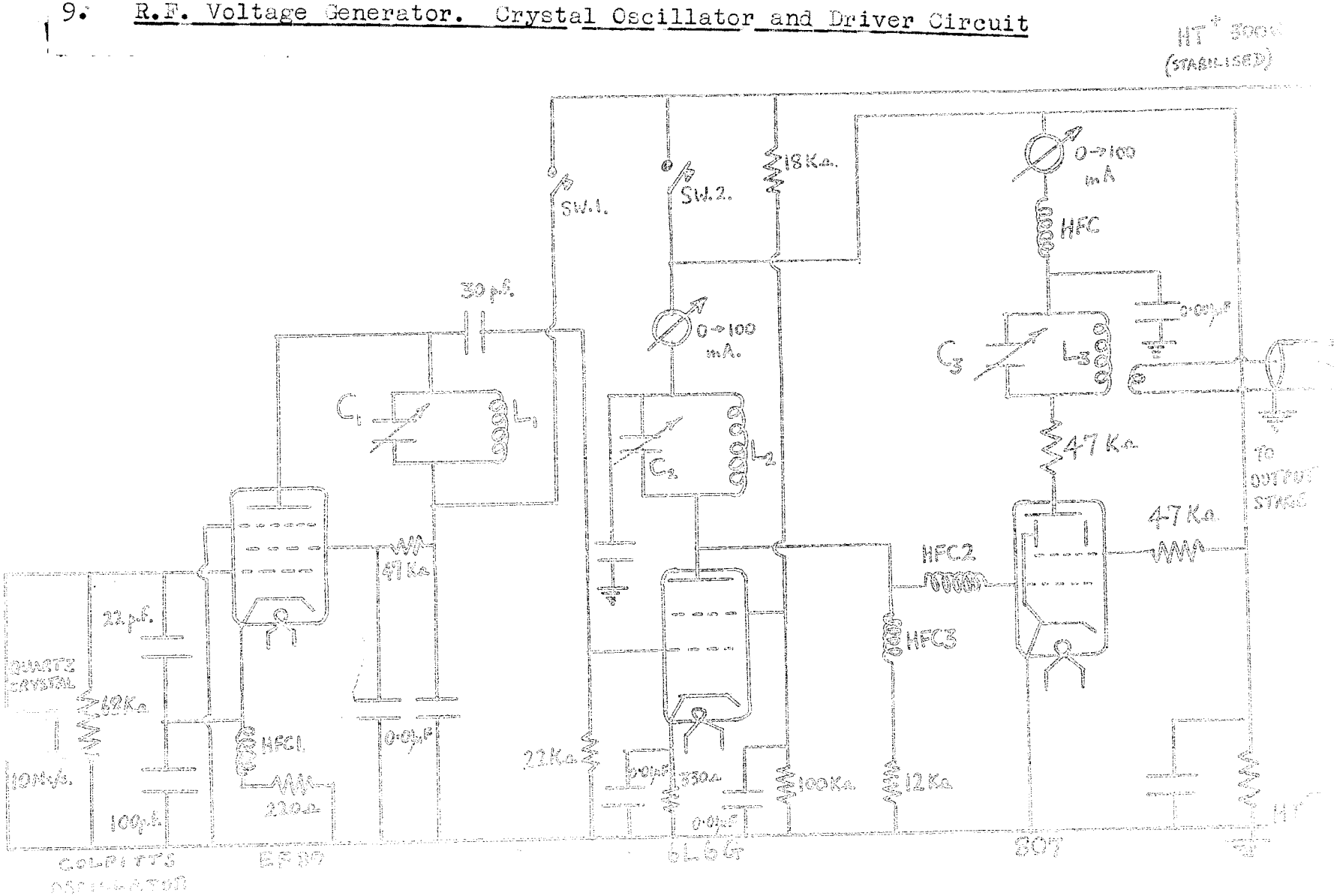

10. R.F. Voltage Generator. Power Amplifier

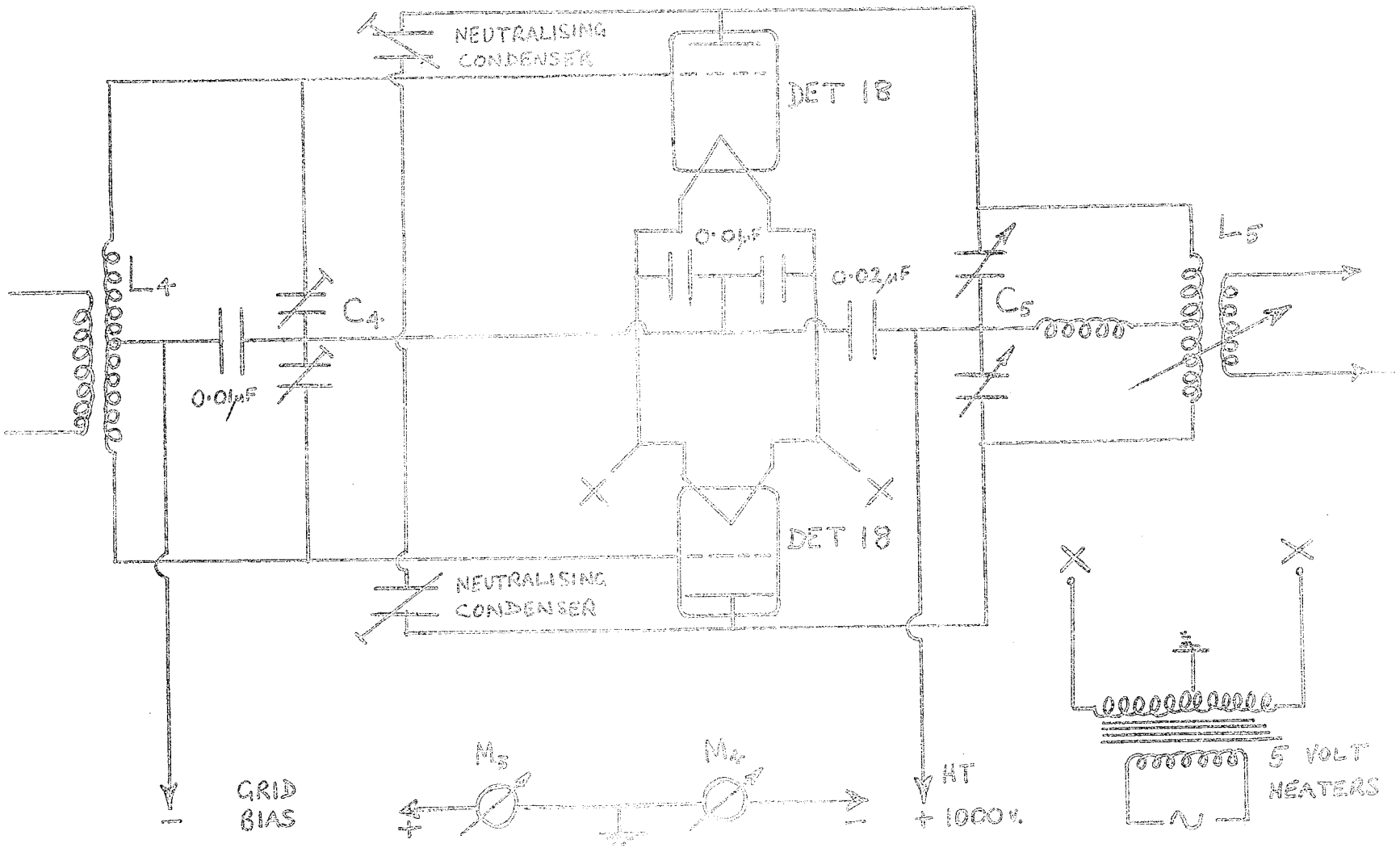

large time intervals and when subjected to varying loads, and less complicated tuning circuits.

A schematic diagram of the generator is shown in Figures 9 and 10. The master oscillator stage, based upon a 10 Mc/s quartz crystal in an evacuated mount and an EF 80 valve, was designed as a Colpitts harmonic oscillator with reference to the preferred circuit suggested by the Quartz Crystal Co.Ltd. A high-Q tuned anode load ensured selective high gain at the fundamental frequency. In addition, three other pre-set coils were available for switching across C_1. By suitably tuning C_1 the parallel circuit could be made to resonate additionally at the second, third and fourth harmonics of the crystal i.e. 20 Mc/s, 30 Mc/s and 40 Mc/s.

By means of R-C coupling the output was fed to the buffer-amplifier. Using this stage, fall-off in amplification due to the Miller effect was minimised. Selective gain at the fundamental or desired harmonic was again effected using tuned-circuit elements, as described above.

Stage three, employing an 807 valve, performed essentially as a driver circuit to feed the final power stage. Transformer coupling was used to transfer the output to the final stage of the generator. Coaxial feed prevented the appearance of unwanted

signals.

The power amplifier used two DET 18 high-frequency triodes, working in linear push-pull operation. Neutralisation by way of preset capacitors linking the anode and grid circuits prevented instability and the risk of parasitic oscillation. A high-Q tuned circuit linking the anodes was used to combine the a.c. outputs of the valves.

Standard de-coupling techniques were employed in all stages to guard against circuit instabilities. Each stage was suitably shielded and screened heater leads were used to all valves. Anode currents were monitored for ease of generator tuning.

The early stages were supplied by a 300 v. stabilised power supply unit. A similar source provided negative bias to the grids of the power valves. E.H.T. for this stage was drawn from a 1200 v. power supply unit, employing metal rectifiers and π -type smoothing filter. Anode voltage was varied by adjustment of the mains input to the E.H.T. unit, using a 'Variac' in the primary circuit of the input transformer.

Oscillations developed across the tuned circuit of the power stage were fed by way of magnetic coupling to the test circuit, as described below.

11. R.F. Voltage Generator. Output Circuit

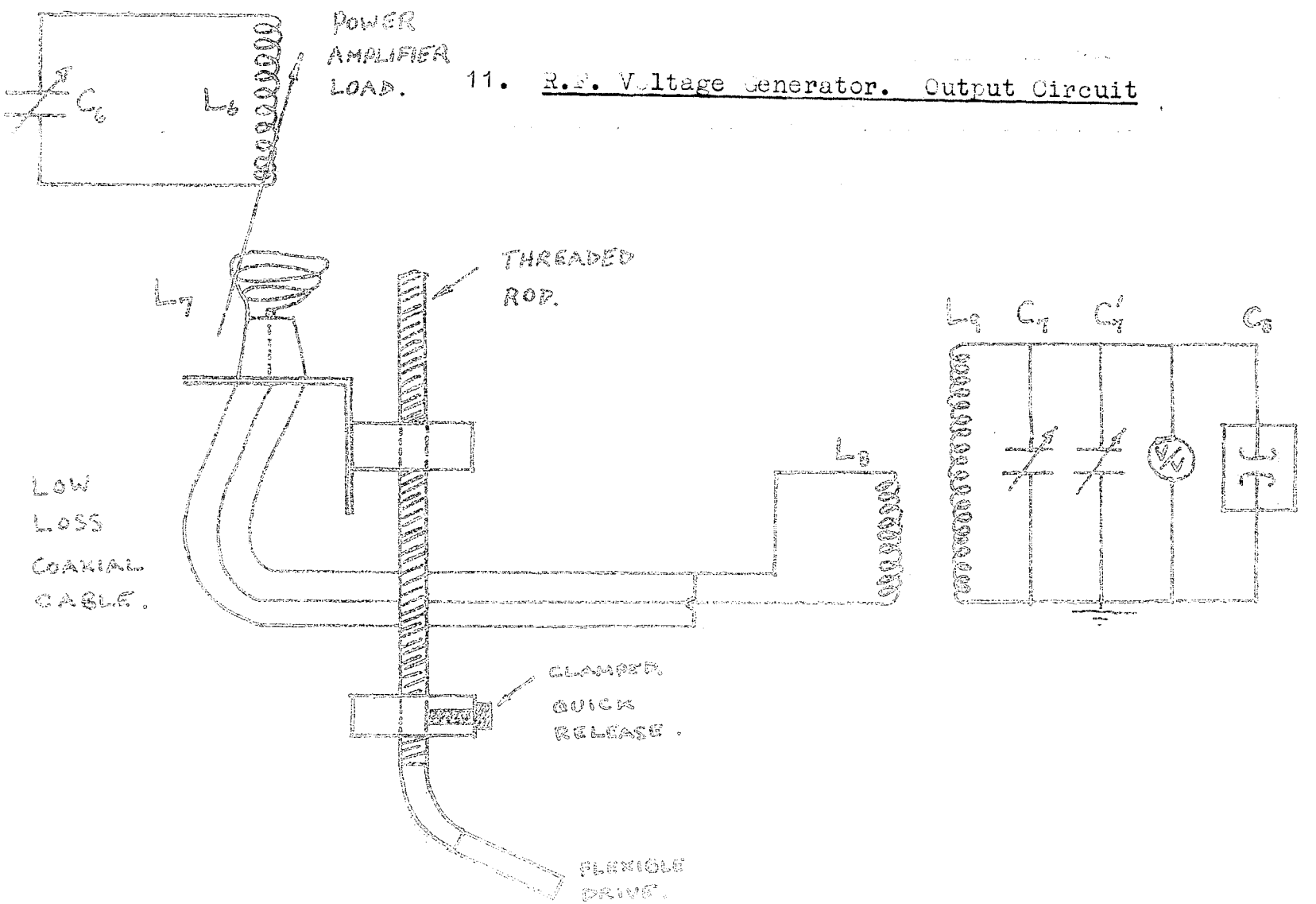

3.4.2 Oscillator output circuit

The circuit by which h.f. voltage of variable strength was made available to the electrodes, is shown in Figure 11.

L_6C_6 represent the output tuned elements of the power amplifier. Coil L_6 plugged into a low-loss ceramic former attached to the front panel of the generator (see photograph). A magnetic coupling coil L_7 was situated coaxially with respect to L_6 and beneath it. Variation of the distance between L_6 and L_7, and hence of their mutual inductance, was used to alter the voltage applied to the test gap. Tests were carried out to establish the position of critical coupling. This was never exceeded.

A mechanical device, shown in the diagram, enabled L_7 to move in a strictly vertical plane. By means of a flexible mechanical drive, fractional adjustments could be made to the position of L_7 (an important requirement in changing the test voltage in the vicinity of breakdown). At the same time a quick release mechanism allowed L_7 to fall away rapidly. This was found useful in extinguishing a maintained discharge across the electrodes.

The electrodes (capacitance C_8 formed part of the parallel circuit L_9, C_7, C_7' and C_8. Variation of C_7 was used to tune

the circuit to resonance at the desired frequency. Plug-in inductance coils were available to alter L_9. Stray capacitance was reduced to a minimum to keep the circuit Q as high as possible.

The tuned circuit of which the electrodes formed part, was energised by magnetic coupling between L_9 and L_8. Low-capacitance, flexible, coaxial cable linked L_8 with the moveable coil L_7.

A Marconi TF 1041 B valve voltmeter was used for voltage measurement (0→300 v. R.M.S. in 6 ranges, with a 10^x voltage multiplier adaptor available). This instrument possesses very desirable input characteristics, having an equivalent input impedance of 2p.F. in parallel with high resistance.

Tests showed that a t frequencies of 10 Mc/s. and 20 Mc/s., the maximum R.M.S. voltage available was about 400 v. The stability of the oscillations was excellent, and no evidence of frequency pulling was found. At 30 Mc/s. and 40 Mc/s. only a small voltage could be derived, due partly to reduction in circuit, Q, (high L/C ratio could not be maintained owing to capacitance of leads, electrodes, etc.) and also to Miller effect attenuation in the early stages.

In view of the time factor, it was decided to confine measurements to the lower frequencies.

3.5 Irradiation

3.5.1 General Comments

The time-lag between the application of a voltage of the necessary magnitude and the consequent breakdown of a gap may be separated into two components.

(a) the statistical time-lag, a consequence of the need for an initiatory electron (or electrons) to appear at a suitable point in the gap, and

(b) the formative time-lag, the interval between the arrival of such an electron and the inception of the discharge.

The formative time-lag is independent of external conditions (other than the strength of the applied field) and with the threshold field applied is usually of the order of $10^{-5} \rightarrow 10^{-6}$ sec.

Statistical lags, on the other hand, can vary from small fractions of a second up to several minutes, depending largely upon the intensity of the external irradiating source.

Irradiation may be effected using 'casual' means, e.g. natural radioactivity and cosmic rays. It is usual, however, to supply electrons at a faster and more steady rate, to reduce statistical lags. Examination of the literature revealed that use has been made of the following methods:

(i) ultraviolet irradiation of electrode surfaces,

(ii) irradiation using radioactive materials,

(iii) irradiation by spark and corona discharges,

(iv) irradiation by X-rays.

3.5.2 Discussion of available methods

The requirement of an irradiating system is to produce a steady source of electrons, without significantly affecting breakdown conditions.

For d.c. breakdown, U-V irradiation of the cathode appears to be satisfactory, particularly in view of the fact that the secondary (γ) source of electrons in such a discharge is rooted in the cathode. In many types of h.f. discharge, however, electrons and ions are unable to reach the electrodes by mobility motion. Under such conditions, a supply of initial electrons within the body of the gas is perhaps desirable to reduce lags to a minimum.

A beam of U-V across the middle of the gap may produce electrons by photoionization. Such a system, originated by Prowse and Jasinski[37], has been successfully used by several workers. In Prowse's method, a discharge (giving rise to U-V quanta) is maintained in pulsed form across a short gap situated in a side-arm of the discharge chamber. The merit of

this is that absorption of the hard U-V quanta by quartz windows etc., is avoided. Unfortunately, Clark[32] found that for pressures below 1 mm. Hg. the irradiating spark becomes diffuse in character and tends to spread into the main chambers.

Radioactive sources, though widely used, have the disadvantage that the radiations cannot be collimated with ease or controlled in intensity. Further, strong sources tend to affect the threshold field value.

Since none of the available methods were entirely free from objections, it was decided to try a slightly different method.

3.5.3 Mid-gap irradiation using external U-V source

In the system adopted, a collimated beam of U-V light was passed through a thin quartz window (centrally situated in a sidearm of the discharge chamber) and directed into the mid-gap region of the test electrodes.

The lamp used was a mains-operated 125 W high-pressure mercury arc lamp (philips MBL/V) with quartz envelope, which produced an arc 30 mm. long and 2 mm. wide. A metal housing was used to afford protection from the radiations. By mounting the assembly on a moveable trolley and by the use of collimating cylinders of variable length and bore, control of

beam width and intensity was obtained. A metal cap was used to block the radiations, when required.

The method worked surprisingly well. Careful tests showed conclusively that a substantial reduction in statistical time-lags was effected without changing the threshold field. Although the times did tend to increase with reduction in gas pressure, the change was not large even at the lowest pressures encountered. (10^{-3} - 10^{-4} mm. Hg.).

Since this method of irradiation may be of interest to other workers, a short discussion of the possible sources of the electrons will now be given.

3.5.4 Irradiation mechanism

As stated, radiations from the mercury arc column were collimated by small holes drilled in metal cylinders. The beam entered the chamber centrally through a quartz window. Geometrically, a slightly divergent beam passed through the interelectrode space about the mid-gap position.

It was first thought that photionization through absorption of a single U-V quantum by a gas molecule could account for the supply of initiatory electrons. In fact, considerable doubt exists as to the possibility of such a mechanism.

A photon is known to ionize an atom with a maximum

probability at a certain critical quantum energy slightly in excess of the first ionization energy,

$$\text{i.e.} \quad E = h\nu > e V_i$$

$$\text{but} \quad \nu = \frac{c}{\lambda}$$

$$\therefore \lambda < \frac{ch}{eV_i}$$

Hence for molecular hydrogen, $\lambda < 805\text{Å}$.

Using the manufacturer's transmission chart for quartz of the thickness and composition used in the side-arm window, radiations in the U-V region below 1800Å are strongly absorbed with a 'cut-off' around 1600Å. If it be accepted that absorption is complete below this value it is obvious that photo-ionization is inoperative. On the other hand, it may be possible that a few high energy photons pass through, sufficient to provide a level of photoionization but too small to be detected by spectroscopic methods. The fact that time-lags increased only slowly with decreasing pressure would indicate that such events are unlikely.

An alternative to the above is that radiations of 1600Å and above enable gas molecules to be ionized in steps. Examples

of cumulative ionization of this type are readily found where molecules possess metastable excitation levels. The mechanism is an unlikely one, however, since in none of the gases used are metastable states to be found (other than neon) and once again a dependence between statistical time-lags and pressure would be necessary (the probability of the process $\propto p^2$ at low pressures).

If photoionization be ruled out, the source of electrons must have been derived from either the electrodes or the glass walls of the chamber opposite the quartz window.

Photoelectric emission from a solid is possible for quantum energies exceeding the work function, Θ, of the surface. Although no value for Θ is available for Pyrex glass, a value of about 4.4 e.v. is common for many insulators. Since the quantum energy of a 1600Å radiation is 7.7 e.v., emission from the glass walls appears to be a very likely source of electrons.

The final possibility, photoelectric emission from the electrodes, cannot be eliminated. Two sources of quanta are possible; from the original beam and by re-radiation from the glass wall. Since the irradiating source successfully provided a regular supply of starting electrons, no further

experimental work was attempted to deduce their true origin (s). Such a study would be useful in view of the essential simplicity of the system.

4. EXPERIMENTAL RESULTS IN HYDROGEN AT 10 Mc/s and 20 Mc/s : BASIC EQUATIONS

4.1 Experimental procedure

Most of the experimental 'runs' involved determining R.M.S. breakdown field as a function of gas pressure; a given set of readings being taken at constant electrode separation.

Gas pressure was varied by initially filling the discharge chamber with hydrogen at the highest pressure to be used (about 1 mm.Hg.) and subsequently reducing pressure in convenient steps.

With the gas in equilibrium at a required pressure, irradiation was introduced and the applied field slowly increased until a discharge occurred. The threshold voltage was determined by re-applying the field at a slightly smaller amplitude than that at which breakdown had first occurred, this process being repeated until a minimum value was established. Upwards of two minutes was allowed between successive readings to ensure charge neutralization. Breakdown fields lower than the true threshold were observed when discharges were started quickly following a previous discharge.

12. Breakdown in Hydrogen at 10 Mc/s and 20 Mc/s. Variation of Breakdown Stress with Gas Pressure for different Electrode Separations

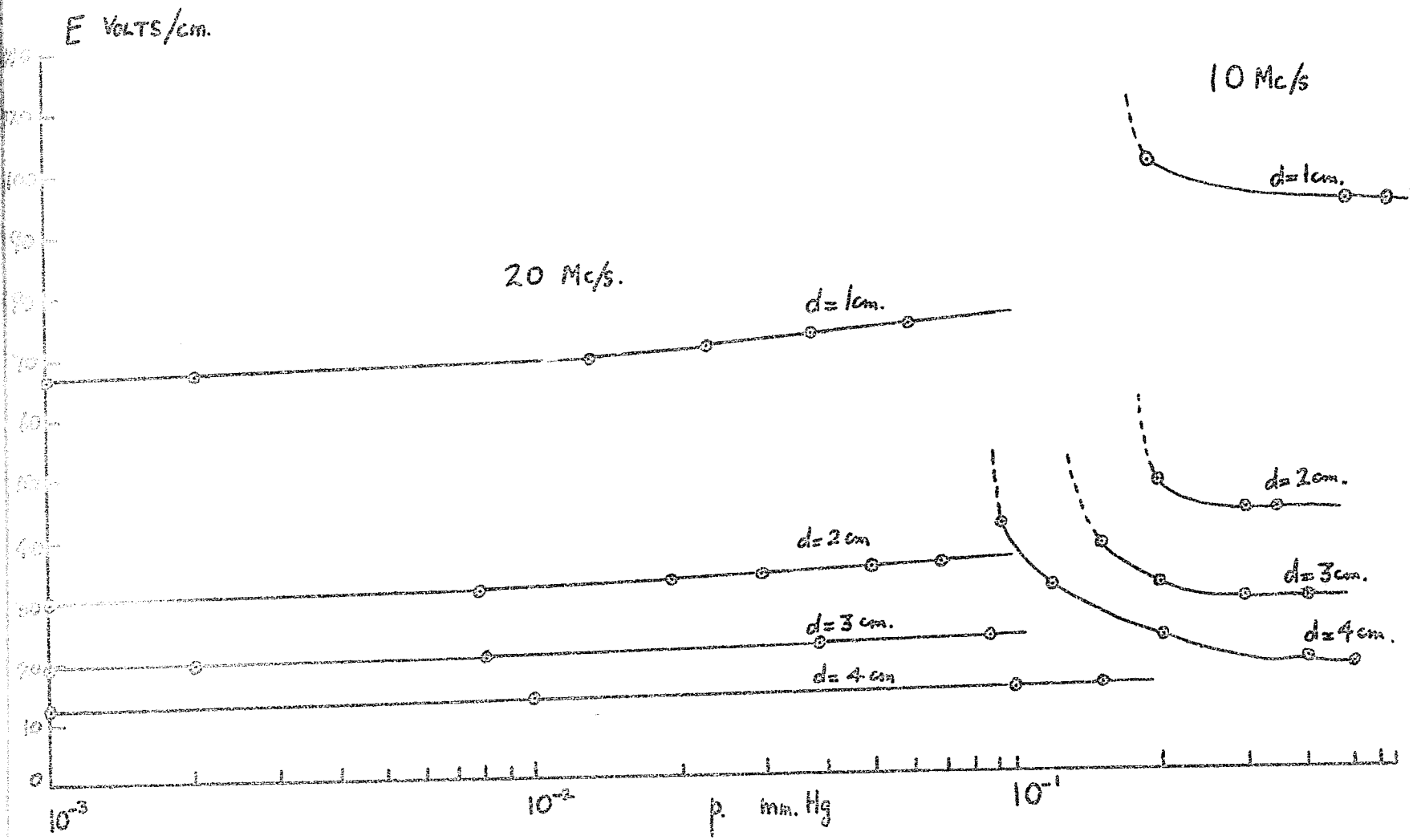

Irradiation was removed during such periods.

Before each run the system was cleaned, as described in Chapter 3. In this way, breakdown values at given electrode spacing and pressure were found to be in close agreement when runs were repeated. Prior to adopting this strict procedure, a spread of experimental results had been noted.

4.2 Breakdown curves at 10 Mc/s and 20 Mc/s

Two families of experimental curves relating RMS breakdown field for different pressures at 10 Mc/s and 20 Mc/s, and for different electrode spacings, are shown in Figure 12.

At 20 Mc/s breakdown at constant gap width is characterised by a slow fall in field strength with reduction in pressure, to an almost constant value which persists down to the lowest pressure investigated, 10^{-4} mm.Hg. With fixed gas pressure, decrease in electrode separation is seen to require an increase in starting field.

Using 10 Mc/s oscillations, abrupt changes in breakdown behaviour occur. The onset field strength at constant electrode separation initially shows a gradual decrease as gas pressure is reduced from the highest value used (somewhat less than 1 mm.Hg.). This decrease is not maintained, however. With further reduction in pressure, the starting field falls to

a broadly-defined minimum value. At pressures below the minimum, field-strength was found to increase sharply, culminating in an abrupt 'cut-off'. Insufficient voltage was available to restart a discharge at still lower pressures. In the work reported by Prowse & Clark[29], breakdown in a wide pressure range down to a few mm.Hg. has been shown to conform with the requirements of the diffusion theory. Departures from the limits of applicability of the theory - discussed in Section 5.4.1 - are to be expected with reduction in gas pressure. Such changes in breakdown behaviour are dependent upon electrode geometry.

The observed cut-offs in the 10 Mc/s curves occur at pressures determined by electrode geometry and an explanation of these effects in terms of departures from diffusion - controlled breakdown is at once suggested by qualitative examination of the results.

Although little information regarding the mechanisms of breakdown can be deduced by inspection, it is clear that the initiation of a discharge according to diffusion theory requirements is not possible at the lower pressures. Simple calculations show that over much of the pressure range the electron mean free path is in excess of the electrode

separation. The probability of an electron making an ionizing event in its mean lifetime must therefore become progressively more remote, as the pressure is reduced.

In Chapters 5 and 6 explanations are put forward of breakdown at 20 Mc/s and 10 Mc/s respectively.

Before offering quantitative interpretations, however, it is necessary to present certain basic equations of electron motion in high frequency fields, and also to deduce, or state, relevant information regarding atomic data such as mean free paths, collision frequencies etc., under experimental conditions.

4.3 Electron mean free path

Calculation of electron mean free path λ_e as a function of gas pressure is complicated by the Ramsaeur effect, i.e. the variation in collision probability with electron energy.

The term "probability of collision", P_c, introduced by Brode[16], is defined as the number of collisions made by an electron in travelling 1 cm. through a gas at a pressure of 1 mm.Hg. and at $0^{\circ}C$.

Hence λ_e and gas pressure p are related by the expression

$$\lambda_e = \frac{1}{pP_c} \quad \ldots \quad \ldots \quad \ldots \quad \ldots \quad (16)$$

TABLE 1

GAS PRESSURES COINCIDENT WITH THE ELECTRON MEAN FREE PATH EQUALLING THE ELECTRODE SEPARATION.

d (cm.)	p (mm Hg)
4	0·0051
3	0·0068
2	0·0102
1	0·0204

Changes in magnitude of P_c with electron energy variations have been studied experimentally by Brode[16]. The published curve for molecular hydrogen shows a complex and largely irregular variation between collision probability and electron velocity. However, for energies below 4 e.v., P_c decreases only slowly with reduced velocity and has an approximate value of 49 $cm.^{-1}$ $mm.Hg.^{-1}$.

Using the approximation

$$\lambda_e = \frac{1}{49p} \quad \ldots \quad \ldots \quad \ldots \quad \ldots \quad (17)$$

Of special interest in the hydrogen results are the pressures at which electron mean free paths coincide with the separation of the electrodes. Applying equation 17 these events are plotted graphically in Figure 13, and are listed in Table 1.

It is seen that within the range of experimental observation, for each of the separations used, breakdown field measurements were recorded at pressures both below and above the values at which electron mean free path equals the gap width.

These transitions are significant in the development of an account of the mechanisms of breakdown; even at this stage it is apparent that ionization by electron collision with gas

molecules is unable itself to promote breakdown of the gas over the full pressure range used.

4.4 Collision frequency/field frequency calculations

It has been shown in Section 1.4.2 that for electrons oscillating under the influence of an a.c. field the principal factor governing the efficiency of energy transfer between field and gas is the ratio of field frequency to collision frequency, ω/ν_c. Margeneau's concept of the 'effective' electric field, equation (2), is an expression of the above statement.

It follows that in cases where electron motion is not disturbed other than by the applied field, changes in breakdown behaviour are to be expected in the region surrounding that corresponding to ω and ν_c being the same order of magnitude.

Exact calculations of collision frequencies are not possible since ν_c, in a similar way to m.f.p., is a function of electron energy. An indirect method of calculation has been found. This relates collision frequency and gas pressure over a fairly broad range of electron energy, and is given below.

From the definition of collision frequency it relates

13. Variation of Collision Probability with Electron Velocity in Hydrogen. Brooke (1933)

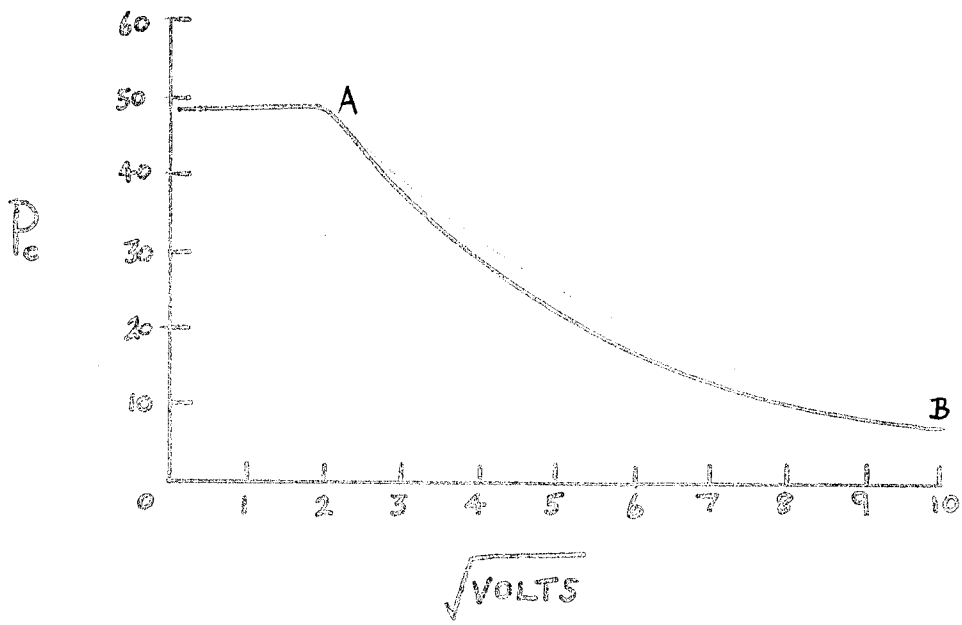

to mean free path and mean (random) electron velocity $\bar{c}$ by the equations:

$$\nu_c = \frac{\bar{c}}{\lambda_e} \quad \ldots \quad \ldots \quad \ldots \quad \ldots \qquad (18)$$

Substituting for λ_e in equation (16)

$$\nu_c = \bar{c} p P_c$$

$$\therefore \quad \bar{c} P_c = \frac{\nu_c}{p} \quad \ldots \quad \ldots \quad \ldots \qquad (19)$$

Brode's experiment relates collision probability and electron energy for hydrogen gas, the curve being shown in Figure 13.

From the figure in region A-B

$$P_c (\bar{u})^{\frac{1}{2}} = \text{constant} = 10^2$$

$\bar{u}$ = mean electron energy, expressed in e.v.

In c.g.s. units

$$\tfrac{1}{2} m(\bar{c})^2 \; 10^{-7} = e \bar{u}$$

$$\therefore \quad (\bar{u})^{\frac{1}{2}} = \left(\frac{m}{2e10^7}\right)^{\frac{1}{2}} \bar{c}$$

$$\therefore P_c(\bar{u}) = \left(\frac{m}{2e10^7}\right)^{\frac{1}{2}} P_c\bar{c} = 10^2 \quad \ldots \quad \ldots \quad (20)$$

Hence from (19)

$$\left(\frac{m}{2e10^7}\right)^{\frac{1}{2}} \frac{\nu_c}{p} = 10^2$$

$$\therefore \quad \nu_c = 10^2 \left(\frac{2e10^7}{m}\right)^{\frac{1}{2}} p$$

$$\nu_c = 5.9 \quad 10^9 p \quad \text{sec}^{-1} \quad \ldots \quad \ldots \quad \ldots \quad (21)$$

(In close agreement with the value derived by Brown & MacDonald[13]).

The collision frequency may be considered constant (at fixed gas pressure) for electrons in the energy range corresponding to A-B, i.e. 4 - 50 e.v., equivalent to a velocity range $1.2.10^8$ - 4.10^8 cm./sec.

It must be admitted that the energy ranges used in the calculations of mean free path and collision frequency do not coincide; unfortunately more complete experimental data is lacking.

The gas pressure corresponding to conditions under which

the average electron makes one collision per oscillation is obtained by equating ν_c in equation (21) to the field frequency

$$\text{i.e.} \quad \omega = 5.9. \quad 10^9 \, P_{c.f.}$$

$$\therefore \quad P_{c.f.} = \frac{2\pi \cdot 2.10^7}{5.9. \quad 10^9} = 0.021 \text{ mm.Hg. at 20 Mc/s.}$$

$p_{c.f.}$ may be called the pressure corresponding to the collision-frequency transition.

Assuming for the moment that electron motion is not hampered by collisions with the electrode faces, i.e. is determined only by the field modulating thermal movement, it is possible to calculate the effective R.M.S. field which delivers the same energy to the gas as a unidirectional field under corresponding conditions. The relevant equation, already introduced in Section 1.4.2 is

$$E_e^2 = \frac{E_R^2 \, \nu_c^2}{\nu_c^2 + \omega^2} \quad \ldots \quad \ldots \quad \ldots \quad \ldots \quad (2)$$

$$\text{i.e.} \quad \left(\frac{E_R}{E_e}\right)^2 = \left(1 + \frac{\omega^2}{\nu_c^2}\right)$$

14. Variation of Effective Yield Strength with Gas Pressure, Hydrogen 10 c/s and 20 c/s

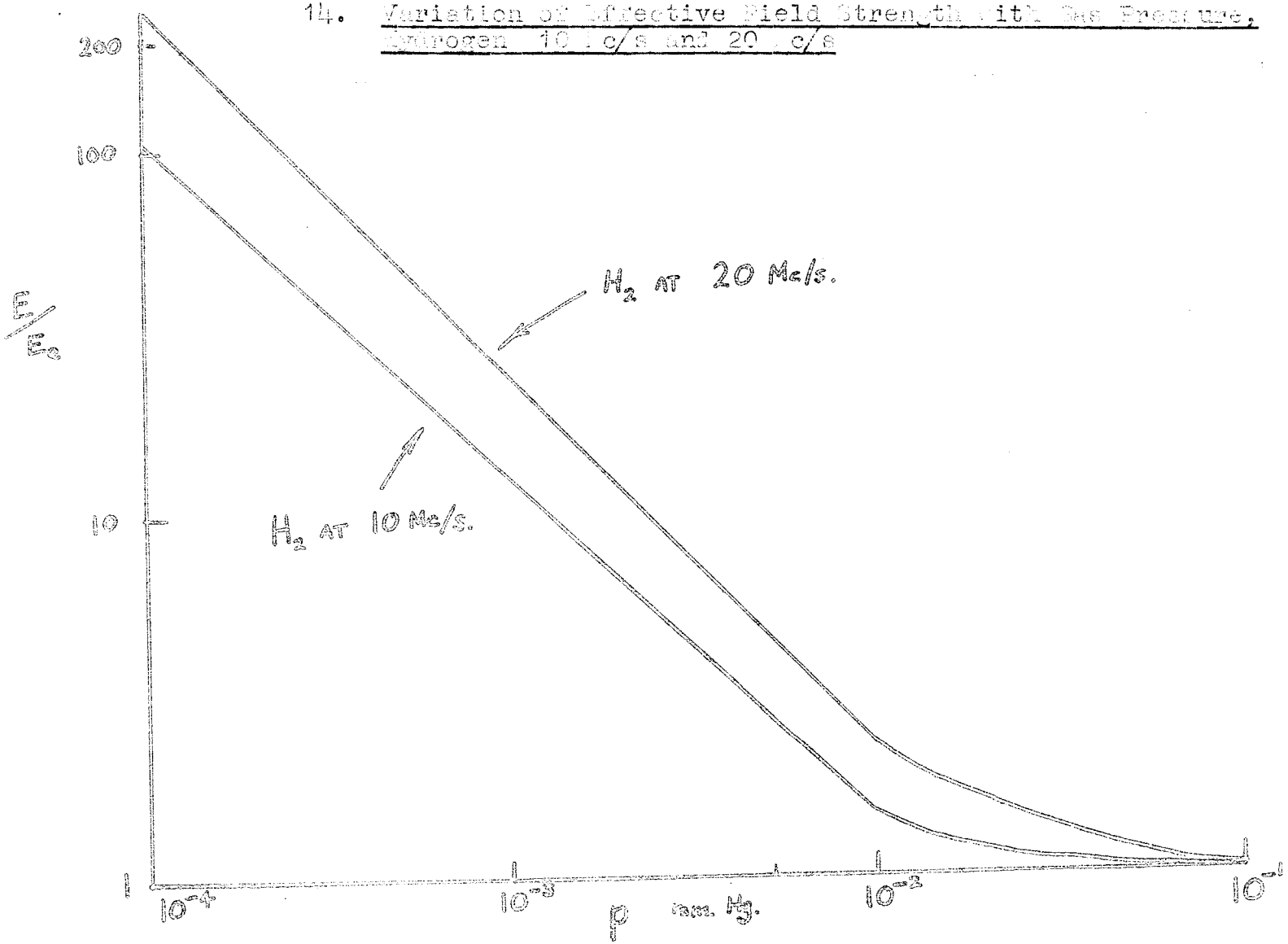

$$\frac{E_R}{E_e} = \left(1 + \frac{4.54 \quad 10^{-4}}{p^2}\right)^{\frac{1}{2}} \qquad \ldots \quad \ldots \qquad (22)$$

using the appropriate values for ν_c and ω .

A double-log plot of E/E_e v.s. p is given in Figure 14, covering the low pressure end of the experimental range studied.

Calculations, using equation 22, show that for pressures in excess of about 0.1 mm.Hg., E_e becomes almost identical with the applied R.M.S. field E_R. However, the ratio E_R/E increases rapidly with reduction in gas pressure and at 10^{-4} mm.Hg. (the lowest recorded in practice) the effective field is only about 1/200 of the applied stress.

The fact that the hydrogen discharges at 20 Mc/s. have been observed to start with comparable field strengths over the whole pressure range - for given values of electrode separation - appears at first sight to contradict the statements and calculations made above regarding energy transfer considerations. However, the 'effective' field concept is only relevant in cases where the to-and-fro movement of electron is not restricted by (for example) the walls of the containing vessel.

An expression for the amplitude of electron oscillation has been deduced in Section 4.5.2.

4.5 Equations of electron motion in high-frequency fields

4.5.1 Electron Drift Velocity

Studies of discharge phenomena in gases are frequently made from the point of view of the behaviour of the (imaginary) 'average' electron. As explained below, the motion of such a particle is unlike that of any individual electron in a swarm or avalanche, but represents the mean properties of such a swarm. Agreement between experiment and theory developed along such lines has, in many cases, proved satisfactory.

Electrons in a gas not subjected to an electric field have random thermally-directed paths and as time goes on diffuse away from their points of origin. Knowledge of the amplitude of electronic oscillation is, therefore, most important in interpreting breakdown behaviour. It is commonly assumed that the particles travel in straight lines between successive collisions. The mean free path λ_e is defined as the average rectilinear distance between impacts - it does not represent a probable value around which the actual paths are closely grouped.

Random motion is altered when an electric field is made to stress the gas. Considering a cloud of electrons the field may be considered as moving the swarm bodily through the gas. The average speed of the centre of the swarm in the field direction gives the (average) drift velocity, v, and defines the drift speed of the 'average' electron. This picture is applicable even in cases where the drift velocity is only a small fraction of the mean random velocity.

Attempts have been made to relate v to unidirectional reduced field strength E/p. At high pressures (low E/p) theory predicts $v \propto (E/p)^{\frac{1}{2}}$ in accordance with experimental observations in many gases[38,39]. Studies at higher E/p are complicated by increasing numbers of inelastic collisions - both exciting and ionizing - occurring in the body of the gas. The dependence of electron random velocity and mean free path upon the reduced field presents a difficulty common to all such problems. Satisfactory correction terms are not available over an extended range of E/p and the approximation is usually taken that such terms as mean free path are invariant. Experimentally, a considerable weight of evidence suggests that drift velocity is directly proportional to E/p

over a wide range of the latter.

4.5.2 Amplitude of oscillation and drift velocity expressions

An expression for the amplitude of electron oscillation with the breakdown field E_R applied will now be derived by considering the high-frequency field $E = E_p \sin \omega t$ applied to electrons moving in an unbounded gas. The effects of finite electrode geometry will then be taken into account by the insertion of suitable boundary conditions.

The ordered motion of an electron in a gas subjected to an alternating field is determined by the equation of motion: (Lorentz),

$$m \frac{dv}{dt} + mv. \nu_c = eE = eE_p \sin \omega t \quad \ldots \quad (23)$$

To solve for v, let the integrating factor $= \exp(\int \nu_c dt)$

$$= \exp(\nu_c . t)$$

$$\therefore \exp(\nu_c t) \frac{dv}{dt} + \nu_c \exp(\nu_c t).v = \frac{e}{m} E_p \exp(\nu_c t) \sin \omega t$$

$$\frac{d}{dt}\left[\exp(\nu_c t).v\right] = \frac{e}{m} E_p \exp(\nu_c t). \sin \omega t$$

since $\frac{d}{dt}\left[\exp(\nu_c t)v.\right] = v.\,\nu_c \exp(\nu_c t) + \exp(\nu_c t).\frac{dv}{dt}$

Hence $\exp t(\nu_c t).\ v = \frac{e}{m} E_p \int \exp(\nu_c t) \sin \omega t.\ dt.$

$$\therefore v = \frac{eE_p}{m(\omega^2 + \nu_c^2)} (\nu_c \sin\omega t - \omega\cos\omega t) + C\exp(-\nu_c t) \quad \ldots \quad \ldots \quad \ldots \quad (24)$$

Equation (24) may also be written

$$\mathbf{V} = \frac{eE_p}{m(\omega^2+\nu_c^2)} (\omega^2+\nu_c^2)^{\frac{1}{2}} \frac{\nu_c}{(\nu_c^2+\omega^2)^{\frac{1}{2}}} \sin\omega t - \frac{\omega}{(\nu_c^2+\omega^2)^{\frac{1}{2}}} \cos\omega t$$

$$+ C\exp(-\nu_c t)$$

whence, $$v = \frac{eE_p}{m(\omega^2+\nu_c^2)^{\frac{1}{2}}} \sin(\omega t - \alpha) + C\exp(-\nu_c t) \quad \ldots \quad (25)$$

where $$= \tan^{-1}\left(\frac{\omega}{\nu_c}\right) \quad \ldots \quad \ldots \quad \ldots \quad \ldots \quad \ldots \quad (26)$$

The electron velocity is seen to have two components. The first is oscillatory due to the action of the field; the second is

unidirectional and decays exponentially with time.

Considering for the moment the oscillatory term alone

$$v = \frac{eE_p}{m(\omega^2+\nu_c^2)^{\frac{1}{2}}} \sin(\omega t - \alpha) \quad \ldots \quad \ldots \quad \ldots \quad (27)$$

Equation (27) shows that the average electron drift velocity varies sinusoidally at the field frequency with a phase difference $\alpha = \tan^{-1}(\frac{\omega}{\nu_c})$ between the two.

Two simple checks can immediately be made which indicate that the equation is of a form compatible with accepted electron behaviour under a.c. conditions.

When $\omega >> \nu_c$, $\tan\alpha \rightarrow \infty$, i.e. $\alpha \rightarrow \pi/2$.

Hence $v \propto \cos\omega t$, i.e. an electron in a vacuum will oscillate in quadrature with the applied field.

On the other hand when $\omega << \nu_c$, corresponding to high pressures or low frequencies, $\tan\alpha \rightarrow 0$, i.e. $\alpha \rightarrow 0$.

i.e. $$v = \frac{eE_p}{m\nu_c} \sin\omega t.$$

The drift velocity, therefore, follows the field variations, a result well established in high-frequency work : the equation agrees exactly with that derived by Brown &

McDonald[13], using a different approach.

The velocity equation can be used to determine the electron displacement and hence the amplitude of oscillation x_o.

From equation (27)

$$v = \frac{eE_p}{m(\omega^2+\nu_c^2)^{\frac{1}{2}}} \sin(\omega t - \alpha) = \frac{eE_p}{m(\omega^2+\nu_c^2)} \left[\nu_c \sin\omega t - \omega\cos\omega t\right]$$

$$\therefore x = \frac{-eE_p}{\omega m(\omega^2+\nu_c^2)^{\frac{1}{2}}} \cos(\omega t - \alpha) + A$$

where $\alpha = \tan^{-1}\left(\frac{\omega}{\nu_c}\right)$

When $x = x_o$, $v = 0$, i.e. $\omega t = \alpha$.

$$\therefore x_o = \frac{-eE_p}{\omega m(\omega^2+\nu_c^2)^{\frac{1}{2}}} + A.$$

$$\therefore x = \frac{-eE_p \cos(\omega t - \alpha)}{\omega m(\omega^2+\nu_c^2)^{\frac{1}{2}}} + \frac{eE_p}{\omega m(\omega^2+\nu_c^2)^{\frac{1}{2}}} + x_o \quad \ldots (28)$$

When $x = o$, v = maximum, i.e. $\frac{dv}{dt} = o$.

15. Amplitude of Electron Oscillation as a function of gas pressure. Hydrogen 20 kc/s.

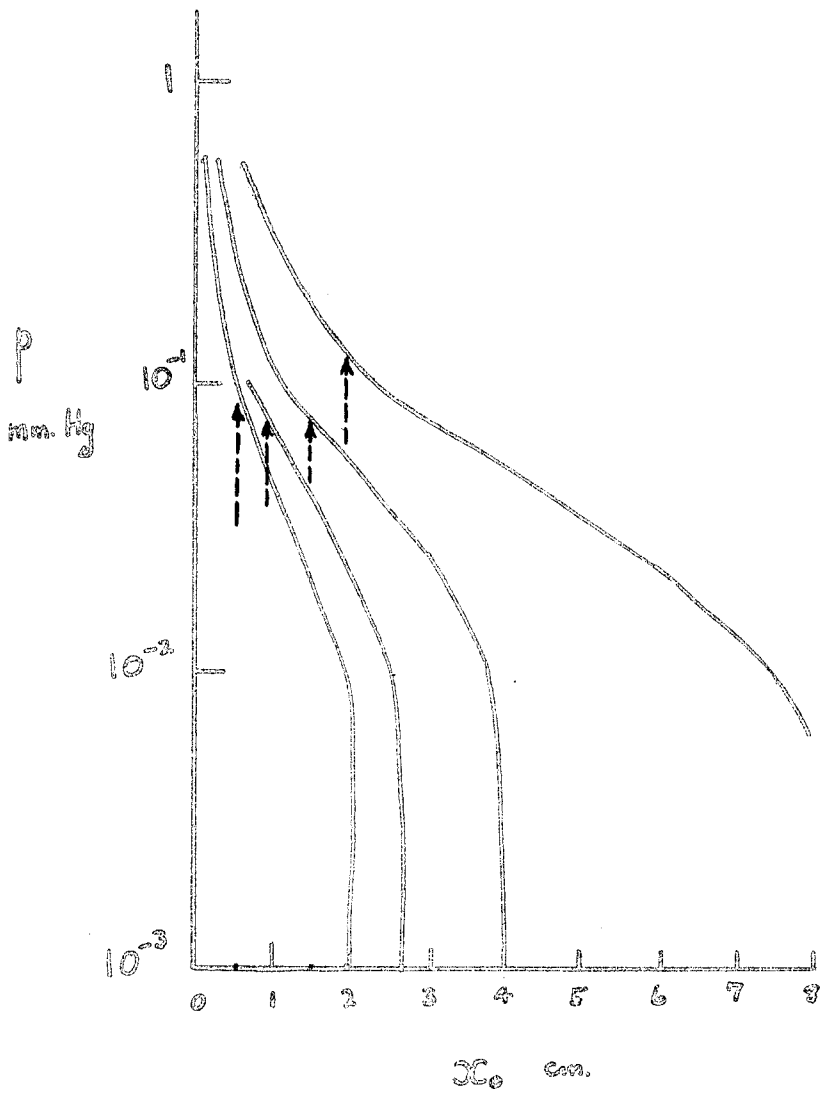

$$\text{i.e. } \frac{dv}{dt} = \frac{\omega e E_p}{m(\omega^2+\nu_c^2)^{\frac{1}{2}}} \cos(\omega t - \alpha) = 0$$

$\therefore \cos(\omega t - \alpha) = 0.$

$\therefore$ Substituting these conditions in equation (28)

$$x_o = \frac{e E_p}{m\omega(\omega^2+\nu_c^2)^{\frac{1}{2}}} \quad \ldots \quad \ldots \quad \ldots \quad \ldots \quad (29)$$

Since collision frequency ν_c is calculable from equation (21), the amplitude of electron oscillation may be determined for any given field strength and gas pressure.

Calculations of this type have been used to produce Figure 15. The curves relate electron amplitude x_o as a function of pressure for the breakdown fields encountered in hydrogen at 20 Mc/s, with electrode separation as the parameter. The electron ambit, i.e. the total traverse in the field direction during a cycle of the field, is equal to $2 x_o$. Hence, if for a given field strength and electrode separation, $\frac{d}{2} > x_o$, electrons will tend to oscillate within the test gap without suffering collisions with the electrodes.

The arrows drawn in Figure 15 indicate the $\frac{d}{2}$ positions

corresponding to each of the experimental curves. It is seen that in all cases, for pressures < 0.2 mm.Hg., the electron ambit exceeds electrode separation.

4.5.3 Summary

Summarising the analyses presented in Sections 4.1 - 4.3 the following deductions may be made:

Mean free path determinations. The fact that electron m.f.p. exceeds electrode separation at the lower pressures is evidence that single-stage ionization by collision is unable, by itself, to promote an increase in electron population leading to breakdown.

Collision-frequency/field frequency determination. The efficiency of energy transfer between an a.c. field of given strength and electrons oscillating within the gas depends upon the ratio ω/ν_c. Calculations given in Section 4.2 and shown diagrammatically in Figure 14 indicate that the average energy transferred to an electron during a cycle of the applied field falls off quickly with reduction in pressure below 0.1 mm.Hg. This effect is directly associated with electron inertia. However, deductions based upon energy transfer can only have real significance when the electron is 'free' in the sense that it is not impeded other than by

collision with gas molecules.

Electron ambits. The calculations based upon equation (27) show that for all but the highest pressures used, an electron starting at any point in the gap must strike an electrode during a period of the supply, provided it does not diffuse laterally away from the influence of the field.

4.5.4 Secondary emission of electrons : discussion

If the electron arrival velocity is sufficiently high, with consequent secondary-electron emission from a surface, the possibility arises that collisions with the electrodes can assist the growth of electron population.

The work of Gill & Von Engel[30] (Section 1.4.5) has established that high frequency electrodeless discharges can be started under 'vacuum' conditions by progressive build-up of electron population by secondary emission. Such a generation process is not encountered in the inception of either d.c. glow discharges or under high-frequency conditions which conform to diffusion-theory requirements.

The diffusion theory implies that there is no need to look beyond single-stage ionization by collision as the electron generation mechanism. Hence, electrons whose thermal motion takes them to the electrodes must be supposed 'lost'

from the system. It is reasonable to suppose that they either suffer surface recombination with positive ions or are accepted into the reservoir of 'free' electrons near the metal surface. The contribution of any secondary electrons towards an overall build-up of electron density would appear to be negligibly small. Further evidence of a direct nature is available.

Prowse & Clark[29] have shown by functional analysis that the relation between $E\Lambda$ and $p\Lambda$ depends only on the nature of the gas. (The diffusion length, Λ, is defined in Section 1.3.3). Hence the curve relating $E\Lambda$ and $p\Lambda$ should be unique for any one gas. This has been verified by suitable comparison of the results of several workers. Significantly, all measurements lie on a single curve, irrespective of the nature of the metal surfaces of the electrodes. Thus in diffusion theory the electrodes serve to stress the gas with the high-frequency field, and limit the extent of the maintained discharge, but play no important role in the development of breakdown. Again in d.c. discharge tubes, numbers of energetic secondary electrons are released from the anode but are returned to it by the unidirectional field. Local ionization and excitation does take place but the really

essential processes occur in the cathode region.

The justification for detailing the point is that, contrary to the above, secondary emission from the electrodes by electron impact is considered to play an important role in initiating low pressure discharges in hydrogen at 20 Mc/s.

5. BREAKDOWN IN HYDROGEN AT 20 Mc/s

5.1 Initiation of the low pressure discharge

An interpretation of breakdown at the lower pressures used will now be given, in terms of a progressive build-up of electron population governed by secondary emission from the electrode faces.

For the effects of secondary emission to be cumulative, a necessary condition for the development of a discharge is that electronstraverse the inter-electrode space in a half-cycle of the applied field.

Equation (24) is used as a starting point in the quantitative expression of the breakdown criterion.

5.1.1 Velocity and displacement equations

The above equation describes the influence of field strength, field frequency, and gas pressure upon the drift motion of electrons in an ocean of gas. The expression becomes applicable to the experimental arrangement used when suitable boundary terms are imposed.

The ultra-violet irradiating source used in the hydrogen experiments provided a small but steady supply of casual electrons within the gap. Let it be assumed that at a time

$t = \frac{\phi}{\omega}$ subsequent to the breakdown field passing through a zero value such an electron be moving with drift velocity v_o away from an electrode surface.

$$v = \frac{e E_p}{m(\omega^2+\nu_c^2)} (\nu_c \sin\omega t - \omega\cos\omega t) + C \exp(-\nu_c t) \quad \ldots \quad (24)$$

Since $v = v_o$ when $t = \frac{\phi}{\omega}$.

$$\therefore v_o = \frac{e E_p}{m(\omega^2+\nu_c^2)} (\nu_c \sin\phi - \omega\cos\phi) + C \exp(-\frac{\nu_c\phi}{\omega})$$

and hence $$v = \frac{e E_p}{m(\omega^2+\nu_c^2)} (\nu_c \sin\omega t - \omega\cos\omega t)$$

$$+ \left[v_o - \frac{e E_p}{m(\omega^2+\nu_c^2)} (\nu_c \sin\phi - \omega\cos\phi) \right] \exp(\frac{\nu_c\phi}{\omega}) \exp(-\nu_c t)$$

$$\ldots \quad \ldots \quad \ldots \quad (30)$$

Considering those cases of breakdown in which the electron ambit exceeds the electrode separation (see Figure 15), let the phase angle ϕ be such that the electron just traverses

the gap in a half-period of the field, π/ω.

Then at a time $t = \frac{\pi + \phi}{\omega}$, the other electorde will be reached with velocity v_i, given by

$$v_i = \frac{e E_p}{m(\omega^2+\nu_c^2)} \left[\nu_c \sin(\pi + \phi) - \omega\cos(\pi + \phi)\right]$$

$$+ \left[v_o - \frac{e E_p}{m(\omega^2+\nu_c^2)} (\nu_c\sin\phi - \omega\cos\phi)\right]\exp\left(\frac{\nu_c \pi}{\omega}\right)$$

$$\therefore v_i = v_o \exp\left(-\frac{\nu_c\pi}{\omega}\right) + \frac{\omega e E_p}{m(\omega^2+\nu_c^2)} \left[1 + \exp\left(-\frac{\nu_c\pi}{\omega}\right)\right](\cos\phi - \frac{\nu_c}{\omega}\sin\phi)$$

... ... (31)

Again, the electron displacement after a time $t = \frac{\pi + \phi}{\omega}$, is equal to the electrode separation d.

Therefore from equation (30)

$$\int_o^d dx = \frac{e E_p}{m(\omega^2+\nu_c^2)} \int_{\frac{\phi}{\omega}}^{\frac{\pi+\phi}{\omega}} (\nu_c\sin\omega t - \omega\cos\omega t)\, dt.$$

(CONT.)

$$+\left[v_o - \frac{e E_p}{m(\omega^2+\nu_c^2)}(\nu_c \sin\phi - \omega\cos\phi)\right] \exp\left(\frac{\nu_c \phi}{\omega}\right) \int_{\frac{\phi}{\omega}}^{\frac{\pi+\phi}{\omega}} \exp(-\nu_c t)\, dt$$

$$\therefore d = \frac{2e E_p}{m(\omega^2+\nu_c^2)} \left(\frac{\nu_c}{\omega}\cos\phi + \sin\phi\right)$$

$$-\left[v_o - \frac{e E_p (\nu_c \sin\phi - \omega\cos\phi)}{m(\omega^2+\nu_c^2)}\right]\frac{1}{\nu_c}\left[\exp\left(-\frac{\nu_c \pi}{\omega}\right) - 1\right] \quad \ldots (32)$$

Equation (31) expresses electron impact velocity in terms of emission velocity v_o, phase angle ϕ and field strength E_p. If v_i is of sufficient magnitude, energy transfer between an impinging electron and electrons in the electrode surface will result in the release of secondary electrons back into the gas.

A build-up of electron concentration by secondary emission is possible provided that the released electrons also cross the gap in a half-period of the applied field i.e. they return to the opposite electrode face at time $\frac{2\pi+\phi}{\omega}$ with velocity v_i, and in their turn cause the release of secondaries. Continuation of the process may ultimately result in breakdown.

The applicability of such a mechanism to the results in hydrogen is now considered.

5.1.2 Relationship at very low pressures

The following quantities involved in equations (31) and (32) are known

peak breakdown field	E_p	experimental measurements
Angular field frequency	ω	
electrode separation	d	

collision frequency ν_c - from measured pressure

specific electron charge e/m - from atomic data.

Three quantities remain unknown: v_i, v_o and ϕ. Solutions for v_i must, therefore, be semi-empirical and can be made in the following way by:

(a) assigning arbitary values to ϕ in equation (32) and hence solving for v_o.

(b) inserting the calculated values for v_o in equation (31) and hence deducing v_i as a function of ϕ.

Simplified expressions for v_o and d may be obtained under certain imposed conditions. Discharges at very low pressures are of particular interest in this respect.

In such cases $\nu_c \ll \omega$, so that

$$\exp\left(-\frac{\pi\nu_c}{\omega}\right) = 1 + \frac{\nu_c\pi}{\omega} + \ldots\ldots$$

Hence from equation (20), to a first order approximation

$$v_i = v_o + \frac{2\,e\,E_p}{m\omega}\cos\phi \qquad \ldots \quad \ldots \quad \ldots \qquad (14)$$

and from equation (21), to a second order approximation

$$d = \frac{2\,e\,E_p}{m\omega^2}\sin\phi + \left[v_o + \frac{e\,E_p}{m\omega^2}\cos\phi\right]\frac{\pi}{\omega} \quad \ldots (15)$$

These formulae are in agreement with expressions derived by Gill & Von Engel[30] (Section 1.4.5) in their study of the growth of electrodeless discharges in evacuated glass containers (pressures < 10^{-4} mm.Hg.). Their equations may be regarded as simplified forms of the general expressions - equations (31) and (32) - with the condition $\nu_c \ll \omega$ realised by the use of extremely low gas pressures.

5.1.3 Impact velocity calculations : secondary emission coefficient

Using the method indicated in the previous section, calculations were made of electron arrival velocity v_i, as a function of phase angle ϕ, using equations (14) and (15).

16. Variation of Electron Impact Energy with Phase Angle. Hydrogen at Low Pressures, 20 Mc/s.

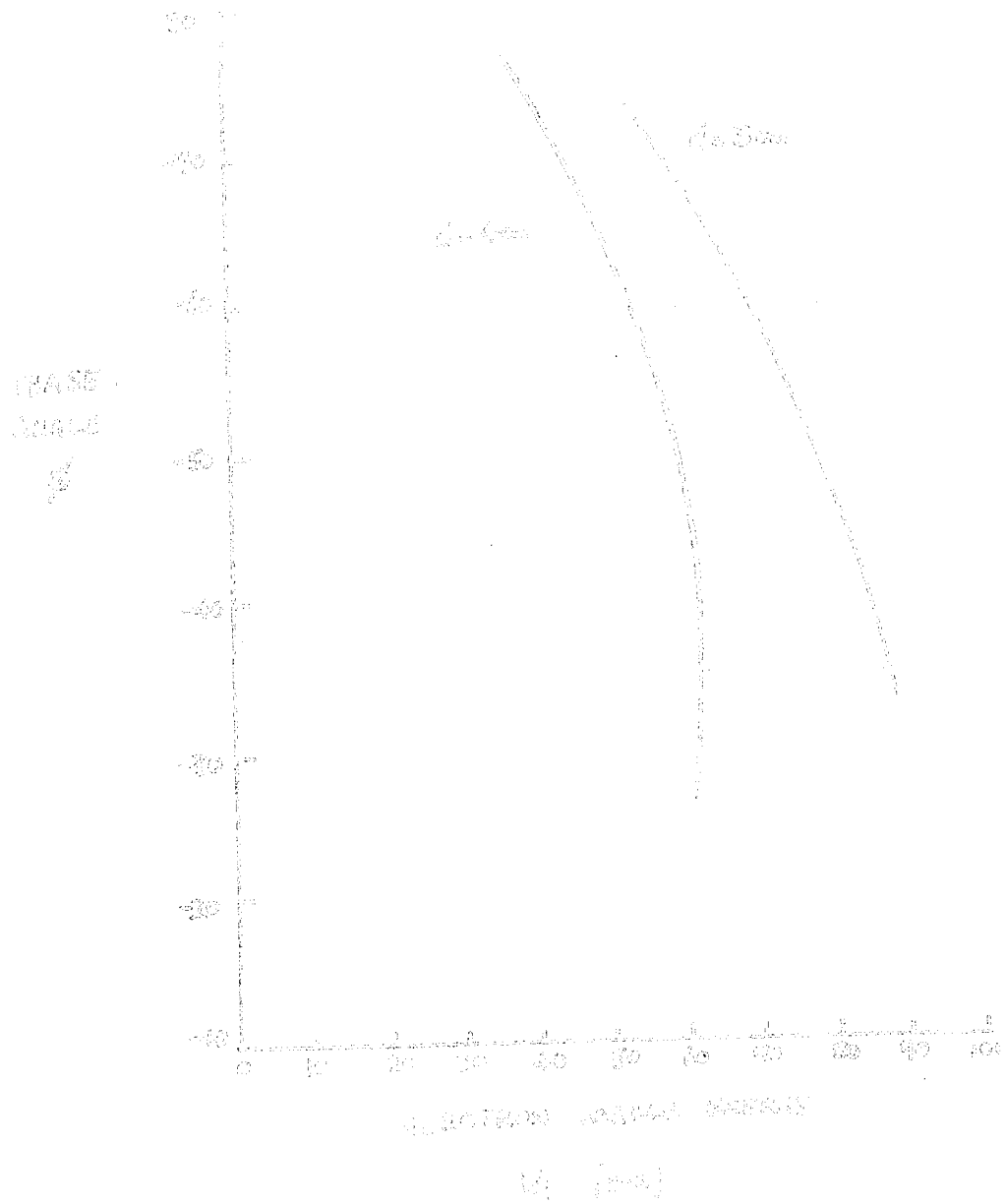

The results are displayed in terms of electron energy, W_i in Figure (16), and refer specifically to measurements at electrode separations of 4 cm. and 3 cm. taken at the lowest pressures used, 10^{-3} mm.Hg. - 10^{-4} mm.Hg. where $\nu_c \ll \omega$.

A strict test of the mechanism of an increase in electron population dominated by secondary emission could be made if experimental data were available regarding secondary emission coefficient, δ, as a function of primary electron energy for the brass electrodes used. It would be expected that electrons leaving one surface at a suitable time ϕ/ω, and arriving at the opposite face at time $\frac{\pi+\phi}{\omega}$, would strike the surface with sufficient energy to cause the release of more than one secondary electron per primary i.e. the emission coefficient δ must be slightly in excess of unity, when account is taken of losses from the system.

Examination of published literature revealed that a few measurements of secondary emission yields have been made involving certain alloys; unfortunately no information regarding brass could be found. However, comparison between the calculated arrival velocities and data obtained from secondary coefficient measurements involving metal alloys (given below), indicates that calculated arrival energies are sufficient to

17. Secondary emission coefficient curves.

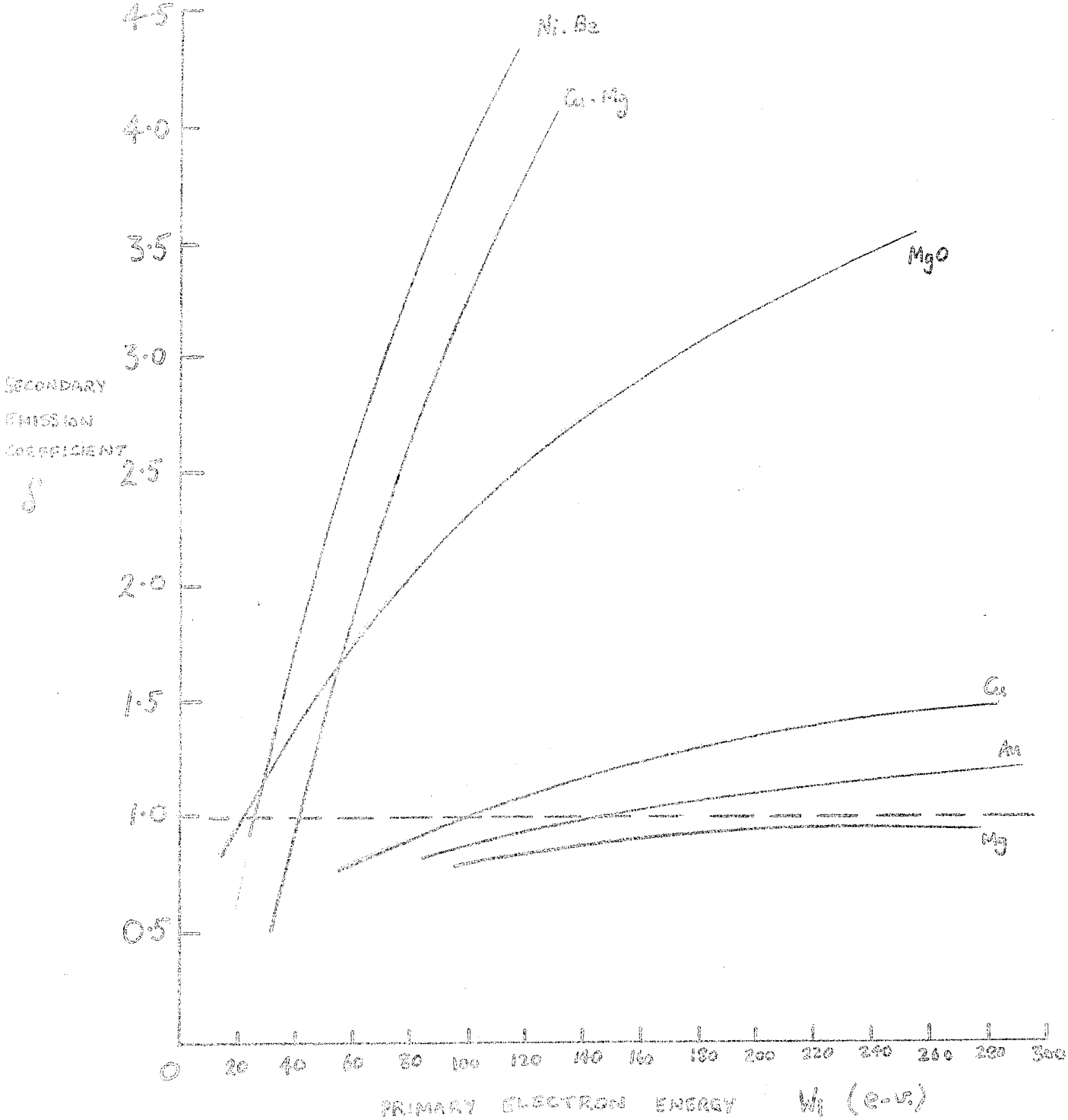

TABLE 2

SECONDARY ELECTRON EMISSION BY ELECTRON IMPACT.

MATERIAL	PRIMARY ENERGY W_i (e-v) for $\delta = 1$	δ_{MAX}	REFERENCE
COPPER	100	1·3	PETRY [46]
GOLD	140	1·46	WARNECKE [47]
BORON	80	1·2	KOLLER + BURGESS [48]
THALLIUM	70	1·7	GOLBRECHT + SPEER [50]
TIN	155	1·35	MOROZOV [51]
NICKEL-BERYLLIUM	25 *	12	MATTHES [43]
COPPER -MAGNESIUM	40*	13	SALOW [44]
SILVER-MAGNESIUM	50*	10·5	SALOW [44]
COPPER-ALUMINIUM	60*	10	SALOW [44]
MAGNESIUM OXIDE	20*	8	SALOW [44]

* OBTAINED BY EXTRAPOLATION

give a yield in excess of unity.

In Figure 17, the coefficient δ is plotted as a function of primary electron energy, expressed in electron volts, for a variety of pure metals, metal alloys and oxidised metal surfaces. The dotted line corresponds to a value $\delta = 1$. Table 2, derived from the same sources, lists primary energies corresponding to $\delta = 1$ and also gives the maximum δ values obtainable.

Relatively low yields are obtained from pure metals[41]. The primary energy required to release one secondary electron varies from metal to metal e.g. 70 e-v (Thallium), 100e-v (Copper); it usually lies in the range 100-200 e-v. Alloys, on the other hand, can give rise to higher values of δ, and the energy values for $\delta = 1$ (obtained by extrapolation of the data) are correspondingly lower, lying between about 25 e-v (nickel - beryllium) and 60 e-v (beryllium-copper). The curves for magnesium and magnesium oxide illustrate the large increases in δ which can be brought about by surface oxidation - an effect particularly associated with metals having a high oxygen affinity.

The brass electrodes used in the present work had an approximate composition of 60% copper and 40% zinc. Standard

chemical surface - cleaning processes were used, as described in Section 3.2.3; in addition, routine clean-up using a glow discharge was frequently carried out. All the early measurements were taken in the reducing gas hydrogen and during this period (lasting many weeks) the electrodes were continuously immersed in the gas. Nevertheless, the exact state of the surfaces was not known and they may have contained absorbed oxygen.

Although conclusive evidence is not available due to lack of data regarding the electrode materials used, a comparison between the calculated arrival energies, Figure 16 and the emission curves shown in Figure 17 suggests that a range of ϕ values exist which will give rise to a secondary emission coefficient sufficiently greater than unity to enable breakdown to take place by the to-and-fro motion of an oscillatory electron stream.

5.1.4 Calculations at smaller electrode separations

Electrons moving away from an electrode at time ϕ/ω (ϕ negative) are retarded in their progress along to positive direction of x until at a time subsequent to t = o, when the field polarity is reversed. Under certain phasing conditions, at the larger electrode separations, electrons may in fact be drawn back for a short distance towards their parent electrode,

before the accelerating field finally sweeps them to the opposite electrode.

A detailed study of electron motion in transit across the gap, given below, shows that for separations below 3 cm., electrons may be returned to their parent electrode surface, making the straightforward phasing mechanism inapplicable.

In order to investigate electron displacement as a function of transit time, it is first necessary to calculate electron velocity at times intermediate between ϕ/ω and $\frac{\pi + \phi}{\omega}$.

Modifying equation (30) for very low pressures

$$v = v_t = \frac{e E_p}{m\omega} (\cos\phi - \cos\omega t) + v_o \quad \ldots \quad (33)$$

If x be the electron displacement at time t, then by integration

$$x = \left(\frac{e E_p}{m\omega} \cos\phi + v_o\right)\left(t - \frac{\phi}{\omega}\right) - \frac{e E_p}{m\omega}\left[\sin\omega t - \sin\phi\right] \quad \ldots \quad (34)$$

$$\left(x = o \text{ when } t = \frac{\phi}{\omega} \right)$$

The variation of v with x can thus be calculated.

16. Motion of Electron in Transit between Electrodes

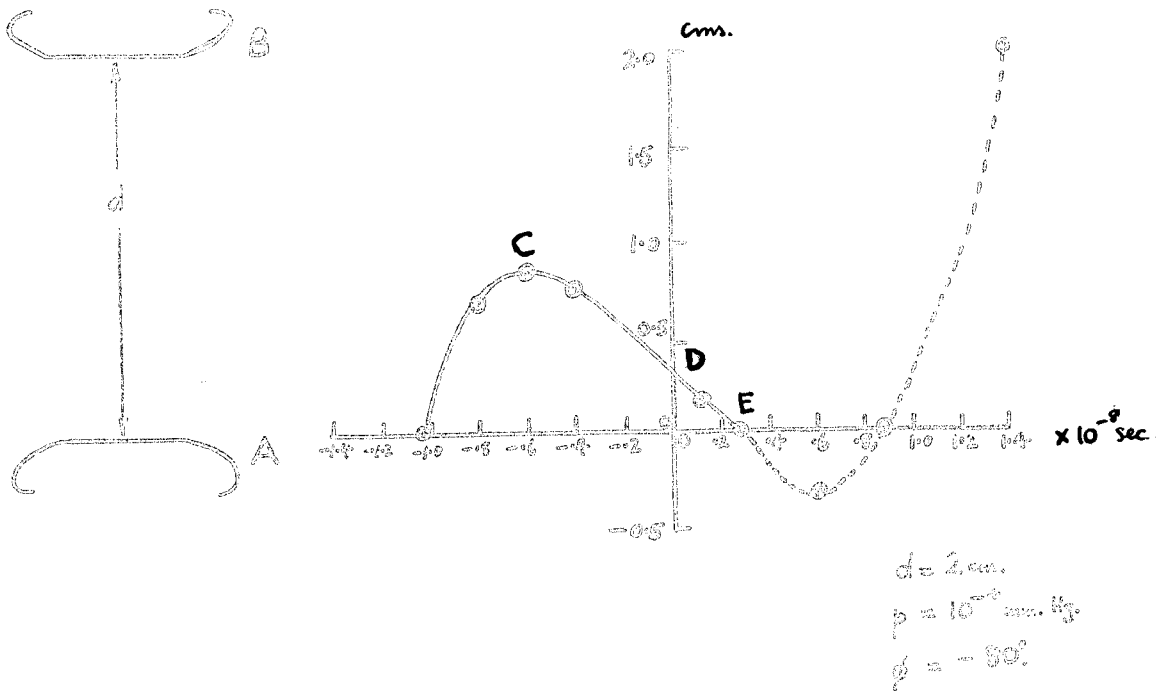

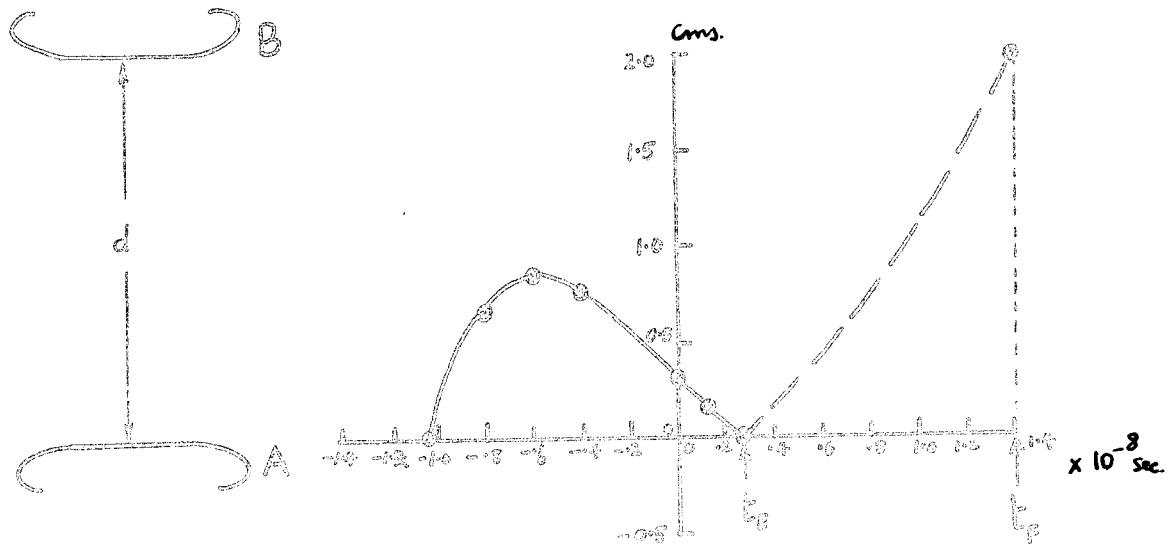

An analysis is given below (typical of the low separation results) for d = 2 cm., $\phi = -80^{\circ}$, p = 10^{-4} mm.Hg. Substituting known values into equation (34)

$$x = 0.27 + (4.49\ 10^{8}t - 4.74 \sin\omega t)$$

The curve relating x and t is shown in Figure 18a.

It is seen that an electron released from electrode A first moves across the gap to point C (a displacement of about 0.8 cm.), whereupon its motion is reversed by the field. At t = o, corresponding to point D, change in field polarity is incapable of preventing return to the parent electrode at time 0;24. 10^{-8} sec. (point E). Mathematically derived values beyond this point using equation (34) which assumes electron motion to be conditional only by theapplied field - cannot therefore have any real significance; the curve beyond E is shown dashed.

A modified breakdown mechanism will now be considered. If n starting electron give rise to $n\delta_A$ electrons due to secondary emission from impact at electrode A and $n_B = n\delta_A\delta_B$ due to emission from electrode B, then for breakdown,

$$n_B > n$$

i.e. $$\delta_A\delta_B > 1$$

The velocities corresponding to both impacts may be calculated. For electrons returning to electrode A (point E, Figure 18a) the arrival velocity V_A may be obtained by direct substitution in equation (33).

New boundary conditions must be fitted to equation(14) to enable impact velocity v_B at electrode B to be determined.

In its simplified form, for low pressures, equation (25) may be written as

$$v = \frac{e E_p}{m\omega} \cos\omega t + C$$

Let the emission velocity of electrons striking the parent electrode, at time t_E, be v_{oE}.

Then $v_{oE} = \frac{e E_p}{m\omega} \cos\omega t_E + C$

$$\therefore \quad v = v_{oE} + \frac{e E_p}{m\omega} (\cos\omega t - \cos\omega t_E) \quad \ldots \quad \ldots \quad (35)$$

When $t = t_F = \frac{\pi + \phi}{\omega}$, $v = v_i = v_B$

$$\therefore \quad v_B = v_{oE} + \frac{e E_p}{m\omega} (\cos\omega t_F - \cos\omega t_E) \quad \ldots \quad \ldots \quad (36)$$

For the case considered:

Impact velocity on parent electrode

$$v_A = 3.95.\ 10^8 \text{ cm./sec.(From (33))}$$

(44 e-v)

$$v_B = 6.72.\ 10^8 \text{ cm./sec.(from (36) neglecting } v_{oA})$$

(128 e-v)

From the available secondary emission data it would appear that the velocity values are large enough to sustain a growth in electron population, though once again a critical test of the mechanism is not possible.

The displacement-time curve for the period $t_E \rightarrow t_F$, obtained by integrating equation (35) is shown by the broken curve in Figure 18b.

Here

$$x = \frac{e E_p}{m\omega^2} (\sin \omega t - \sin t_E) - \frac{e E_p}{m\omega} \cos \omega t_E (t_F - t_E) \quad \ldots \quad (37)$$

In the above calculations it has been assumed that the time interval between an electron striking a metal surface, and a secondary electron leaving it, is small compared with a period of the applied field. The emission interval has, in fact, been found experimentally to be about 10^{-12} sec.,

negligibly small compared with the field period; 2×10^{-8} sec.

5.2 Breakdown at intermediate pressures

5.2.1 Effect of increasing gas pressure

The breakdown field values at 20 Mc/s show no abrupt changes for increased gas pressure. However, it will be shown that the initiation of a discharge through a mechanism dominated by secondary emission from the electrode faces cannot be sustained at pressures corresponding to the electrons making many collisions in transit across the gap. For the highest pressures used, the breakdown data conforms with the diffusion theory of high frequency breakdown. From the absence of discontinuities in the breakdown curves, it would appear that a smooth transition takes place between the two mechanisms.

Quantitative analysis of results in this region proved very difficult and it must be admitted that it has not been possible to formulate a complete picture of events leading to breakdown. Nevertheless, it can be shown that as the pressure is increased beyond values for which the mean free path is small compared with electrode separation, the efficiency of ionization increases, and the impact velocity of electrons on electrode faces decreases. The points are

19. Variation of electron arrival velocity with gas pressure hydrogen 20 l c/s.

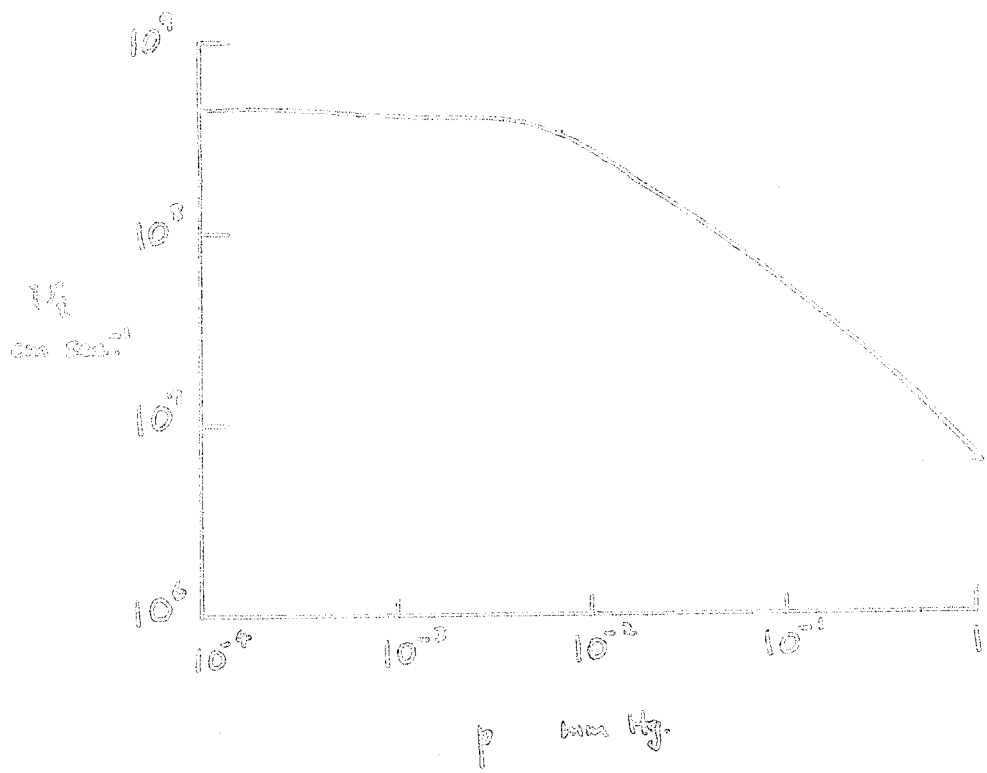

established below.

Changes in impact velocity v_i as a function of pressure are calculable from equation 31, namely,

$$v_i = v_o \exp\left(-\frac{\nu_c \pi}{\omega}\right) + \frac{e E_p}{m(\omega_c^2+\omega^2)} \left[1 + \exp\left(-\frac{\nu_c \pi}{\omega}\right)\right] \left(\cos\phi - \frac{\nu_c}{\omega}\sin\phi\right)$$

Also $\nu_c = 5.93 \cdot 10^9 \, p$ ... ... (21)

Using known atomic data together with experimentally determined values of E_R, v_i can be found at a given phase angle for a range of gas pressures.

A set of results is shown in Figure 19. The impact velocity is seen to remain substantially constant at its 'free space' value for pressures up to the point at which the mean free path fills the tube and thereafter exhibits a steady decrease with further increase in pressure. Thus the contribution of secondary electrons towards a build-up of electron population becomes progressively less effective.

5.2.2 Change of ionizing efficiency with gas pressure

Collision ionization in a gas is usually described in terms of Townsend's primary coefficient α , or in related terms such as ionization rate v_i and ionizing efficiency S_e.

Both theory and experiment show that in a given gas α /p is a continuous function of the reduced field E/p.

In evaluating the increase in ionization due to increase in gas pressure, recourse must be made to the experimental data available.

Two approaches were made, one based upon Von Engel & Steenbeck's[5] ionizing efficiency - electron energy curve, the other using Von Engel's[40] $\frac{\alpha}{p} - \frac{E}{p}$ plot. In each case analysis was complicated by the necessity of introducing the time variation of electric field strength.

(a) Evaluation based upon the ionizing efficiency-electron energy curve

At a given pressure, the number of ion pairs produced by an electron in a lifetime limited by mobility capture may be deduced from the breakdown data by finding

(i) electron velocity (and hence, energy) as a function of displacement across the gap,

(ii) ionizing efficiency S_e as a function of displacement x, and

(iii) integration of S_e dx over the whole gap.

(i) Electron velocity at various times in transit across the gap is given by the generalised equation

$$v = \frac{e\,E_p}{m(\omega^2+\nu_c^2)}\,(\nu_c \sin\omega t - \omega\cos\omega t)$$

$$+ \left[v_o + \frac{e\,E_p}{m(\omega^2+\nu_c^2)}\,(\nu_c\sin\phi - \omega\cos\phi \right]$$

$$x \quad \exp\left(\frac{\nu_c\phi}{\omega}\right) \quad \exp(-\nu_c t) \qquad \ldots \quad \ldots \quad \ldots \qquad (30)$$

To obtain a displacement-time relationship it is necessary to integrate the above equation i.e.

$$\int_o^x dx = \frac{e\,E_p}{m(\omega^2+\nu_c^2)} \int_{\frac{\phi}{\omega}}^{t} (\nu_c \sin\omega t - \omega\cos\omega t)\,dt$$

$$+ \left[v_o - \frac{e\,E_p}{m(\omega^2+\nu_c^2)}\,(\nu_c\sin\phi - \omega\cos\phi) \right] \exp\left(\frac{\nu_c\phi}{\omega}\right) \int_{\frac{\phi}{\omega}}^{t} \exp(-\nu_c t)\,dt$$

$$\therefore\ x = \frac{e\,E_p}{m(\omega^2+\nu_c^2)} \left[\left(\frac{\nu_c}{\omega}\cos\phi + \sin\phi\right) - \left(\frac{\nu_c}{\omega}\cos\omega t + \sin\omega t\right) \right]$$

$$- \frac{1}{\nu_c} \left[v_o - \frac{e\,E_p}{m(\omega^2+\nu_c^2)}\,(\nu_c\sin\phi - \omega\cos\phi) \right] \exp\left(\frac{\nu_c\phi}{\omega}\right) \left[\exp(-\nu_c t) \right.$$

$$\left. - \exp\left(-\frac{\nu_c\phi}{\omega}\right) \right] \qquad \ldots \quad \ldots \quad \ldots \qquad (38)$$

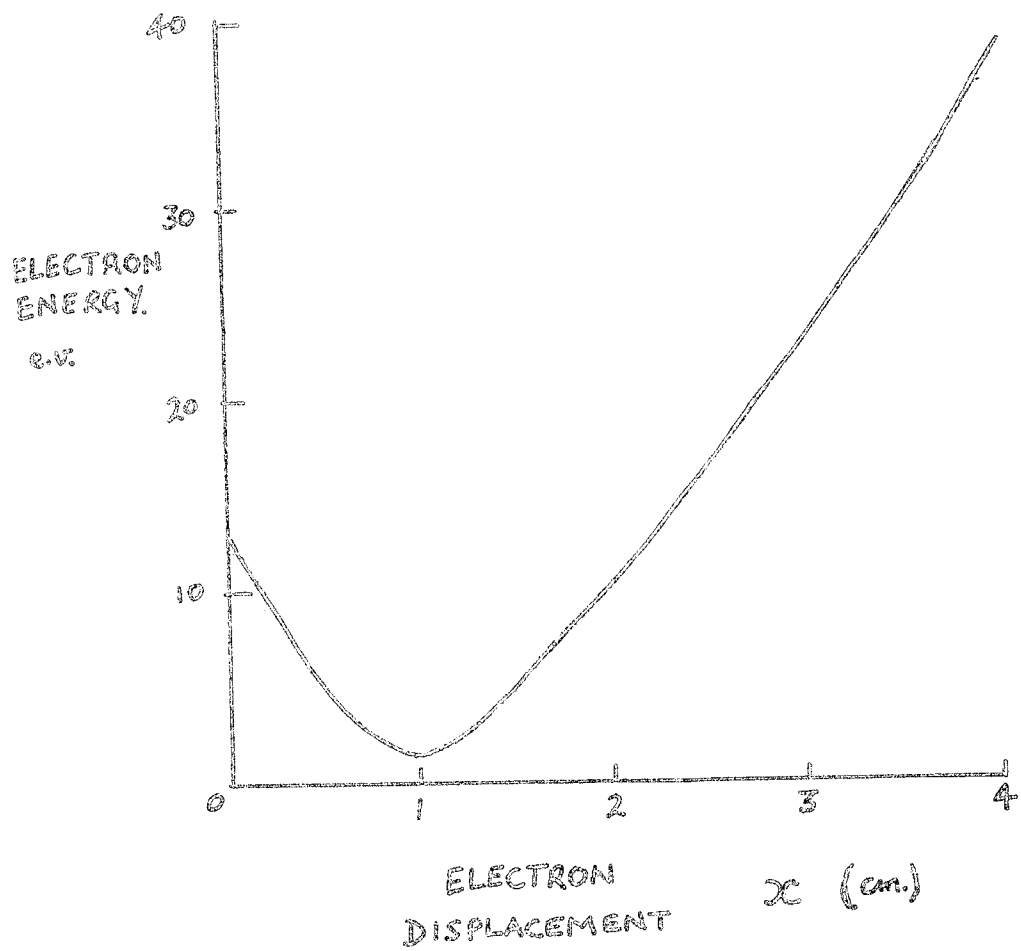
40
30
20
10
0
1
2
3
4
ELECTRON ENERGY.
e.v.
ELECTRON DISPLACEMENT
x (cm.)

To produce a continuous v - x curve at a particular pressure, tedious calculation is required to obtain sets of values of v and x at corresponding times, using equations (30 and (38).

For the case d = 4 cm., $\phi = -60^{\circ}$, p = 0.005 mm.Hg., the velocity-time is given in Figure 20a and the velocity-displacement in Figure 20b. The early decrease in velocity is a result of the field initially retarding the electrons.

Since $\frac{1}{2} mv^2 = e V$, an energy displacement curve msy be drawn. This is shown in Figure 21.

(ii) The electron ionizing efficiency S_e is defined as the number of ion pairs produced by one primary particle, reduced to 1 mm.Hg.

If the probability of a collision resulting in ionization is f_e, it is related to S_e by

$$S_e = \frac{f_e}{\lambda_e} \quad \left(= Q_i \text{ which is the cross-section for ionization by electron collision} \right)$$

Von Engel[5] reproduces measured values of S_e in hydrogen as a function of electron energy. The curve rises sharply from zero $V = V_i$ (as expected on Bohr theory), reaches a maximum at energies a few times V_i and then decreases.

22. Ionizing Efficiency vs. Electron Displacement.

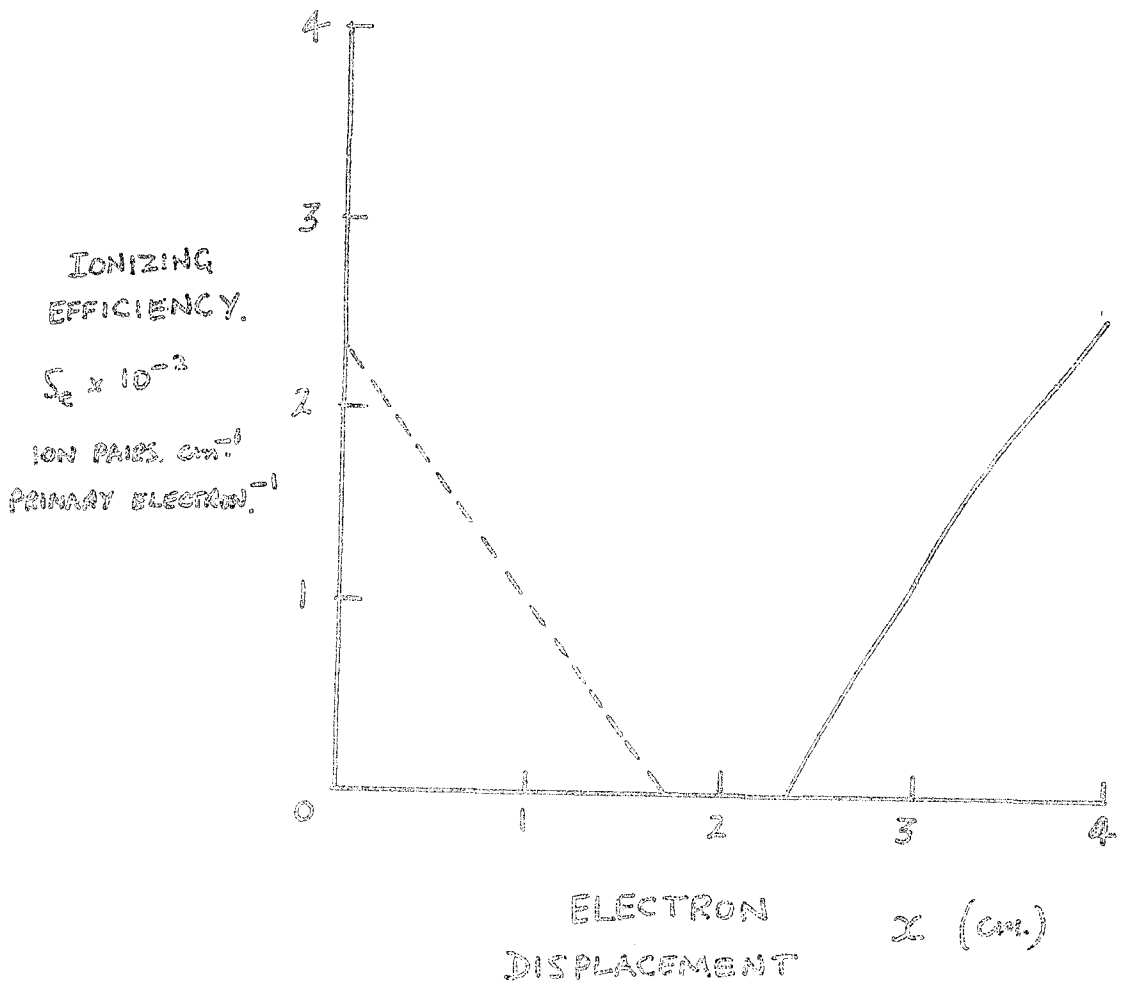

Due to double-log plotting, values of S_e cannot easily be read from the curve. However, it is found[5] that for energies below the maximum, the rise in S_e is approximately linear, obeying the empirical equation:

$$S_e = ap\,(V - V_i) \qquad \ldots \quad \ldots \quad \ldots \qquad (39)$$

where 'a' is a constant for a particular gas.
For hydrogen 'a' = 21.10^{-2} in appropriate units.

Using equation (38) in conjunction with figure 21, it is, therefore, possible to calculate values of S_e at various points in the gap. This is shown in Figure 22.

It is seen that for $x < 2.3$ cm., $S_e = 0$. This separation corresponds to $V = V_i$. Between 2.3 and 4 cm., S_e rises steadily as the electron gains energy. The dotted curve in the figure shows the ionizing effect of an electron travelling in the reverse direction.

(iii) The number of ion pairs produced per electron in transit across the gap is given by $n_f = \int_o^d S_e\,dx$.

By graphical method, for the case considered, $n_f = 0.02$ ion pairs.

The above analysis affords calculation of the number of

ion pairs produced in the gap and could be extended to other pressures. However, in view of the lengthy nature of the calculations, an alternative approach was made, making use of known variations of α /p with E/p.

(b) Evaluation using α /p - E/p curve

From the definition of Townsend's primary coefficient,

$n = \exp\left(\int_0^x \alpha \, dx\right)$ where n is the normalised number of electrons emerging from a plane x cm. from the origin, in the field direction.

Hence $n_f = \exp\left(\int_0^x \alpha \, dx\right) - 1$ ... ... (40)

For a given gas $\frac{\alpha}{p} = F_1 \left(E/p\right)$

The instantaneous value of α in an h.f. field may be considered the same as the steady value in a steady field of the same strength (see, for example, Pim[31]).

Using this concept,

$$\frac{\alpha}{p} = F_1 \left(E_p \frac{\sin \omega t}{p}\right)$$

Experimentally[40], the variation of α/p with increasing E/p in hydrogen shows an initial increase up to an E/p value of about

23. Variation of α/p with phase of Applied Field.

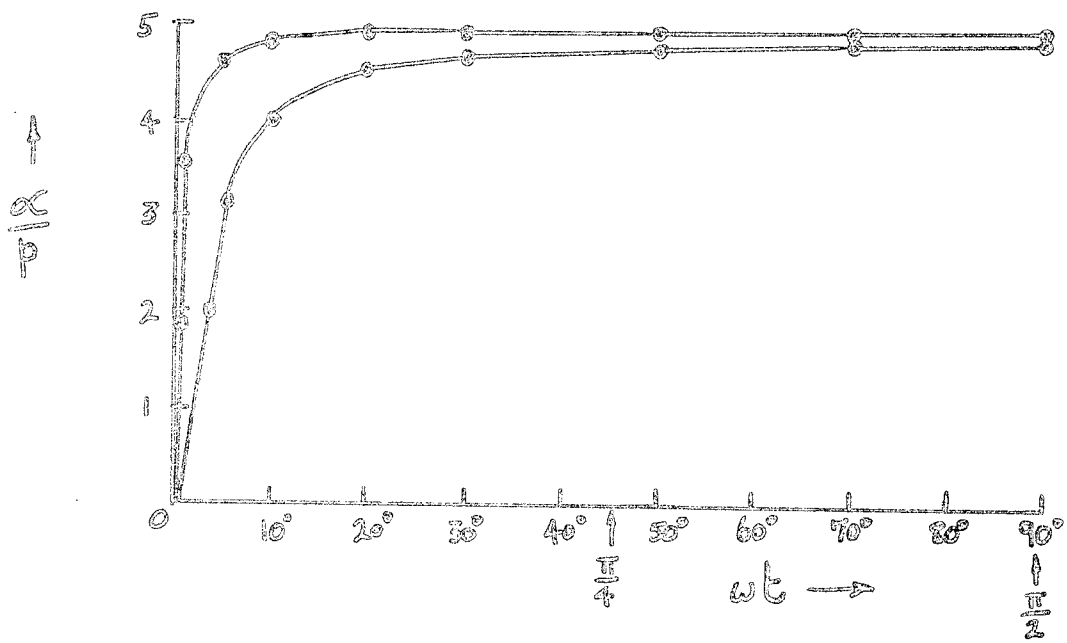

600; for higher values of E/p values of α/p remain approximately constant.

Mathematically the curve is represented by a semi-empirical relation[5],

$$\frac{\alpha}{p} = A \exp\left(-\frac{B}{E/p}\right) \quad \ldots \quad \ldots \quad \ldots \quad (41)$$

A and B being constants.

Range of validity of E/p,

22 - 1000.

$$\therefore \int \alpha \, dx = pA \int \exp\left(\frac{-B}{E_p \sin \omega t/p}\right) v. \, dt \quad \ldots \quad (42)$$

Values of v in transit across the gap are given by equation (30). Hence, by calculation of v and the experimental term at various times in transit across the gap, the integral may be evaluated by graphical method.

A simplified, though less exact, form of equation (42) will now be considered.

At the lower pressure it is seen that for all but very small values of ωt (and hence $E = E_p \sin \omega t$), α/p remains almost at a value close to A. (5 ion pairs/cm. mm.Hg.). The

24. Calculated ion-pair production as a function of gas pressure.

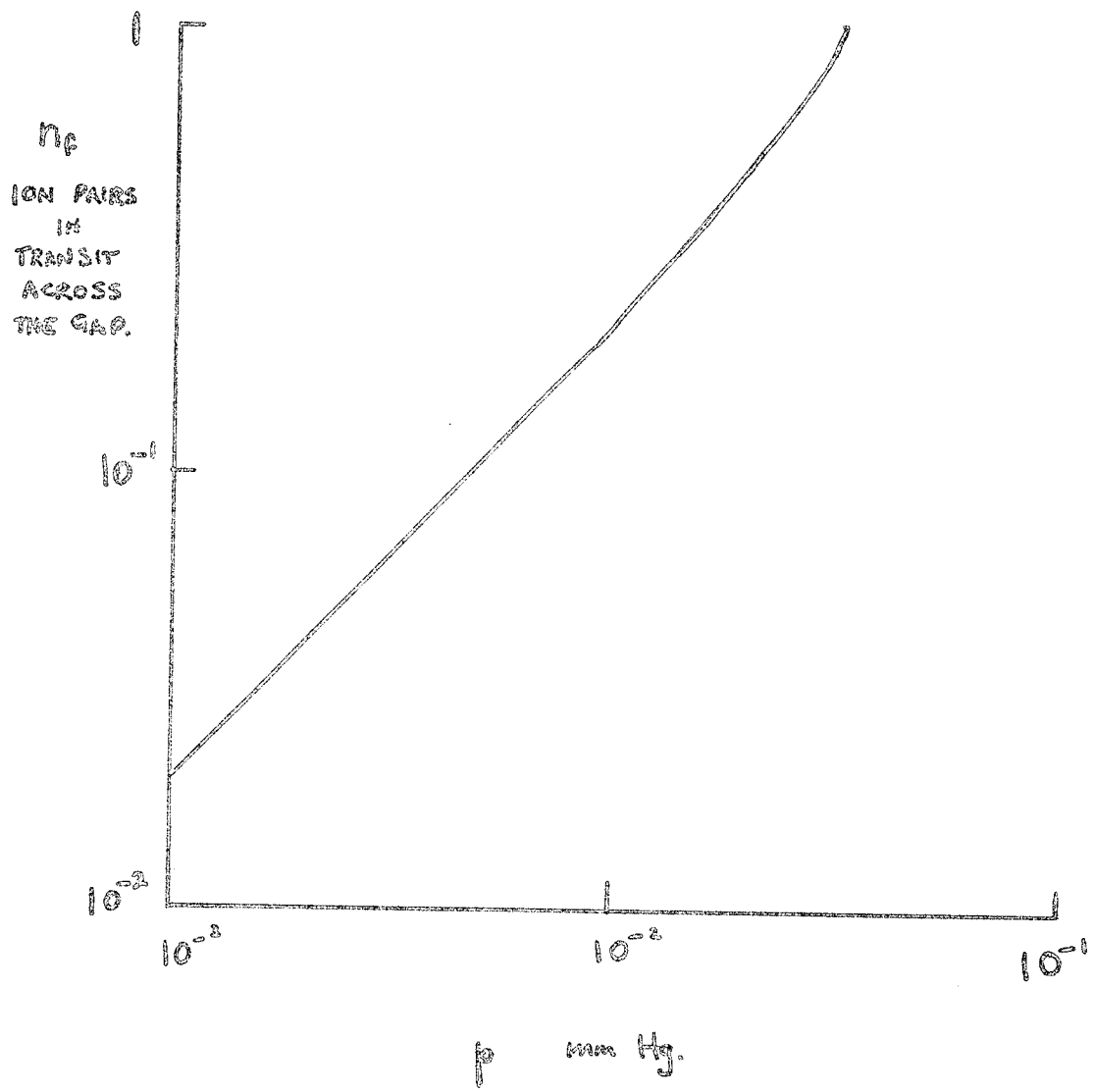

slope of the curve indicates that at the high E/p values encountered during most of a cycle of the applied field, almost all collisions will result in ionization, making α/p virtually independent of the reduced field strength. The curve plotted for a pressure of 0.005 mm.Hg. is similar, although the flat portion of the curve is reached more gradually and the maximum value of α/p is slightly smaller.

Over much of the intermediate pressure range α/p may be considered roughly constant, independent of both time variation of the electric field and of E/p i.e. the exponential term in equation (41) tends to unity.

Hence $\alpha/p \rightarrow A$.

Equation (34) then reduces to

$$\int_0^d \alpha \, dx = Ap \int v \, dt = Ap \int dx = Apd.$$

$$\therefore \quad n_f = \exp(Apd) - 1 \quad \ldots \quad \ldots \quad \ldots \quad \ldots \qquad (43)$$

i.e. the number of ion-pairs created in the gap rises steadily with increasing gas pressure.

For the 4 cm. gap, the variation of n_f with gas pressure in the intermediate region, as expressed by equation (43), is shown in Figure 24. At higher gas pressures, the n_f values

are undoubtedly too large, due to the approximations introduced. Agreement between the two calculations at $p = 0.005$ mm.Hg. is not good (n_p values being 2.10^{-2} and 10^{-1} for the first and second calculations, respectively) probably due to the fact that the E/p value at this pressure is well outside the quoted range of validity of equation (41).

5.3 Electron losses

To establish a regular increase in electron population, their net rate of increase must exceed the rate of loss.

In a build-up dominated by secondary emission, removal from the system, at the lower pressures, is accounted for by the primary electrons entering the electrodes. In the general case the effective secondary emission coefficient of the electrode surfaces must be sufficiently in excess of unity to replace any further losses.

Depopulation - in terms of total removal from the cylinder of gas contained by the electrodes - is largely pressure dependent. A qualitative account of the possible processes will now be given.

(a) Volume Recombination

Volume recombination was considered to be unimportant in the range of pressures employed.

Neutralisation by way of direct ion-electron collision is an improbable event, due to the high relative velocities involved. Three-body processes are in general more effective. Such collisions are unlikely at low pressures and hydrogen is virtually a non-attaching gas.

The special type of dissociative recombination described by Fucks[11], and discussed in Section 1.3.2., can give rise to electron generation. However, the necessary sequence of events is most improbable below a few mm.Hg. Corrigan & Von Engel, who have studied excitation and dissociation in hydrogen by an electron swarm, neglect volume recombination in the pressure range 0.7 mm.Hg. - 12.mm. Hg.

(b) Diffusion

Thermal diffusion of electrons in a gaseous medium may be pictured as a 'random walk' of the particles away from regions of high concentration. Electron drift is therefore accompanied by a radial spread of charge.

By its very nature, losses from the system should be very small in the low pressure region $\nu_c < \omega$, corresponding to much of the experimental range. At higher pressures where electrons make many collisions per oscillation, diffusion becomes increasingly important, particularly when electrons are unable to reach the electrodes by oscillatory drift. Results at the higher pressures used are seen in the following section to conform to such behaviour.

Quantitatively, little headway could be made at the low pressures. The basic diffusion equations were found to be inapplicable under experimental conditions.

5.4 Applicability of diffusion theory at higher pressures

5.4.1 Limits of the diffusion theory

For the highest pressures investigated, breakdown may be expected to conform with the diffusion theory of high-frequency breakdown.

The requirements of the diffusion theory- that under threshold conditions the gain in electron population due to collision ionization shall just replace diffusive losses - demand a number of experimental conditions to be observed,[13] namely:

(a) that each electron make at least one ionizing collision before it leaves the tube.

In the limiting case, the electron mean free path λ_e becomes equal to the characteristic diffusion length A and to conform with theory $\lambda_e \leq \Lambda$.

The characteristic diffusion length Λ is determined by the geometry of the electrode system and for a cylinder of height d and radius R has been evaluated[13] as:

$$\frac{1}{\Lambda^2} = \left(\frac{\pi}{d}\right)^2 + \left(\frac{2.405}{R}\right)^2$$

TABLE 3.

CHARACTERISTIC DIFFUSION LENGTHS.

d (cm.)	Λ (cm.)
4	1·08
3	0·87
2	0·61
1	0·30

TABLE 4.

PRESSURES AT WHICH $\lambda_e = \Lambda$,

FOR VARIOUS GAP WIDTHS.

d (cm.)	p (mm. Hg.)
4	0·019
3	0·023
2	0·032
1	0·068

Calculations of Λ for various values of electrode separation d are given in Table 3. The proper value of R is a matter of some doubt, since the field strength gradually decreases away from the flat central region of the electrodes: the value used is that between the centre and periphery of an electrode.

Since $\lambda_e = \frac{1}{49_p}$ (over a fair range of electron energies) ... ... (17)

the condition becomes:

$$p \geq \frac{1}{49\Lambda}$$

Hence the limiting pressure for various electrode separations d may be calculated. These are given in Table 4.

(b) that uniform field conditions are obeyed.

A further requirement can be written in terms of the size of the discharge tube permissable to sustain a single loop of a standing wave of the applied field i.e. $\frac{\lambda}{2} \geq \Lambda$.

Since $d \ll \lambda$ for all the electrode separations used, the uniform field condition is obeyed.

(c) that electrons, by virtue of their oscillatory motion, oscillate within the confines of the gap.

Hence $x_o \leq d/2$ ... ... (44)

TABLE 5.

d (cm.)	p (mm. Hg.)
4	ALL PRESSURES
3	$3{\cdot}5 \cdot 10^{-2}$
2	$1{\cdot}3 \cdot 10^{-1}$
1	$0{\cdot}5 \cdot 10^{-1}$

Alternatively, defining the electron ambit d_e as the displacement in a half-cycle of the field

$$d_e = 2x_o$$

$$\therefore \quad d_e \leq d.$$

From equation (29)

$$x_o = \frac{e E_p}{m\omega(\omega^2+\nu_c^2)^{\frac{1}{2}}}$$

the variations of x_o with p under experimental conditions have been plotted in Figure 15. (It should here be restated that the accuracy of the plot - and all calculations involving the collision frequency term - is dependent upon the assumption that $\nu_c \propto p$ (Section 4.4)).

Using Figure 15, the limiting pressures corresponding to equality of equation (44) are given in Table 5.

The limiting pressures thus decreases with increasing separation, as expected.

For the 4 cm. gap, the electron ambit and electrode separation are almost equal for pressures below about $5.\ 10^{-3}$ mm.Hg. However, in this range electrons are still capable of crossing the gap during a half-cycle under suitable

initial conditions, as previous analysis has shown - values given in the table refer specifically to motion which is purely oscillatory.

It is evident from the calculations based upon diffusion theory requirements that the oscillation amplitude condition effectively limits the pressure range under which diffusion theory may be applied. To test the theory use may be made of the expression derived by Prowse & Clark[29], namely that under diffusion controlled conditions.

$$F_1\left(\frac{E_R}{p\Lambda}\right) = \frac{m}{3e} \cdot \frac{1}{E_R \Lambda_p \Lambda} \cdot F_2\left(\frac{E_R}{p\Lambda}\right) \quad \ldots \quad \ldots \quad (45)$$

F_1 and F_2 are functions depending upon the nature of the gas. The curve relating $E\Lambda$ and $p\Lambda$ is thus unique for any one gas and provides a stringent test for the applicability of the theory. For low gas pressures where ν_c is comparable with ω, the R.M.S. field E_R in equation (45) should be modified to read E_e; where E_e is the effective field for energy transfer (see Section 4.4).

E_e is related to E_R by

$$E_e^2 = \frac{E_R^2 \nu_c^2}{\omega^2 + \nu_c^2} \quad \ldots \quad \ldots \quad (22)$$

25. Diffusion Controlled Breakdown

$E_b\Lambda \propto 1/\ $, results of various workers

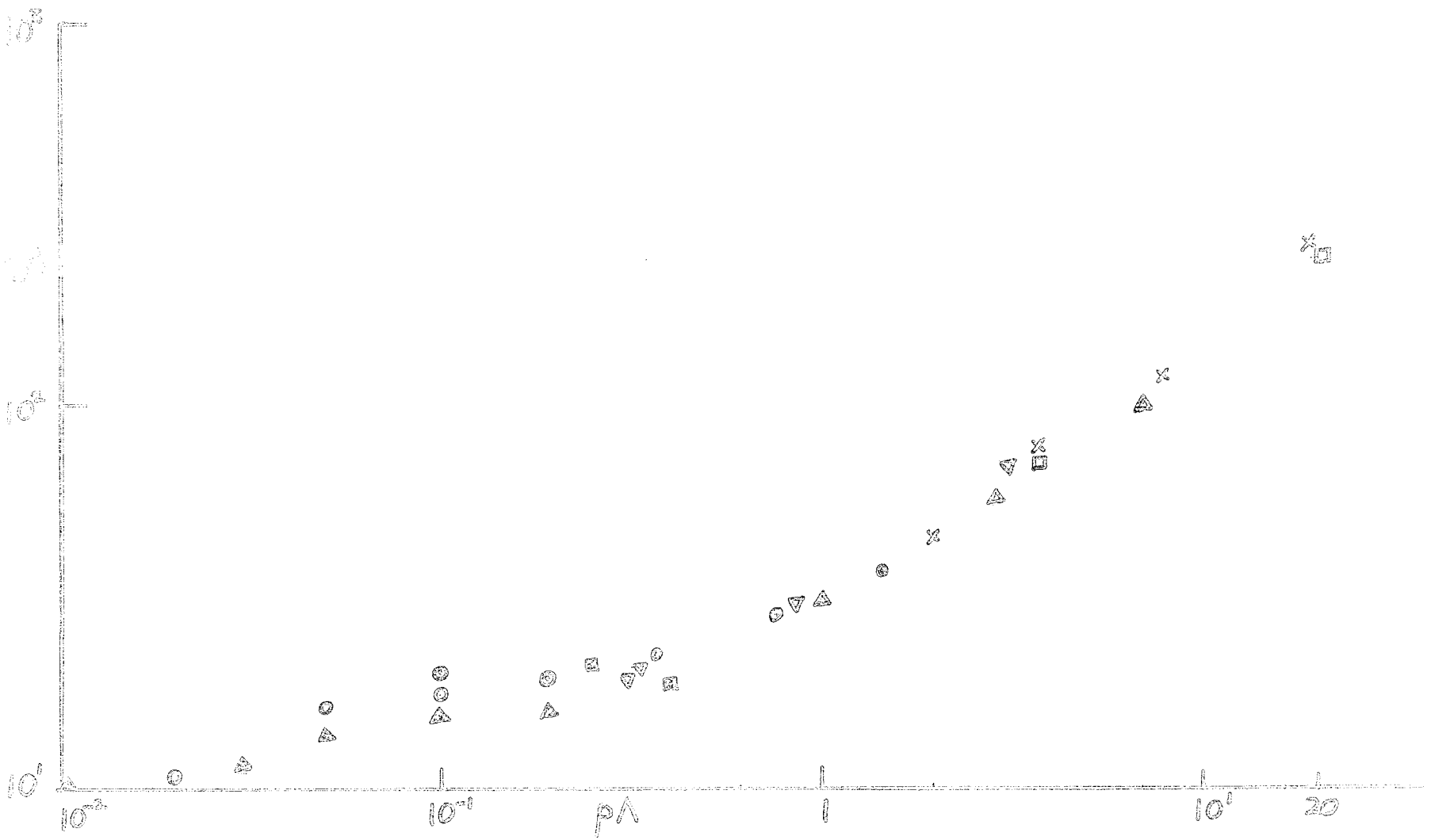

5.4.2 $E_e\Lambda$ - $p\Lambda$ Results

Since the $E_e\Lambda$ - $p\Lambda$ curve is unique for hydrogen in the diffusion controlled region, and therefore independent of frequency, the experimental results at 20 Mc/s should be on the same curve as measurements taken by other workers, using different electrode geometries and field frequencies.

The plot is shown in Figure 25, using the author's results and those of Brown and McDonald[13], Thompson[27] and Clark[32].

It is seen that by a short smooth extrapolation of the other worker's data, the 20 Mc/s results are in reasonable conformity with the diffusion theory.

For constant $p\Lambda$, corresponding values of $E_e\Lambda$ for different gap widths tend to exhibit a small but characteristic increase as d is decreased. It is difficult to conclude whether or not this change is significant - the spread of results is little more than that between those on the common curve at higher $p\Lambda$ values. Also, pressures measured above 0.1 mm.Hg. were subject to error due to a cramping of the Pirani gauge near the limit of its scale. Apart from this reservation, it may be concluded that breakdown at the high pressures is initiated when the loss of electrons by diffusion is slightly more than made up by

production through collision ionization.

5.4.3 Onset field values in diffusion controlled discharges. - Discussion

One of the features of the hydrogen results shown in Figure 12, is that the minimum values of field strength recorded for breakdown under diffusion-limited conditions are lower than have been hitherto reported. A comparison with the results obtained at microwave frequencies[13] is particularly interesting.

It has already been mentioned[29] that the curve relating $E_p\Lambda$ and $p\Lambda$ is unique, for a given gas, when breakdown conditions accord with the diffusion theory. For a system with fixed electrode geometry (Λ and hence d constant) reduction in gas pressure gives rise to a progressive lowering of onset field strength, provided that the electrons make many collisions/oscillation. This is a consequence of the fact that as pressure is reduced, electron mean free path is increased, and hence the energy gained from the field per collision rises.

Under such conditions field frequency is not significant and similar field values are required for breakdown in a frequency range extending from a few megacycles up to the microwave region (as evidenced by results at widely different frequencies lying on a common $E\Lambda$ - $p\Lambda$ curve).

At microwave frequencies, reduction of field strength with

TABLE 6.

DIFFUSION-CONTROLLED BREAKDOWN IN HYDROGEN. LIMITING CONDITIONS AND TRANSITIONS AT 3000 Mc/s AND 20 Mc/s.

CHARACTERISTIC DIFFUSION LENGTH $\Lambda = 1{\cdot}08$ cm. $(d = 4$ cm.$)$.

		LIMITING CONDITION	LIMIT AT FREQUENCY OF	
			3000 Mc/s.	20 Mc/s.
a	COLLISION FREQUENCY TRANSITION	$\nu_c \gg \omega$ $p \geqslant \frac{2\pi}{5{\cdot}9.10^9} \cdot f$ mm. Hg.	$p \geqslant 3{\cdot}2$ mm. Hg.	$p \geqslant 2{\cdot}1.10^{-2}$ mm. Hg.
b	MEAN FREE PATH LIMIT	$\lambda_e < \Lambda$ $p \geqslant \frac{1}{p_e \Lambda} = \frac{1}{49\Lambda}$	$p \geqslant 1{\cdot}8.10^{-2}$ mm. Hg.	
c	OSCILLATION AMPLITUDE LIMIT	$d \geqslant d_e = 2x_o$ CALCULATION FROM EQUATION 29.	$d > d_e$ for all fields and pressures encountered	$p \geqslant 5.10^{-3}$ mm. Hg.
d	UNIFORM FIELD LIMIT	$\lambda/2 \geqslant \pi\Lambda$ $\Lambda \leqslant \frac{c}{2\pi\Lambda} \cdot \frac{1}{f}$	$\Lambda \leqslant 1{\cdot}6$ cm.	$\Lambda \leqslant 240$ cm.

decreasing pressure is not continuous, even within the limits of diffusion control. For a frequency of 3000 Mc/s., the Collision Frequency transition ($\nu_c = \omega$) occurs at p = 3.2 Mm.Hg. (Case (a), Table 6). Further reduction in p necessitates a rise in field strength, since transfer of energy between field and gas becomes less efficient.

On the other hand, at 20 Mc/s, the transition occurs at $p \simeq 2.10^{-2}$ mm.Hg. Hence, providing the natural limits of the diffusion theory are complied with within the range 3.2 mm.Hg. - 2.10^{-2} mm.Hg. lower ultimate values of breakdown stress are possible at this frequency.

Table 6 relates the limiting pressure values for the gap ($\Lambda = 1.08$ cm.) with reference to the Mean Free Path and Oscillation Amplitude limits (cases (b) and (c)); it is seen that diffusion control is limited by the mean free path filling the tube at $p \simeq 1.8.10^{-2}$ mm.Hg., a value close to that for the Collision Frequency transition.

Increase in size of the discharge tube - and hence increase in Λ - causes a reduction in threshold field strength, since diffusion losses from the system are reduced. The scaling process is limited, however, by the frequency-dependent Uniform Field limit, if the diffusion theory is to be applicable. Maximum

values of are given in Table Case (d) and show that a value $\Lambda = 1.6$ cm. must not be exceeded at 3000 Mc/s. The corresponding value at 20 Mc/s, on the other hand, is much larger than has yet been used in practice.

It may be concluded that the low breakdown fields here reported in hydrogen arise from a choice of field frequency and electrode geometry which enable the diffusion theory, in the region where electrons make more than one collision per oscillation, to be complied with down to relatively low pressures.

6. BREAKDOWN IN HYDROGEN AT 10 Mc/s. RESULTS FOR OTHER GASES

6.1 Breakdown in hydrogen at 10 Mc/s.

6.1.1 Experimental procedure

The experimental techniques employed in recording breakdown measurements at 10 Mc/s were very similar to those described for 20 Mc/s experiments. The tuned circuit master oscillator, based upon a 10 Mc/s quartz crystal, was tuned to resonate in the fundamental mode and the driver, power and coupling circuits appropriately adjusted.

Ultraviolet irradiation of the gap was again used. The threshold field was established by increasing the applied field in small steps until a discharge occurred; the process being repeated a number of times. Adequate intervals were allowed to take into account statistical lags and deionization times.

6.1.2 Variation of breakdown field with gas pressure at 10 Mc/s

The experimental plots are shown graphically in Figure 12, with R.M.S. breakdown field E_R given as a function of gas pressure for different electrode separations.

The form of the breakdown curves differ markedly from

the corresponding results at 20 Mc/s. With decreasing pressure the onset field strength rises sharply after an initially uniform region, measurements terminating in an abrupt cut-off.

At pressures above cut-off, field values were observed to decrease as the electrode separation was increased, in a manner similar to recordings at 20 Mc/s. Again, the cut-off pressures showed a characteristic decrease as the separation was increased.

6.1.3 Interpretation of the 10 Mc/s results

As described in Section 5.4.1 the application of the diffusion theory of high-frequency breakdown is restricted to certain ranges of the parameters involved (electrode separation, gas pressure, field frequency), in accordance with the limits prescribed by Brown & McDonald[13].

At 10 Mc/s, the experimental results lie within the mean free path and uniform field limits.

However, it will now be shown that the increases in field strength culminating in cut-offs may be attributed to departures from the diffusion theory, caused by progressive increases in the amplitudes of electron oscillation to the points at which the ambits completely fill the spaces between

26. Electron Emit as a Function of Gas Pressure. Hydrogen 1 a.c/s.

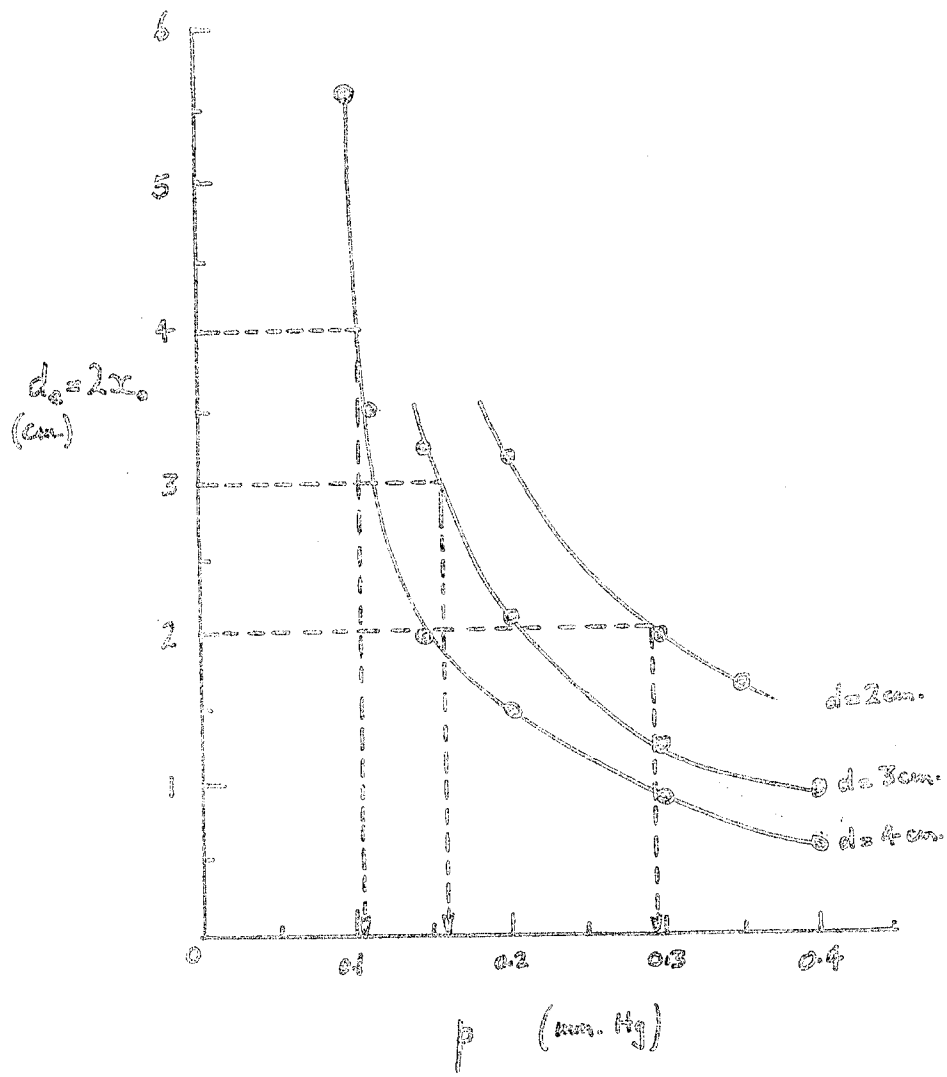

the electrodes.

From equations (29) and (44)

$$d_e = 2x_o = \frac{2e\,E_p}{m\omega(\omega^2+\nu_c^2)^{\frac{1}{2}}} \quad \ldots \quad \ldots \quad (46)$$

Using the data from figure 3 in conjunction with equation (46), changes in electron ambit with gas pressure may be plotted, and are given in Figure 26. From these curves, the critical pressures at which the electron ambits fill the interelectrode spaces may be located; these are marked in the figure using dotted lines. By transferring these calculations to the experimental E - p curve (see Figure 3) it is seen that for each value of electrode separation, the critical pressure lies on the sloping part of its relevant curve, at a point somewhat above the cut-off value.

From this evidence it seems reasonable to suppose that the characteristic rise of E with decreasing p is brought about by the gradual removal of electrons from the test gap by mobility capture, removal commencing at apressure corresponding to the foot of the slope and being complete at the cut-off value.

It should be pointed out that although precise theoretical information is lacking regarding the distribution of individual amplitudes in a swarm of electrons oscillating

at high frequency, a large body of experimental evidence indicates that the oscillation amplitude limit of the diffusion theory is a gradual process covering a finite range of the parameter involved - in this case, gas pressure.

6.2 Results in other gases

6.2.1 Experimental procedure

Breakdown measurements were also recorded in a second diatomic gas (nitrogen) and a monatomic gas (neon). Spectroscopically pure samples of gas provided by the British Oxygen Company Ltd. were used; no additional purification was attempted. In this respect the neon results must be treated with some reserve. (A. von Engel, in conversation with J.L. Clark, pointed out that small but significant amounts of argon must be expected in neon samples used from the above source. Additional ionization due to the Penning effect will, therefore, take place, causing variations in breakdown field values).

Standard methods of flushing the vacuum system were undertaken, as described inSection 3.3. Initiatory electrons were again provided by ultraviolet irradiation; statistical lags were found to vary between a few seconds and a minute or two, in extreme cases. There appeared to be no sigificant

27. Breakdown in Nitrogen, Neon and Hydrogen.

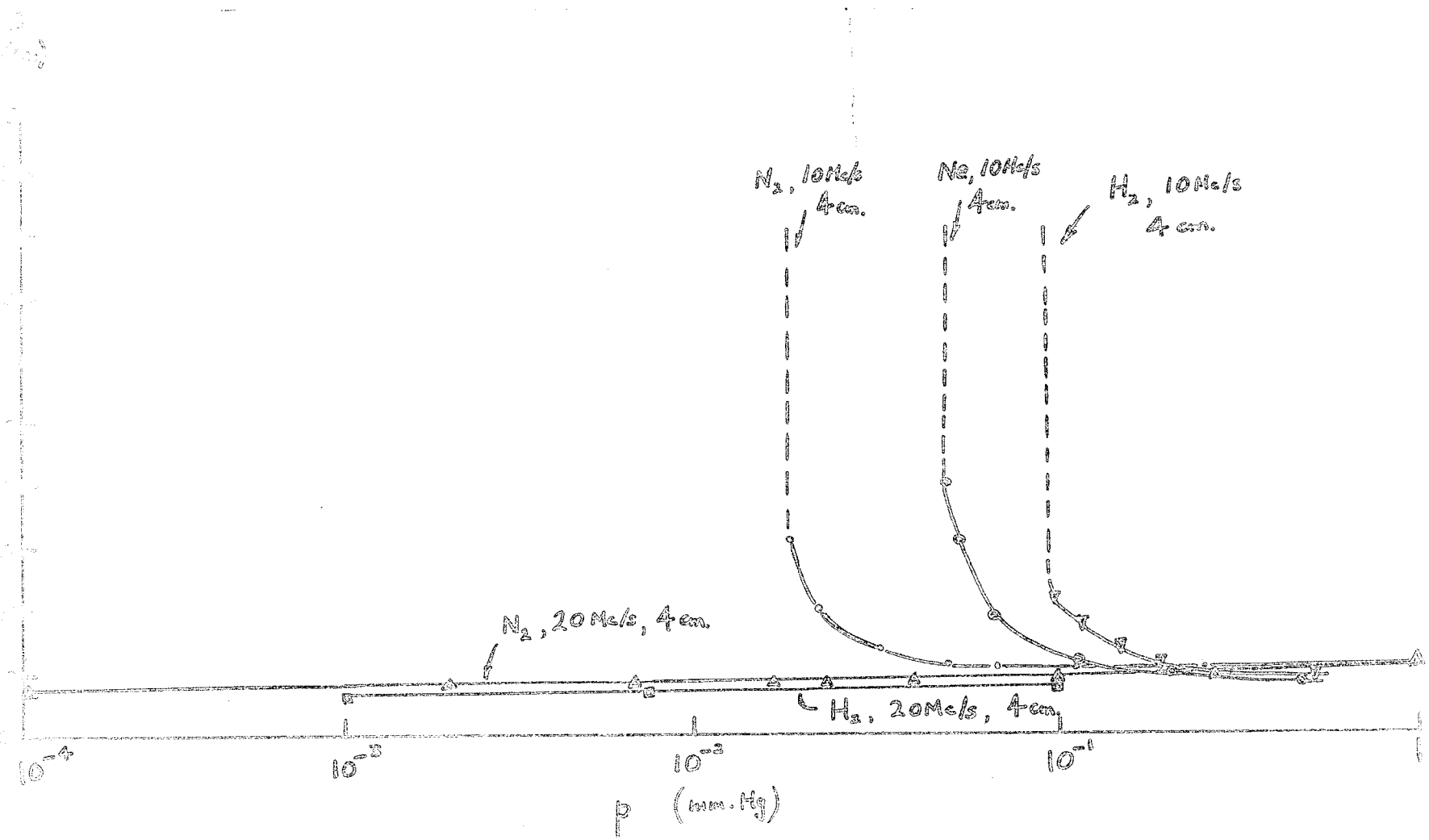

relationship between statistical times and the nature of a particular gas.

6.2.2 Results in Nitrogen and Neon

Several runs were taken using these two gases. As in previous cases the variation of threshold field was obtained as a function of pressure, for various fixed electrode spacings. A number of experimental curves are shown in Figure 27; results in hydrogen are also given for comparison.

At 10 Mc/s, cut-offs were again observed, though the transitions were not quite so abrupt as in hydrogen. The cut-off pressures, however, varied significantly from gas to gas at constant electrode separation.

Assuming that the nature of the cut-offs is associated with the amplitudes of electron oscillation increasing to fill the gap, as in hydrogen, the variations in cut-off pressures are to be expected, since properties such as collision probability, mean free path etc., are dependent upon the nature of the gas as well as its pressure.

For nitrogen, using the collision probability - electron energy curve of Brode,[16], and substituting the proper variables, it is found that over a range of electron energies from 4 - 50 e.v. collision frequency and gas pressure are

related by the equation:

$$\nu_c = 1.28.\ 10^{10} p \qquad \ldots \quad \ldots \quad \ldots \quad (47)$$

(the numerical value varies within 10% of the value over the range given above).

According to equation (29) the amplitude of electron oscillation increases with decreasing collision frequency, and hence with decreasing pressure.

In qualitative agreement with experimental observations, it is to be expected that cut-offs in nitrogen occur at relatively lower pressures than in hydrogen, since at a given pressure the respective collision frequencies are in a ratio of more than two to one (2.16 : 1). Quantitatively it can be shown that at cut-off the ratio $(\frac{E_R}{\nu})_c$ should be approximately constant whatever gas is used, at constant electrode separation. Unfortunately, this could not be tested due to the abrupt nature of the cut-offs.

No simple relationship appears to exist between collision frequency and gas pressure in neon, as shown from Brode's[16] probability curve. The reasoning given above suggests that the collision frequency should lie between the values for hydrogen and nitrogen (at constant pressure).

At 20 Mc/s, results in nitrogen show that the breakdown fields at low pressures are similar in magnitude to those encountered in hydrogen at the same frequency and gap width. This may be regarded as evidence in support of the analysis of the hydrogen results at low pressures, in which breakdown initiation was explained in terms of a build-up of electron density through secondary emission at the electrode surfaces. Such a mechanism is dependent upon the nature of the electrodes rather than upon the nature of the gas and would give rise to similar breakdown values.

7. DISCUSSION OF RESULTS

The diffusion theory of breakdown proposes a breakdown mechanism whereby the rate of growth of electron population within a test gap, is restricted by a rate of deionization dominated by diffusive losses of electrons from the system. Within the natural limits of the theory, Brown et al. of M.I.T. have demonstrated the validity of the theory in a variety of gases it frequencies in the microwave region.

More recently, Prowse & Clark[29] have verified by measurements at 9.5 Mc/s that the theory is applicable to breakdown in the radio-frequency region.

Using microwave sources, decrease in gas pressure within an electrode system of given geometry results in an initial decrease in threshold field values. However, such decreases are not usually maintained below pressures of a few mm.Hg., since reduction in pressure has the effect of causing departures from diffusion theory requirements. Breakdown fields rise, because outside the diffusion controlled region either the rate of electron loss is increased or the rate of production becomes less effective. Similar evidence of departures from the theory have been observed by several workers at radio frequencies. On

the other hand, measurements by Clark[32], at 9.5 Mc/s suggested that with suitable electrode geometries the theory might hold at pressures below 1 mm.Hg., with a further decrease of breakdown field values below the minima obtainable in the microwave region.

The work here reported in hydrogen shows that departures occur at somewhat lower pressures than have hitherto been reported. At 10 Mc/s analysis has indicated that the cut-offs may be attributed to the fact that the amplitudes of electron movement can be no longer confined to the inter-electrode distance. Mobility capture greatly enhances the net rate of loss of electrons and demands an increase in applied field strength to break down the gap.

At 20 Mc/s breakdown fields decrease slowly with reduced pressure (at fixed electrode separation) to an almost constant value. The absence of sudden changes in breakdown field strengths and the lack of basic data regarding the properties of the electrode surfaces has led to a semi-empirical analysis of breakdown for low pressures at this frequency.

By writing down the basic equation of electron motion in an alternating field, a theoretical picture of breakdown has been built up in terms of a to-and-fro movement of electrons

across the interelectrode space. Electron density is considered to increase largely by secondary emission from the electrode surfaces. At very low pressures (corresponding to breakdown in a 'vacuum') the field equations are in agreement with those of Gill & Von Engel[30], who have explained the inception of electrodeless discharges at very low pressures in terms of secondary emission from the walls of the glass discharge capsule.

A basic requirement of breakdown under such conditions is that electron motion be suitably phased with respect to the sinusoidal applied field and that the interelectrode space be traversed in a half period of the supply. Assuming that breakdown occurs at a field value such that a net gain in electron density is just maintained during each half period, knowledge of the secondary emissive properties of the electrodes would enable a critical test of the theory to be made. As previously mentioned, this has not proved possible. However, calculations of impact velocities etc. suggest that the observed breakdown field values are sufficient to permit an increase in electron populations, leading ultimately to breakdown. For the smaller electrode spacings a modification to the straight-forward to-and-fro mechanism, is proposed, whereby electrons

traverse the gap in a half-period during which they restrike the parent electrode.

With increasing gas pressure, calculations show that for pressures below the region in which the electron mean free path becomes comparable with the electrode spacing, breakdown behaviour approximates closely to 'vacuum' conditions. For further increase in pressure, the mechanism becomes progressively less efficient and fails when electrons make numbers of collisions in transit across the gap. At the same time the amplitude of electron oscillation (in the purely oscillatory sense) decreases with increasing pressure, giving rise, at pressures between about 10^{-2} mm.Hg. to 5.10^{-1} mm.Hg. (depending on the gap spacing) to breakdown in reasonable conformity with the diffusion theory. Intermediate conditions have not been explained quantitatively but results indicate a smooth transition between the two.

For a given electrode separation and field strength, the electron oscillation amplitude (one half the total distance moved in a half-cycle of the field, d_e) is given by equation 18, namely

$$x_o = \frac{d_e}{2} = \frac{e E_p}{m (\omega^2 + \nu_c^2)^{\frac{1}{2}}}$$

Also $\nu_c \propto p$.

The pressure at which an electron just crosses a gap of length d, in a half-period, thus increases as field frequency decreases. At 10 Mc/s pressures corresponding to $d_e = d$ are too high to give electrons striking the electrode faces sufficient energy to release surface electrons by secondary emission. Hence electrons striking the walls are lost from the system and 'cut-offs' occur. With 20 Mc/s oscillations, the corresponding pressures are low enough and hence impact velocities sufficiently high to permit suitably phased electrons to release further electrons from the electrodes.

No theoretical treatment was attempted for the results, in other gases. Qualitatively results support the work in hydrogen. At 20 Mc/s, field values at low pressures for corresponding electrode separations are very similar, supporting the view that breakdown is not significantly influenced by the nature of the gas. The characteristic changes in cut-off pressures at 10 Mc/s are as expected from considerations of departures from the diffusion theory.

REFERENCES

1. E.L.E. WHEATCROFT - Gaseous Electrical Conductors, Clarendon Press, Oxford (1938)

2. M.J. DRUYVESTEYN, F.M. PENNING - Revs. Mod. Phys. 12, 87, (1940)

3. P.T. SMITH - Phys. Rev. 36, 1293 (1930)

4. W. BLEAKNEY - Phys. Rev. 36, 1303, (1930)

5. A. VON ENGEL - Ionised Gases, Clarendon Press, Oxford (1955)

6. L.B. LOEB - Basic Processes of Gaseous Electronics, Univ. of California Press, (1955)

7. R.N. DITCHBURN ET AL. - Proc. Roy.Soc., A 181, 386 (1943)

8. K.G. McKAY - Adv. in Electronics, 1, 65 (1948)

9. F.W. LIKE - J. App. Phys., 12, 396, (1941)

10. J. FRIEDMANN & J.G. WEISS, 29, 777, (1941)

11. W. FUCKS - Appl. Sc. Res., B 5, 109

12. S.J.B. CORRIGAN & A.VON ENGEL - Proc. Roy. Soc. A. 245, 335 (1958)

13. S.C. BROWN & A.D. McDONALD - Phys. Rev. 76, 1629, (1949)

14. F. LLEWELLYN JONES & G.D. MORGAN - Proc. Phys. Soc. B. LXIV,56, (1951)

15. F. LLEWELLYN JONES & G.C. WILLIAMS - Proc. Phys. Soc. B. LXVI,17, (1953)

16. R.B. BRODE - Rev. Mod. Phys., 5, 257, (1933)

17. H. MARGENAU - Phys. Rev., 60, 508, (1946)

18. K. MASCH - Arch. Elektrotech, 26, 589, (1932)

19. M. IAAVOLA - Arch. Elektrotech, 22, 443, (1929)

20. H. RAETHER - Zeitz Phys., 117, 375, (1941)

21. L.B. LOEB & J.M. MEEK - Mechanism of the Electric Spark, Stanford U.P. (1941)

22. F. LLEWELLYN JONES & A.B. PARKER - proc. Roy.Soc. A. 213, 185, (1952)

23. F. LLEWELLYN JONES - Extract from B.A. Meeting 1952

24. E. REUKEMA - Trans. Am. I.E.E., 47, 38, (1928)

25. W.A. PROWSE & F.E. LANE - Appl. Sc. Res., 5, 127, (1955)

26. S. GITHENS - Phys. Rev. 57, 822, (1940)

27. J. THOMPSON,- Phil. Mag., 23, 1, (1937)

28. M.A. HERUN & S.C. BROWN - Phys.Rev., 74, 291, (1948)

29. W.A. PROWSE & J.L. CLARK - Proc. Phys. Soc., LXXII, 625, (1958)

30. E.W.B. GILL & A. VON ENGEL - Proc.Roy. Soc. A, 192, 446 (1948)

31. J.A. PIM - J.I.E.E., 96, 117, (1949)

32. J.L. CLARK - Ph.D. Thesis, Univ. of Durham (1957)

33. R.A. PASKA - Ballistic Labs. Rep. No. 1944, 1955 (Restricted Circulation)

34. W.A. PROWSE & J.I. CLARK - E.R.A. Report I/T 365 (1957)

35. W. ROGOWSKI - Arch. Elekt. 16, 73 (1926)

36. J.D. STEPHENSON,- J.I.E.E., 73, 69 (1933)

37. W.A. PROWSE & W. JASINSKI - I.E.E. Monograph No. 32 (1952)

38. N.E. BRADBURY & R.A. NIELSON - Phys. Rev. 49, 338, (1936)

39. N.E. BRADBURY & R.A. NIELSON - Phys. Rev. 51, 69, (1937)

40. A. VON ENGEL - Hand der Phys., Springer, Berlin (1956)

41. H. BRUINING - Phys. & Appl. of Sec. Electron Emission Pergammon Press (1954)

42. J. MATTHES - 2 Tech. Phys., 22, 232, (1941)

43. ZWORYKIN et al - T.Appl. Phys. 12, 696, (1941)

44. H.SALOW - Am. Phys. 5, 417, (1950)

45. H. BRUINING & J.H. de BOER - Physica 6, 823 (1939)

46. R.L. PETRY - Phys. Rev., 28, 362, (1926)

47. R. WARECKE - J. Phys. Radium, 7, 270 (1936)

48. L.R. KOLLER & J.S. BURGESS - Phys. Rev. 70, 571, (1946)

49. H. BRUINING & J.H. de BOER - Phys. 5, 17, (1938)

50. H. GOLBRECHT & F. SPEED - 2 Phys. 135, 602 (1953)

51. P.M. MOROZOV - J. Exp. Theoret. Phys. USSR 11, 410(1941)

46a. E. UHLMANN, Arch. Electrotech. 20, 589, (1929)